# A Closed-Loop System between Intra-Ear Canal Monitoring and General Anesthesia

by

Tiro Setati

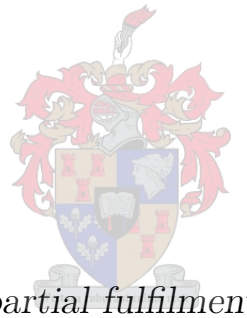

*Thesis presented in partial fulfilment of the requirements for the degree of Master of Engineering (Electronic) in the Faculty of Engineering at Stellenbosch University*

Supervisor: Prof. W. J. Perold
Co-supervisor: Dr. D. Withey, Dr. P. Fourie

March 2021

# Declaration

By submitting this thesis electronically, I declare that the entirety of the work contained therein is my own, original work, that I am the sole author thereof (save to the extent explicitly otherwise stated), that reproduction and publication thereof by Stellenbosch University will not infringe any third party rights and that I have not previously in its entirety or in part submitted it for obtaining any qualification.

Date: 2020 / 08 / 31 .....

# Abstract


## A Closed-Loop System between Intra-Ear Canal Monitoring and General Anesthesia

T. Setati

*Department of Electrical and Electronic Engineering,*
*University of Stellenbosch,*
*Private Bag X1, Matieland 7602, South Africa.*

Thesis: MEng (Electronic)

March 2021

South Africa has a shortage of workers in the healthcare sector, and this shortage extends into anesthesiology as well. With this need, it would be helpful to introduce a system that administers anesthesia automatically to lighten the load on anesthesiologists as well as to help distribute available anesthesiologists more evenly across the South African population. Therefore, a closed-loop control system maintaining a patient's depth of anesthesia was designed.

The system designed consists of an intra-ear electrode and monitor, reading mid-latency auditory evoked potentials (MLAEP) from a patient, a control system and an infusion pump to infuse anesthetic to a patient. The focus of this study will be the design of the closed-loop control system interfacing the intra-ear monitoring system and the infusion of anesthetic.

The closed-loop control system will have a reference MLAEP latency or plasma concentration that it will need to follow, and the intra-ear monitor will send the latencies read from the patient. These will be the inputs to the control system's model predictive controller (MPC), which incorporates a model of the patient within the controller so that the infusion regime it determines is based on patient-specific parameters. Once the amount of infusion is determined, the system will send infusion instructions to the infusion pump to administer the correct amount of anesthetic to the patient.

The designed control system was simulated, and its performance was compared to a simulated closed-loop control system based on a PID controller. This controller shows overall better control because of the shorter settling time, smaller overshoot, and smaller errors between the reference value and

the measured output that the MPC control loop achieves. The effect of measurement noise on MPC control system was also investigated and the results showed that the system was able to operate adequately with signal-to-noise ratio (SNR) down to 15 dB.

From the simulations conducted, it was shown that the closed-loop control system could keep a simulated patient adequately sedated using the MLAEP as an adequate control signal to keep the patient sedated.

# Uittreksel

## 'n Geslotelussisteem tussen Intra-oorkanaal Monitering en Algemene Narkose

T. Setati

*Departement Elekries en Elektoniese Ingenieurswese,*
*Universiteit van Stellenbosch,*
*Privaatsak X1, Matieland 7602, Suid Afrika.*

Tesis: MIng (Meg)

Maart 2021

Die tekort aan gesondheidswerkers in Suid-Afrika sluit ook narkotiseurs in. 'n Stelsel wat narkose outomaties kan toedien sal die werklas van narkotiseurs verminder asook help om die dienste wat narkotiseurs aanbied, meer eweredig oor die Suid-Afrikaanse populasie te versprei. Met hierdie as agtergrond en motivering is die ontwerp van die geslote-lus-beheerstelsel vir die instandhouding van die narkosediepte by pasiënte uitgevoer.

Die stelselontwerp bestaan uit 'n intra-oorkanaal elektrode wat die MLAEP (Middle Latency Auditory Evoked Potentials) van die pasiënt monitor, 'n kontrolesisteem asook 'n narkose infusiepomp wat aan die pasiënt se veneuse sisteem gekoppel is. Die fokus van hierdie navorsing was gemik op die ontwerp van 'n geslotelus sisteem tussen die intra-oorkanaal moniteringsisteem en die infusiepomp narkose.

Die beheerstelsel monitor die MLAEP sein in pasiënte, en bepaal dan die pasiënte se plasma narkosekonsentrasie waardeur effektiewe sedasie gedurende die instandhoudingsfase van die narkose bewerkstellig kan word. Die beheerder maak gebruik van die sogenaamde MPC (Model Predictive Control) wat 'n model van die pasiënt insluit en dus die infusie algoritme, gebaseer op die pasiënt se spesifieke liggaamsparameters, insluit. Sodra die infusietempo bepaal is, word die instruksie na die infusiepomp gestuur waardeur die korrekte narkose aan die pasiënt toegedien word.

Die stelsel ontwerp is met 'n geslote-lus-sisteem, wat 'n PID (Proportional-Integral-Derivative) beheerder insluit, vergelyk en gevolglik 'n beter beheer a.g.v. die kleiner oorskiet en kort stabilisasie-tyd wat deur die MPC beheer

lus bereik kan word tot gevolg het. Die stelsel-ontwerp het ook die effek van metingsgeruis op die stelsel evalueer en kan bevestig dat die stelsel gemaklik binne die 15 dB geruisvlak kon funksioneer. 'n Bykomstige ontwerp om die narkotiseur in staat te stel om die diepte van narkose te beheer, is suksesvol deur die stelsel gedemonstreer.

Die simulasieresulate kon aantoon dat die geslotelus beheersisteem die pasiënt effektief gesedeerd hou. Verder het die simulasie getoon dat die MLAEP 'n voldoende beheersein verteenwoordig en dus die gesimuleerde pasiënt oor 'n wye spektrum suksesvol kon sedeer.

# Acknowledgements

I would like to express my sincere gratitude to the following people and organisations.

Firstly, thank you to my supervisors Prof. Willem Perold, Prof Pieter Fourie and Dr. Dan Withey. Without the help of Prof Pieter Fourie and Prof. Willem Perold, I would not have known of, or have been able to work on this incredibly interesting topic and their support was invaluable. Dr. Dan Withey's assistance throughout this journey was immeasurable. His guidance helped in understanding the elements of this project and his support during the valleys of this journey made it all possible.

The assistance from the anesthesiologists Dr. Ettienne Coetzee and Dr. Theodi Lombard is highly appreciated. Their help in understanding the field of anesthesiology and the role this system would play in practice helped me understand the context in which this project would apply.

The funding from the Council for Scientific and Industrial Research (CSIR) throughout the duration of this thesis is also greatly appreciated.

# Dedications

*Praise **God** from whom all blessings flow.*

*To my parents **Malesela** and **Chokoe Setati** and sisters **Theresho Setati** and **Maweshi Nkoana** for their unending love their support.*

*To my family, friends and colleagues at the CSIR for all the support and encouragement.*

# Contents

# List of Figures

# List of Tables

# Nomenclature

### Variables

| | | |
|---|---|---|
| $\phi$ | Electrochemical potential | [mV] |
| $C_e$ | Effect-site concentration | [$\mu$g.ml$^{-1}$] |
| $C_p$ | Anesthetic plasma concentration | [$\mu$g.ml$^{-1}$] |
| $K$ | Exposed surface area per unit time | [mm$^2$.s$^{-1}$] |
| $k_{ij}$ | Pharmacokinetic model rate constants moving from origin $i$ to destination $j$ | [ ] |
| $N_b$ | Trough latency from the MLAEP signal | [ms] |
| $q_i$ | State-space variable of the drug mass in compartment $i$ | [mg] |
| $S_0$ | Total surface area | [mm$^2$] |
| $t$ | Contact time | [ms] |
| $\tau$ | Dielectric relaxation time constant | [ms] |
| $u$ | Anesthetic infusion rate | [mg.min$^{-1}$] |
| $V_a$ | Artefact voltage | [$\mu$V] |

### Units

| | |
|---|---|
| $dB$ | Decibels |
| $^\circ$ | Degree |
| $Hz$ | Hertz |
| $mg$ | Milligrams |
| $mg.min^{-1}$ | Milligrams per minute |
| $mg.kg^{-1}.min^{-1}$ | Milligrams per kilogram per minute |
| $mm^2$ | Square millimetres |
| $mm^2.s^{-1}$ | Square millimetres per second |
| $ms$ | Milliseconds |
| $mV$ | Millivolts |
| $\mu g.ml^{-1}$ | Micrograms per millilitres |
| $\mu V$ | Microvolts |

**Abbreviations**

| | |
|---|---|
| AEP | Auditory Evoked Potential |
| AEPidx | Auditory Evoked Potential index |
| AR | Autoregressive |
| BAEP | Brainstem Auditory Evoked Potential |
| BIS | Bispectral Index |
| DC | Direct Current |
| EEG | Electroencephalogram / Electroencephalography |
| EP | Evoked potentials |
| ERG | Electroretinogram |
| GUI | Graphical User Interface |
| IAE | Integral Absolute Error |
| ICU | Intensive Care Unit |
| IDE | Integrated Development Environment |
| ISE | Integral Squared Error |
| ITAE | Integral Time-weighted Absolute Error |
| ISTE | Integral of the Squared Time Error |
| $\text{IST}^2E$ | Integral of the Squared Time-Squared Error |
| $\text{IST}^3E$ | Integral of the Squared Time-Cubed Error |
| MAC | Minimum Alveolar Concentration |
| MDAPE | Median Absolute Performance Error |
| MDPE | Median Performance Error |
| MEF | Median Edge Frequency |
| MLAEP | Mid-latency Auditory Evoked Potential |
| MIMO | Multi-Input Multi-Output |
| MPC | Model Predictive Controller |
| NaCl | Sodium Chloride |
| PD | Pharmacodynamic |
| PE | Performance Error |
| PK | Pharmacokinetic |
| PK-PD | Pharmacokinetic and Pharmacodynamic |
| PID | Proportional-Integral-Derivative |
| SEF | Spectral Edge Frequency |
| SEP | Somatosensory Evoked Potential |
| SNR | Signal-to-Noise Ratio |
| TCI | Target-controlled infusion |

| | |
|---|---|
| TIVA | Total intravenous anesthesia |
| USB | Universal Serial Bus |
| VEP | Visually Evoked Potential |
| WAV | Wavelet |

# Chapter 1

# Introduction

## 1.1 Problem statement

South Africa has a shortage of workers in the healthcare sector, and this shortage extends into anesthesiology as well [1]. With this shortage, it would be helpful to introduce a system that assists in the administration of anesthesia to help bridge the gap in the shortage of skilled anesthesiologists. This system would need to operate without the need for constant supervision from an anesthesiologist, and therefore, it would need to be able to provide the desired anesthetic to a patient at reliable, safe quantities without the risk of under-dosing and overdosing. The system would also need to be able to operate effectively with a wide range of patients despite the possibility of a wide window of inter-patient variability.

## 1.2 Background information

Anesthesia is the controlled loss of sensation and/or consciousness in a medically controlled setting. There are three types: local, regional and general anesthesia. Local anesthesia is the loss of sensation in a specific, smaller area of the body, for example the right hand; and regional anesthesia is the loss of sensation to a large area in the patient's body, for example the right arm. General anesthesia is the loss of both consciousness and sensation. Anesthesia can involve analgesia, the loss of pain sensation; paralysis, the loss of muscle functionality; amnesia, the loss of memory; or unconsciousness [2].

Anesthesiologists have a great responsibility in sedating and maintaining the comfort of a patient in surgery by administering enough drug to keep the patient from experiencing the pain or stress of surgical stimulation while making sure the drugs administered cooperate with the patient's pharmacological requirements. Under-dosing of the drugs could lead to intraoperative awareness that could cause postoperative post-traumatic stress disorders [3] while

overdosing could be fatal as anesthetics can block the central nervous system from sending and receiving information needed for normal bodily functions, like breathing and maintaining a normal cardiac rhythm [3].

The skills shortage in anesthesiology could be attributed to the loss of experienced practitioners in rural areas, high personnel turnover and inadequate training in anesthesiology. The automation of anesthesia could provide a great benefit in hospitals that lack the presence of professional anesthesiologists [4].

To address the shortage of skilled anesthesiologists available, a system delivering anesthetic to a patient autonomously needs to operate for the duration of a surgery without the constant need for human intervention. It will be best if the system operated as a closed-loop control system. A control system is a system that governs the behaviour of a defined variable. It controls the variable by either keeping it constant in the face of external disturbances, or it changes its outputs in order to satisfy a specified set-point [5].

It would be beneficial to implement a closed-loop control system to automate the delivery of an anesthetic. The controller would read signals from a patient through some sort of monitoring apparatus, such as an electrode and signal acquisition, into the control system and the control system would be responsible to determine how much anesthetic to administer based on the current readings. It would also be beneficial if the system incorporated a model of the patient receiving the infusion so the system can base its infusion algorithm on the patient receiving the infusion.

Monitoring the depth of anesthesia that a patient is experiencing would require analysing one of the various electroencephalogram (EEG)-derived signals that are available, like the Bispectral Index Scale (BIS) [6] and the Auditory Evoked Potentials (AEPs) [7], and there are various monitors available to monitor these signals [8]. Mid-latency Auditory Evoked Potentials (MLAEPs) are signals derived from EEG signals generated as the brain responds to an audio stimulus. These signals have shown to decrease in the speed of their response based on the depth of anesthesia experienced by a patient [9].

In [10], a novel intra-ear monitor has been developed to track the MLAEP of a patient during anesthesia. Using this latency acquired from the monitor, a closed-loop control system delivering anesthetic drug and incorporating the pharmacokinetic and pharmacodynamics of the patient [11] can be designed to autonomously control the depth of anesthesia experienced by a patient.

## 1.3 Significance and motivation

Automating anesthesia could assist the available anesthesiologists by providing consistent, accurate dosages of anesthetic to the patients, potentially requiring

less oversight. The system could also immediately alert the anesthesiologist if a problem is detected either in the patient or with the infusion system. [1].

According to the South African Society of Anesthesiologists [1], anesthesiologists are responsible for overseeing one anesthetic procedure at a time. Automating anesthesia could allow the anesthesiologist to be able to oversee more than one procedure at a time from a control room. The system would maintain the patients in a state of anesthesia and alert the anaesthesiologist in the case that an intervention is needed.

## 1.4 Contributions

Firstly, this thesis highlights that a non-invasive intra-ear monitor can be used to estimate a patient's propofol plasma concentration by correlating the concentration with the latencies of the MLAEP signals generated as the patient experiences deeper levels of anesthesia. This correlation is achieved through plasma concentration to MLAEP latency modelling.

The thesis shows the benefit of incorporating a patient model into the control system. It also shows that the MLAEP latencies, or plasma concentrations, are adequate control variables that can be used in a closed-loop feedback controller administering anesthetic to a sedated patient through simulation-based evaluation of an MPC controller with an integrated patient model.

Additionally, this thesis provides a simulation-based comparison of a PID-controlled closed-loop system and an MPC-controlled closed-loop control system, intended for automated delivery of anesthetic.

## 1.5 Research questions

Upon understanding the background of the problem, one can determine research questions with the intention of answering them during the investigative procedure. The research questions include:

- Can a closed-loop feedback control system be designed to interface the intra-ear canal monitor and general anesthesia and what type of control system would be suitable for use in automating anesthesia?
- How effective are MLAEP latencies as a control signals for use in closed-loop control?
- How would such a system operate with the wide variety of patients which exist?

- Is such a system capable of handling the requirements that an anesthesiologist would need to meet to keep a patient adequately sedated under various conditions?

## 1.6 Assumptions, definitions and limitations

In the field of anesthesiology, the anesthesiologist, also referred to as an anesthetist, is the practitioner administering the anesthetic to sedate the patient. The anesthesiologist relies heavily on a thorough understanding of pharmacokinetics and pharmacodynamics of a patient, which define how a drug moves through the patient's body as well as the effect that the drug has on the patient's brain.

To automate the delivery of anesthesia safely and reliably, it would be valuable to have the closed-loop control system incorporating some information about the patient for improved control [12]. Therefore, it would be advantageous to incorporate a patient model into the control system to optimize the anesthetic delivery to the patient, based on the knowledge of the drug dynamics in the patient [12].

Another factor to be considered is that the system needs to accommodate a wide variety of patients. This can cause the controller performance to decrease because the same type and quantity of anesthetic drug could affect various patients in different ways [13]–[15].

Finally, a potential concern to be considered is if the automation of anesthesia will be accepted by anesthesiologists and other health care practitioners. Although the goal of the system is not to replace the job of the anesthesiologist but rather to automate the task of maintaining the patient in a state of anesthesia [16], such a system could be seen as a threat to anesthesiologists and anesthesiologists could question whether the system would be able to perform adequately.

## 1.7 Theory base and general literature review

Anesthesia is the controlled loss of awareness and sensation in a patient. This allows for surgeons to operate on a patient without the patient being awake or experiencing or reacting to the pain of the surgery. The first recorded successful use of anesthesia was administered by William T.G. Morton who sedated a patient, Edward Gillbert Abbott, by administering ether. This was conducted on 16 October 1864 in "The Ether Dome" at Massachusetts General Hospital [17].

When a patient is anesthetized, there are a number of responses and signals from the patient that the anesthetist could use to measure the patient's depth

of anesthesia at a given time. These responses and signals include a varied heart rate, a varied breathing rate, varying oxygen saturation in the blood, changing temperature of the blood, and changing frequency of brain activity [18]. These are influenced differently depending on the anesthetic drug used and many of these responses have no linear correlation between their rate of change and the depth of anesthesia. What has been noticed is that brain activity does have a linear correlation to the depth of anesthesia, and so it would be worth investigating these correlations [19].

Administering anesthetics to patients requires a thorough knowledge of pharmacokinetics, the movement of drugs in the body, and pharmacodynamics, the influence of the drugs within the body. There are various pharmacokinetic models used to represent the movement of various anesthetic drugs in different patient categories. For total intravenous anesthesia, the 3-compartment model is commonly used [20] and for volatile anesthetics, like servoflurane, the 5-compartment model is used [21]. Also, for intravenous anesthesia, the Schnider and Marsh models are used for healthy adults [22], and the Paedfusor [23] and Kataria models for children [24].

The interest in closed-loop control of general anesthesia has grown since the bispectral index (BIS) monitor was introduced to determine the depth of anesthesia [25]. Closed-loop control of anesthesia involves a controller that adjusts its output based on the difference between the current input and a reference setting. The inputs to the controller are measurements from the process that is being controlled. There are various closed-loop control designs available for use, each with their own advantages and disadvantages. Model predictive control (MPC) is a type of controller that makes use of a model of the system to make predictions of the system's dynamics based on the actual measurements.

## 1.8 Overview

This section introduces the shape of the dissertation. The chapters within will be the following:

- Chapter 2 presents a literature review of concepts of anesthesia to give the necessary background on which the ideas and methods of this dissertation are based.
- Chapter 3 presents a literature review of concepts in control systems to provide the necessary background for control system design considerations.
- Chapter 4 describes the methodology used to conduct the work in this dissertation.

- Chapter 5 compares the control system constructed from a Proportional-Integral-Derivative (PID) controller, to that constructed from a Model Predictive Control (MPC) controller.
- Chapter 6 describes the effect of measurement noise on the system and how the system would operate under those conditions.
- Chapter 7 discusses the results obtained as well as the how the system would be incorporated in the field.
- Chapter 8 concludes the dissertation by summarizing the results and highlighting potential future work.

# Chapter 2

# Literature Review: Anesthesiology

## 2.1 Introduction

This chapter investigates the literature available in the field of anesthesiology as well as literature available in monitoring the depth of anesthesia a patient experiences.

## 2.2 Anesthesia

Anesthesia is the controlled loss of sensation and/or consciousness in a medically controlled setting. Anesthesia can involve analgesia, the loss of pain sensation; paralysis, the loss of muscle functionality; amnesia, the loss of memory; and/or unconsciousness [2].

### 2.2.1 Types of anesthesia

There are 3 types of anesthesia available in medicine. They are local anesthesia, regional anesthesia and general anesthesia. The type of anesthesia administered to a patient could depend on the type of surgery to be undertaken, the age of the patient, the underlying medical condition that the patient has, or the patient's personal preference [26].

#### 2.2.1.1 Local anesthesia

Local anesthesia is the loss of sensation in a relatively small area of the body without causing a loss of consciousness. The effects of local anesthesia are caused by suppressing the stimulation of nerve endings which are responsible for transmitting pain signals to the brain.

There are a number of methods used to induce local anesthesia, which include applying a low temperature to the area, depriving the area of oxygen, mechanical trauma and the use of local anesthetics [27].

It is important that the method used to induce local anesthesia is reversible, impermanent and it should not irritate the area where it is applied. The method used should also have low toxicity, the onset of the anesthesia should be as quick as possible and the effects should last long enough for the procedure to be completed without it wearing off. Furthermore, the chemicals used should not need to be used at dangerous concentrations to have lasting effects, they should not produce allergic reactions, they should easily undergo biotransformation in the body and they should not deteriorate when sterilized by heat. Every local anesthetic available cannot meet all the criteria mentioned, but they do satisfy the majority of the requirements [27].

Local anesthesia is commonly used for smaller procedures, like the removal of wisdom teeth or a filling in dentistry, removing a mole and other minor skin operations, biopsies and certain eye operations like cataract removal [28].

#### 2.2.1.2 Regional anesthesia

Regional anesthesia involves administering anesthetic to a part of the body larger than that involved in local anesthesia. Regional anesthesia blocks a cluster of nerves in a certain part of the body to prevent pain and discomfort during surgery. Similar to local anesthesia, regional anesthesia does not cause unconsciousness, but it only blocks the nerves of an affected area to prevent pain signals from reaching the brain [29].

There are mainly two types of regional anesthesia. The first includes peripheral nerve blocks, where anesthetic is injected near the desired nerve or bundle of nerves to prevent pain sensations from being experienced at that specific region, like the hands, feet or face. The second type is epidural and spinal anesthesia, where the anesthetic is injected near the spinal cord and this affects major nerves that block pain sensations from entire regions of the body, like the lower abdomen, legs or hips [30].

The administration of regional anesthesia requires great skill and experience because the anesthetic needs to be injected at precise locations location as this affects which regions are affected, and it reduces the risk of complications associated with incorrect administration, like nerve damage and infection. For epidural and spinal anesthesia, it is even more important to be precise because mistakes could affect heart rate, breathing, blood pressure and other vital functions [30]. Patients receiving regional anesthesia also need to be closely monitored because the location of administration may affect the central nervous system, respiratory system or the cardiovascular system [30].

Compared to general anesthesia, regional anesthesia is considered to be more time-consuming and less reliable. The duration of its effects vary and the depth of the anesthesia experienced by the specific region cannot be regulated [31].

#### 2.2.1.3 General anesthesia

General anesthesia involves an overall loss of consciousness for the patient. General anesthesia involves experiencing a reversible state of unconsciousness, coupled with a lack of awareness, pain suppression and memory loss [32]. Although these are all the elements involved in the successful administration of general anesthesia, each of these effects is achieved by administering different drugs to the patient.

Using general anesthesia has a number of advantages over the other types of anesthesia. General anesthesia in children is associated with fewer cases of nausea and vomiting after the surgery, reduced procedural costs and less operating room pollution and fewer cases of emergence delirium. Another advantage is that general anesthesia has shown fewer interferences with evoked potential monitoring [33].

## 2.3 General anesthesia

Anesthesiologists have the choice of two types of anesthetics to administer to a patient to induce sedation. The anesthesiologist could opt for either of the two options for the duration of the surgery or to use both at different points in the surgery.

### 2.3.1 Inhalation anesthesia

Inhalation anesthesia was introduced in the 1940s accompanied by the development of fluorine technology [34]. Inhalation anesthetics, also known as volatile anesthetics, are delivered to a patient through the respiratory system via a breathing mask.

The uptake and distribution of volatile anesthetics is depicted in Figure 2.1. Initially, the volatile anesthetic is released from an anethesia delivery machine with a vaporizer into a fresh gas mixture which is then delivered to a breathing circuit. From the breathing circuit, the gas mixture is taken in by the patient and it enters the patient's lungs and alveoli. Through transcapillary diffusion, the anesthetic then travels from the alveoli to the pulmonary veins which transfer oxygen and the anesthetic to the blood. The blood is then distributed to various tissues, like fat, muscle and vessel-rich groups, (the brain, liver and kidneys). When the blood flows out of these tissues, it travels as deoxygenated

blood to the pulmonary artery and it returns to the lungs' alveoli. Here, the blood is reoxygenated and receives more anesthetic to flow through the patient again, and some of the anesthetic is returned to the alveoli and exhaled [35].

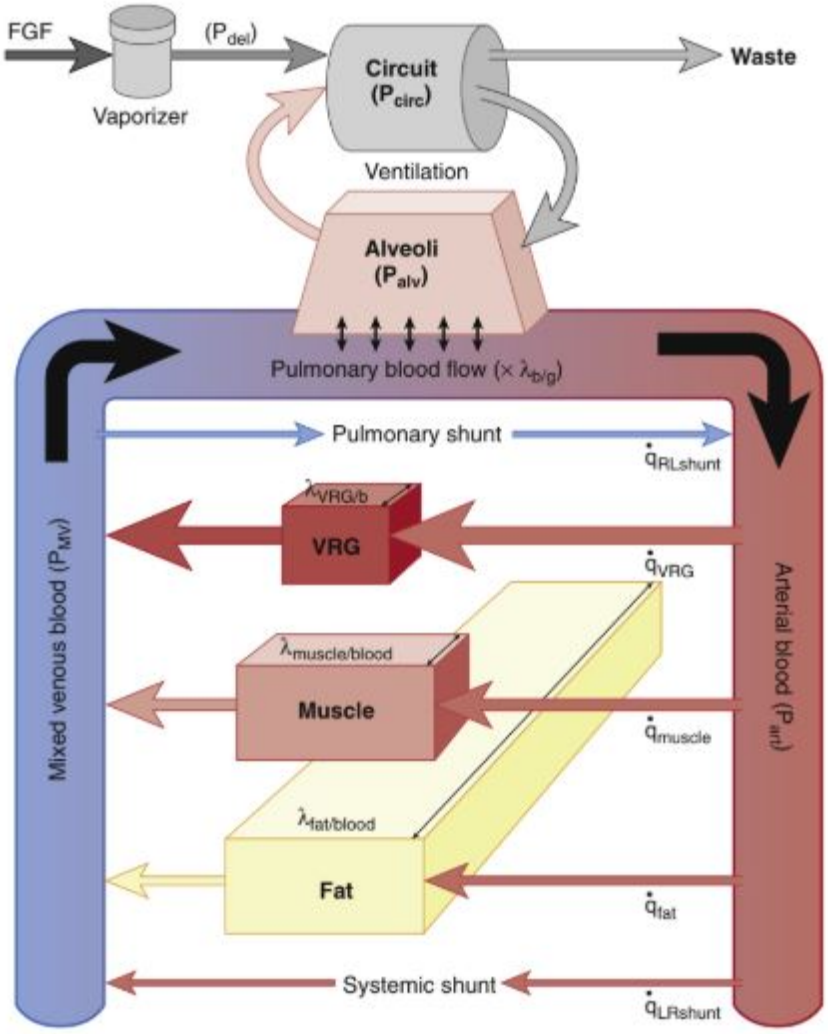


Figure 2.1: Flow diagram representing the administration and transportation of inhaled anesthetic [35]

The inhaled anesthetic that is mixed with the fresh gas mixture is delivered as a partial pressure, which is a portion of the total gas pressure delivered to the patient. If the anesthetic is delivered at 1.5% in air at 760 mmHg or 1 atm, then the ratios stand as follows: 157.2 mmHg of $O_2$, 591.4 mmHg of $N_2$ and 11.4 mmHg of the anesthetic [35]. Some common anesthetics used in volatile anesthesia include isoflurane, desflurane and sevoflurane.

One advantage of volatile anesthetics is that their concentration in the patient can be easily determined. By measuring the amount of drug expired

by the patient through a mass spectrometer, the concentration of the drug within the patient can be determined by comparing it to the amount of drug administered to the patient [34].

### 2.3.2 Intravenous anesthesia

Intravenous anesthesia involves injecting the desired anesthetic directly into the patient's bloodstream. This has the advantage of the anesthetic being administered with more precision by the infusion pump, as well as having greater depth of anesthesia experienced by the patient during the surgery [34].

Intravenous anesthesia was established by Christopher Wren in 1656. He used "a goose quill and a bladder to inject wine and ale into a dog's vein" [36]. In 1843 and 1853, the hollow needle and hypodermic syringe were invented and this allowed for the intravenous injection of drugs. By the 1900s, a wide variety of drugs had been developed for intravenous anesthesia. One of these includes the drug ether [36].

Intravenous anesthesia is also commonly governed by target controlled infusion (TCI) where the anesthesiologist administers the anesthetic to reach a targeted effect and/or plasma concentration. The infusion starts with the injection of the anesthetic into the patient's blood through a vein in the patient's arm. The initial administration is a large bolus dose which is then followed by a step-down infusion scheme. This step-down infusion scheme administers anesthetic at decreasing rates of infusion until the patient is at the desired plasma concentration or shows signs of adequate sedation [37]. Once adequately sedated, the surgeon can begin with the surgery.

### 2.3.3 Drugs used in general anesthesia

Intravenous anesthetics at normal concentrations only function as hypnotic drugs and do not contribute to any pain suppression. Anesthetics in this category can be categorized as Barbiturates, Benzodiazepines such as midazolam and diazepam, Phencyclidine like ketamine, Carboxylated imidazole like etomidate, and Isopropylphenol like propofol [37]. Since the early 1990s, propofol has become a popular anesthetic in total intravenous anesthesia because of its quick redistribution and metabolism, which then relates to quicker emergence times for the patient [37].

Alongside the anesthetic, there are other drugs used during general anesthesia. These drugs are used to numb the patient's pain responses as well as to suppress muscle movements. Opioids, such as morphine, fentanyl, sufentanil, alfentanil, or remifentanil, are commonly used in practice to suppress the sensation of pain during the surgery. Opioids primarily target specific receptors of

the central nervous system and limit neurotransmitter signals that would register pain, from reaching the brain. One major side effect of using opioids during surgery, especially in large doses, is that they affect the patient's breathing. For this reason, a patient needs to be assisted with breathing through artificial ventilation [34].

Neuromuscular blocking drugs are the drugs used as muscle relaxants to prevent the patient from moving during the surgery. Using these drugs make it easier for the insertion of the artificial ventilation tubing as well as preventing involuntary muscle movements and twitching during the surgery. Neuromuscular blocking drugs have no effect on the patient other than blocking muscle movements, so they do not interfere with the anesthetics or opioids. When short-duration muscle relaxation is required, succinylcholine can be used and for longer effects, derivatives of curare such as mivacurium, rocuronium or pancuronium, can be used [34].

### 2.3.4 Phases of general anesthesia

To achieve a stable plasma concentration of anesthetic in the patient for the duration of the surgery, delivering the drug in varied amounts and infusion rates is required. The steps taken to achieve this desired concentration are divided into the three main phases of general anesthesia. These include: induction, maintenance, and emergence [3].

In the case of intravenous anesthesia, the induction phase involves inserting venous and arterial catheters, setting up EEG monitoring devices, starting the administration of anesthetics and intubation. A bolus infusion is administered, which is followed by a decreasing rate of infusion until the patient reaches the desired plasma concentration and the desired effect is achieved [37]. This phase needs much of the anesthesiologist's attention because it can cause heavy stress responses from the patient by increasing the patient's heart rate and blood pressure which could lead to fatal strokes and heart attacks in vulnerable patients [3].

Then the operation begins and the anesthesiologist is responsible for the maintenance of anesthesia. In this phase, the anesthesiologist monitors the patient's depth of anesthesia to prevent underdosing that could cause intraoperative awareness, or overdosing during the surgery. This phase, though critical, does not require as much attention from the anesthesiologist as compared to the induction phase.

Lastly, at the end of the surgery, the emergence phase is conducted. This is the phase when the anesthetic infusion is stopped and the patient slowly gains consciousness. The monitoring devices and tracheal tube are removed at the end of this phase [3].

## 2.4 Depth of anesthesia

One of the most important steps in delivering appropriate amounts of anesthesia to a patient is being able to determine the current depth of anesthesia experienced by the patient. Without monitoring the current level of anesthesia experienced, the anesthesiologist runs the risk of either underdosing the patient with not enough anesthetic, which could lead to awareness during the surgery. On the other end, overdosing the patient with the anesthetic could lead to the patient taking longer to gain consciousness at the end of the surgery as well as potentially experiencing postoperative complications [32].

### 2.4.1 Electroencephalography (EEG)

The anesthetic delivered to the patient during anesthesia serves the purpose of making sure that the patient remains unconscious throughout the duration of the surgery. It, therefore, makes sense to monitor how conscious a patient is right at the source of consciousness: the brain.

Electroencephalography (EEG) is the measuring and recording of the electrical activity generated within the brain. The electrical signals are generated from neurons which generate bio-electromagnetic fields through the electrical impulses when they communicate. These impulses are then propagated through the brain tissue, brain and scalp [8].

The EEG signal shows no repetitive patterns nor does it show any correlation to specific underlying events. However, there are some measurable characteristics of the EEG signal that show a monitoring of some brain functionality [38]. The randomness of the EEG stems from neurons acting independently because higher cortical function is associated with desynchronization. This desynchronization and neuron independence is the root of conscious human behaviour. Mechanisms that decrease levels of consciousness, like anesthesia or sleep, have been shown to increase cortical synchrony [38], [39]. To an extent, this decreases the randomness of the EEG signals.

When the EEG signals are generated, the overall postsynaptic current is transmitted through the highly conductive cerebrospinal fluid and scalp, and the less conductive skull. As the signals move through the highly conductive layers, there is a significant amount of spatial smearing of regional voltage differences [38]. From the transmissions, the EEG signals can be detected on the surface of the skin using skin surface electrodes.

#### 2.4.1.1 EEG monitoring on the scalp

To standardise the monitoring of EEG signals on the scalp for comparability in research, the International 10-20 System layout was selected [40]. The name is based on the 10% and 20% relative placement of the electrodes after identifying

anatomical landmarks, and the system ensures that the symmetric spacing of electrodes over the correct anatomical location on the patient's head.

The first referential line is created by connecting the midline of the scalp from the depressed concave region between the eyebrows, called the nasion, to the inion, which is the convex point at the back of the skull. The second referential line is created by forming a line from one ear's tragus (the small cartilage found on the anterior of the pinna of the ear) to the opposite ear's tragus, cutting through the first referential line. The two referential geometries are then divided into segments:

$$S = \{10\%, 20\%, 20\%, 20\%, 20\%, 10\%\}$$

with $S$ as the section spacing percentages of the relative total distance between adjacent reference points. The placement of the electrodes is depicted in Figure 2.2.

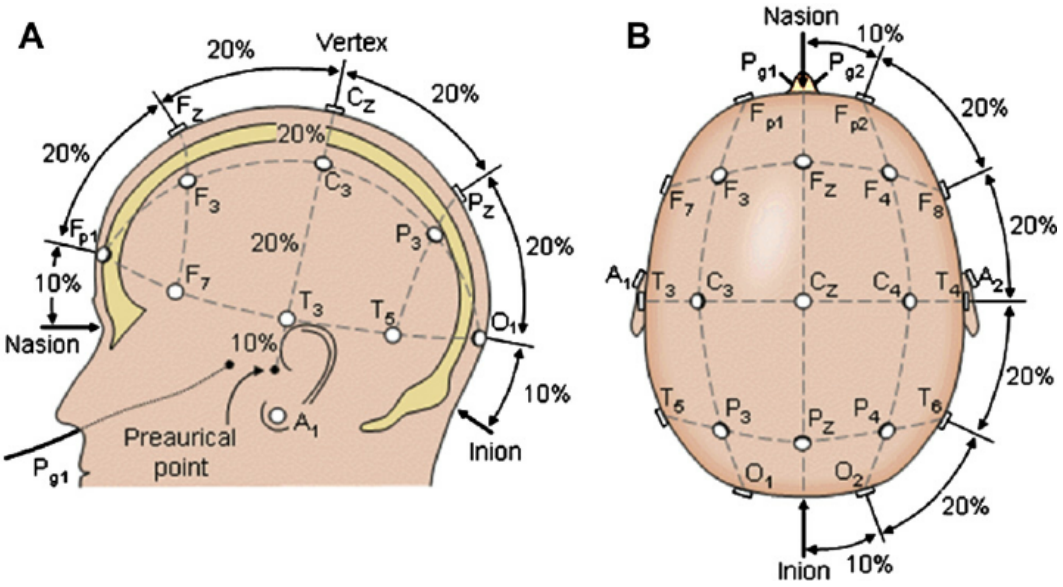


Figure 2.2: International 10-20 electrode placement system as seen from the left (A) and from above (B). From the figures: $A$: ear lobe. $C$: central. $F$: frontal. $F_p$: frontal polar. $O$: occipital. $P$: parietal. $P_g$: nasopharyngeal. $T$: temporal. $Z$: zero (midline saggital) [41]

The placement of electrodes for the International 10-20 System layout is an arduous process, but the placement of the 21 electrodes, with the two reference earlobe electrodes included, ensures reliable reading of EEG signals generated in the brain across the surface of the scalp. Using fewer electrodes is possible, but this would introduce the risk of losing information during the propagation of EEG signals from their sources in specific areas in the brain. Additionally, patient cooperation is necessary as the patient's hair then

becomes an obstruction in the placement of the electrodes, so the patient's hair needs to be trimmed or removed to allow the electrodes to make sufficient contact with the scalp for accurate readings.

#### 2.4.1.2 EEG monitoring in the ear

As mentioned in [38], EEG signals's postsynaptic current is transmitted through cerebrospinal fluid, skull and scalp. As the EEG signal can be detected throughout the mediums of propagation, [42] has investigated the possibility of recording EEG signals from within the ear canal.

Figure 2.3 shows a cross section of the human ear consisting of 3 parts: the outer ear (pinna and external auditory canal); the middle ear, the parts that couple sound to the inner ear; and the inner ear (cochlea) that converts sound to nerve signals, and has a bony casing. The auditory canal, from the pinna to the eardrum, is roughly 26 mm long with a diameter of about 7 mm in the average human ear.

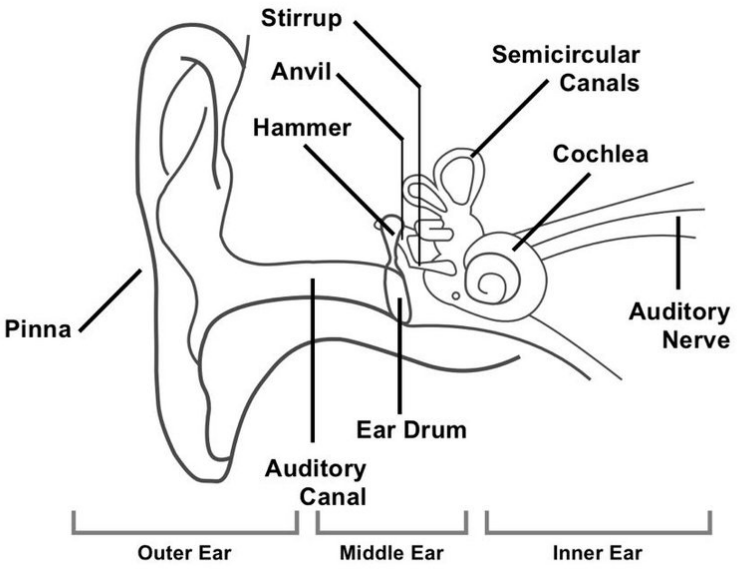


Figure 2.3: Cross section of the average human ear [43]

Evoked potentials are electrical signals which propagate from within the brain throughout the interior of skull in the conductive cerebrospinal fluid and scalp [38] after the onset of a stimulus [44]. These signals can be picked up from the inner ear and on the surface of the skin of the auditory canal [38] and can therefore be picked up by the electrodes of an intra-ear EEG monitor embedded on an earpiece designed to fit within the patient's ear.

Although intra-ear monitors have shown to record 10-20 dB lower amplitudes than the scalp monitor's recordings, both systems maintain a similar signal-to-noise-ratio (SNR) [45]. Additionally, this development is a simpler alternative to scalp EEG monitoring because it does not require lengthy setup procedures and it alleviates the risk of artefact generation caused by skin stretching and electrode movement that are common in scalp EEG monitoring.

### 2.4.2 Monitoring the depth of anesthesia

The administration of anesthetics has a number of effects on the patient. With these effects, there are a number of variables that can be measured from the patient to determine the influence of the anesthetic that has already been administered. During anesthesia, variables include the patient's blood pressure, muscle activity, and breathing. Unfortunately, these parameters have no direct correlation to the current state of hypnosis experienced by the patient, as they rather indicate whether the patient has received adequate muscle relaxant or other drugs that affect these variables [46].

One other parameter that has been identified to correlate with the level of hypnosis experienced is a patient's brain activity. Therefore, it has been identified that a patient's electroencephalogram (EEG) can be analysed to determine the depth of hypnosis experienced [38]. To derive insightful, information from the EEG, a number of parameters have been derived from the EEG to determine the level of hypnosis experienced by the patient.

#### 2.4.2.1 EEG modelling

Sharma and Roy [46] sought to predict movement due to surgical stimulation [47] sought to predict movement due to surgical stimulation. By measuring blood pressure, heart rate and anesthetic concentration of volatile anesthetics in terms of minimum alveolar concentration (MAC). Along with the autoregressive (AR) parameters, all these parameters were used as inputs to an autoregressive model and neural network analysis to predict movement.

This study great improvement when EEG data was combined with other parameters. However, the functionality of such a system comes at the expense of large networks and computational power [38].

#### 2.4.2.2 Power Spectrum Analysis

The power spectrum analysis is used in determining the distribution of the EEG in its frequency domain. EEG signals can be classified into 5 frequency bands at a range of frequencies. These include:

- $\delta$ band ranging from 0.25 Hz to 3.5 Hz
- $\theta$ band ranging from 3.5 Hz to 7.5 Hz
- $\alpha$ band ranging from 7.5 Hz to 12 Hz
- $\beta$ band ranging from 12 Hz to 32 Hz
- $\gamma$ band ranging from 32 Hz to 70 Hz

Anesthetics administered to a patient affect the frequency distribution of the EEG signals generated [48]. In an awake state, the EEG signal is predominantly in the $\delta$ and the $\alpha$ bands. As the patient falls deeper into anesthesia, the activity monitored in the $\alpha$ band decreases and the activity in the $\delta$ band starts increasing.

To make findings from the power spectrum analysis useful for monitoring the depth of anesthesia, the measurements need to be normalized to indices using Fourier analysis as well as the spectral distribution. Two of such indices are the Median Edge Frequency (MEF) [49] [50] and the Spectral Edge Frequency (SEF) [51].

#### 2.4.2.3 Bispectral Index (BIS)

The Bispectral Index (BIS) is an index that tracks the changes in EEG signal and its properties during anesthesia. It has been found to be a more reliable monitor of anesthesia when compared to the power spectral analysis since anesthesia slows or suppresses the EEG signals generated and the power spectral analysis only tracks changes in the magnitude of the EEG signal [38].

BIS is a combination of a number of variables derived from the EEG signal acquired via skin contact electrodes on a patient's forehead [52]. The score determined ranges from 100 and declines the deeper into anesthesia a patient falls, with its minimum at 0 [53]. The scores are labelled as follows:

- 100 - 90: Awake
- 89 - 70: Light and moderate sedation
- 69 - 60: Deep sedation
- 59 - 40: General anesthesia
- 39 - 1: Deep hypnotic state
- 0: Flatline

#### 2.4.2.4 Wavelet Analysis

As functional as BIS is, one problem is that it is derived from the preceding 15 to 30 seconds worth of EEG data. This introduces problems if the score and the patient's current depth of anesthesia need to be used in real-time, or the score needs to be implemented into a third-party system because of the use of the prior 15-30 seconds of data which could be irrelevant to the current depth of anesthesia [6].

It has been shown that the WAV Index [54], derived from wavelet analysis, and the BIS are closely correlated. However, the WAV index analyses quick changes in a patient's EEG signals during induction, emergence and intra-operative awareness and movement better than BIS does [55]. BIS has been found to exhibit abrupt changes during anesthesia, but the WAV index has shown a more gradual increase and decrease during anesthesia because it is based on a per-second analysis of the EEG signals from the patient [55].

#### 2.4.2.5 Evoked Potentials

Another method identified to detect variations in EEG is by monitoring evoked potentials. Evoked potentials are electrical signals generated by the brain and other parts of the central nervous system as a response to the agitation of an external signal. Evoked potentials can be analysed based on the amplitudes and latencies of the various peaks and troughs found in the signal. The changes found in evoked potentials measured in succession can signify that the patient is undergoing a change in response to the stimulus experienced [7], and thus the patient's state of anesthesia is changing.

## 2.5 Evoked Potentials

Evoked potentials (EP) are the responses generated by the nervous system when an external stimulus is introduced. They provide quantitative numerical data of neurological signals generated. They can be measured in terms of the amplitudes, in volts, and latencies, in seconds [44].

The use of evoked potentials in clinical settings is favoured based on the detail EP can reveal. They have the ability to detail abnormal sensory system conduction in ambiguous neurological examinations, they can reveal the inconspicuous involvement of a sensory system when a nerve's protective sheath is damaged by disease, known as demyelination, and they can assist in monitoring changes in a patients' neurological state and the changes the patient might be experiencing. Furthermore, the sensitivity and objectivity of their examinations, as well as their ability to be recorded in patients that are comatose or anesthetized, are further advantages to using evoked potentials over other detailed examinations [44].

The disadvantage of evoked potentials is that they are susceptible to diseases affecting the points of stimulation (for example, visual evoked potentials are affected by the ocular disease in a patient), yet they are predominantly disease unspecified, so the disease affecting the EP cannot be specified. Additionally, they show significant change as patients get older. To acquire artefact-free recordings, they require some patient cooperation [44].

In theory, any external sensory stimulus can be tested and measured, but in medicine, only a few have been found to be reliable in their measurements. The problem with many of the evoked potentials that could be measured is that they are longer latency responses related to higher cognitive functions [44]. The most commonly used stimuli include auditory stimuli, visual stimuli and somatosensory stimuli and they generate the visual evoked potentials (VEP), somatosensory evoked potentials (SEP) and auditory evoked potentials (AEP), respectively [56].

### 2.5.1 Visual Evoked Potentials

Visual evoked potentials (VEP) are the evoked potentials generated from visual stimuli. They are used to detail the conduction within the visual pathway from the retina to the optic nerve, through the optic chiasma and optic radiations, to the primary visual cortex [44], [57], depicted in Figure 2.4.

VEPs are recorded by placing three electrodes across the occipital region of the scalp, with a fourth electrode placed on the mid frontal region as a voltage reference. Two more electrodes are placed on the lower eyelid of each eye to record the average activity taking place in that region [44]. These are depicted in Figure 2.5. The visual stimulus is a high contrast black-and-white "checkerboard" image occupying 20° - 30° of the field of vision. The black and white squares periodically change positions and the averaged responses recorded during these transitions is the VEP [44].

The average responses of the VEP of binocular and monocular "full-field" simulations are depicted in Figure 2.5 [44]. The components of the VEP signal are named according to their polarity ($P$ for positive when the wave deflection is downward or $N$ for negative when the wave deflection is upward) and the approximate time to which they occur after the "checkerboard" pattern reversal. Therefore, the electrode placed at the midline occipital region reads a negative N75 component, followed by a significant P100 component. The P100 latency of the midline electrode is taken as the time from the stimulus generation to its registration. The vertical lines represent a normal patient's mean and 99.5% confidence intervals of the P100 latency [44].

The latency of the P100 trough in normal patients can be affected by the brightness and contrast of the checkerboard displayed and even the viewing angle of the checkerboard [58]. Additionally, other factors like the pupillary

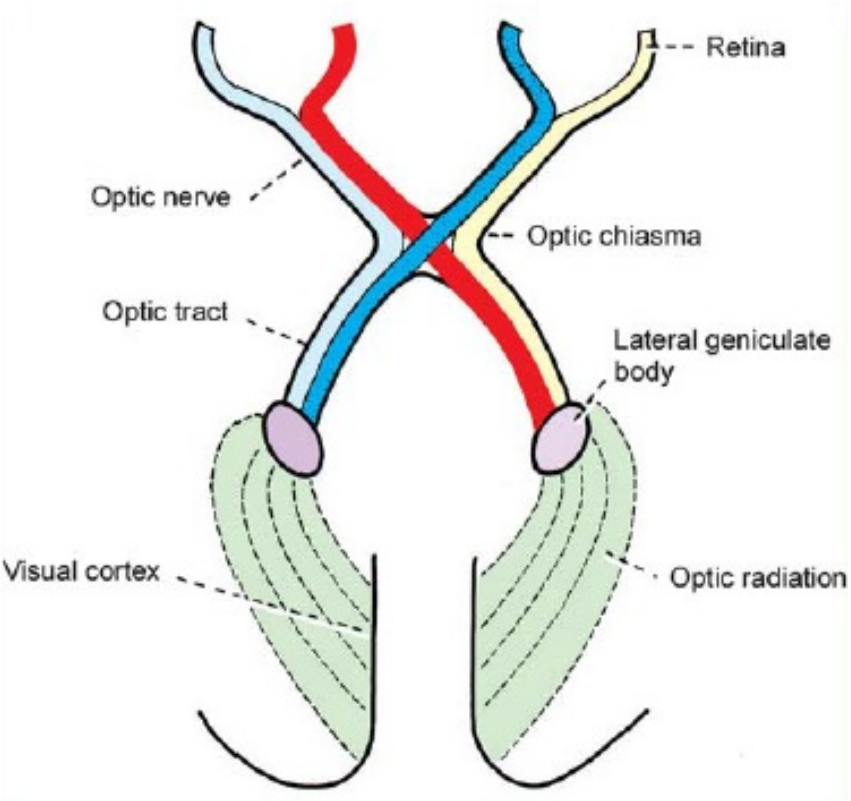


Figure 2.4: Diagram representing the visual pathway from the retina to the visual cortex [57]

size, gender and age of the patient affect the VEP [59]. Therefore, for older patients with deteriorated visual acuity, it may be necessary to use larger checks to acquire usable VEP data. It has also been shown that sedated patients and those in anesthesia show deteriorated VEPs [60].

If the P100 latency falls out of the confidence interval range of 99.5%, it can be assessed as a visual abnormality in the patient. These abnormalities can range from binocular delay, monocular delay, monocular absence or monocular waveform abnormality, as depicted in Figure 2.6 [44]. Causes of these abnormalities could range from optic nerve damage or inflammation, glaucoma, diabetes, tumours compressing the optic nerve and many others [56].

### 2.5.2 Somatosensory Evoked Potentials

Somatosensory evoked potentials (SEP) are evoked potentials measured at various points on the skin as a response to nerve stimulation on the surface of the skin. The electrical activity measured over the scalp from this nerve stimulation depicts cerebral action potentials and these potentials are best observed contralateral to where the nerve was stimulated [61].

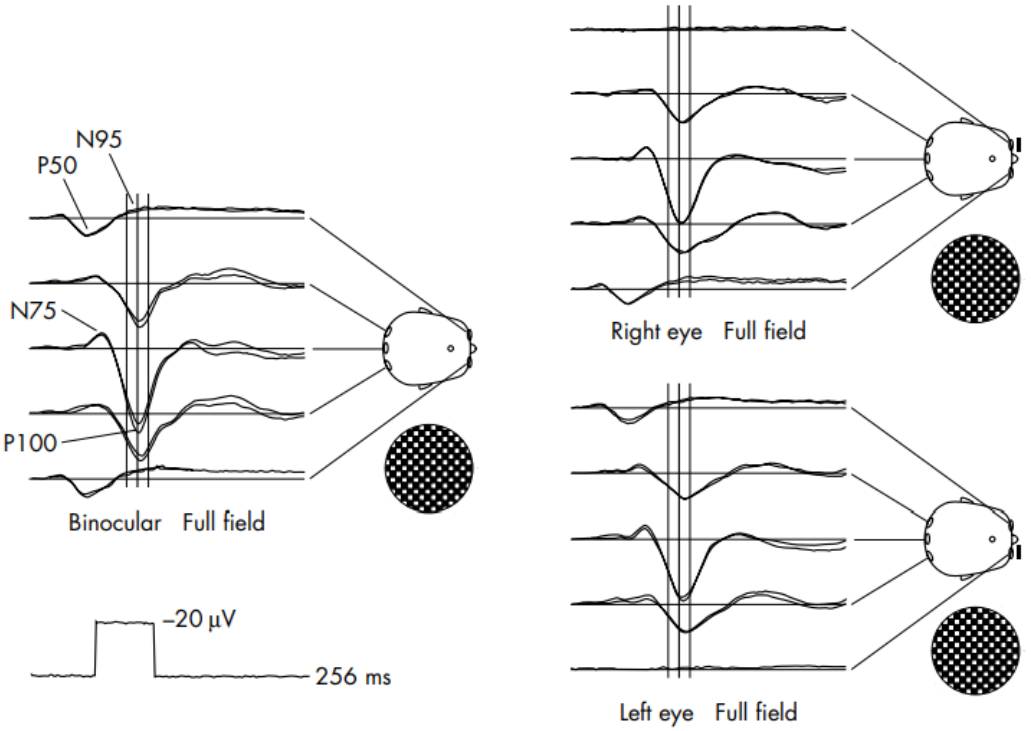


Figure 2.5: Visual evoked potentials (VEPs) and pattern electroretinograms (ERGs) generated by full field stimulation. The vertical cursors show the mean latency and its 99.5% confidence limits [44]

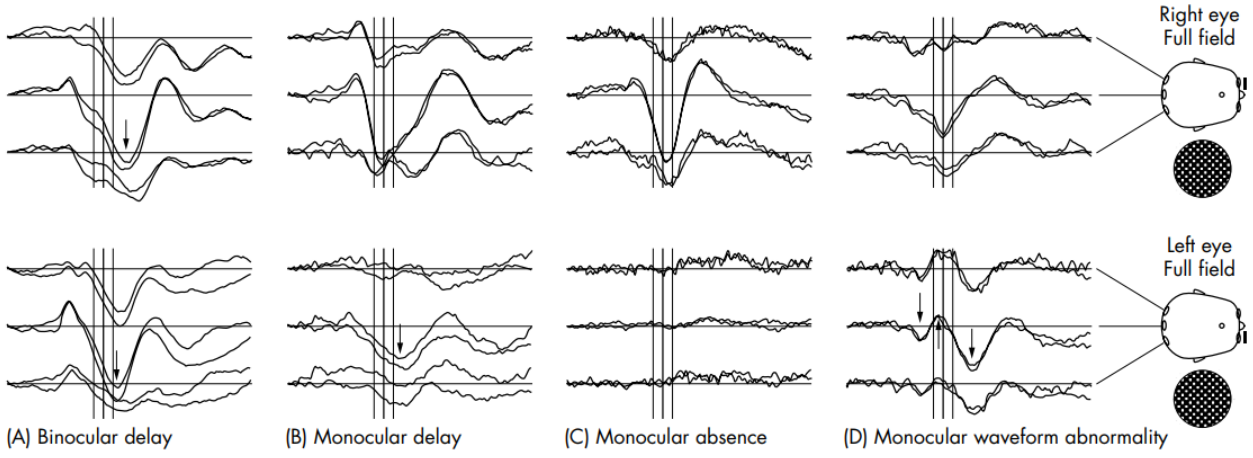


Figure 2.6: Examples of abnormalities in the VEP [44]

The SEPs are recorded relative to a stimulus with a pretrigger. To generate the stimulus, the recommended electrical stimulus should be a continuous square wave pulse of a 0.1 - 0.2 ms duration. Additionally, when stimulating a motor- and sensory-fibre containing nerve, the intensity of the stimulus should exceed the motor threshold necessary for evoking a muscle twitch, but not too high as to cause pain [61].

To record the SEP most effectively and efficiently from the scalp, skin surface electrodes should be placed according to the International 10-20 System [62], depicted in Figure 2.2. Only seven electrodes are necessary: $F_z$, $C_z$, $P_z$, $F_3$, $C_3$, $P_3$ and a reference earlobe electrode. The electrocortical locations that should be used contralaterally to the side which the stimulation occurs are the $F_3$ and the $P_3$. The impedance of the skin on which the electrodes are placed needs to be less than 5 k$\Omega$ [61].

Similar to the VEPs, the waveform peaks are labelled according to their polarity and their latency. The size of the amplitudes represent the magnitude of the incoming conducted stimulus and the length of the latency shows the anatomical location along the somatosensory pathway where the stimulus was administered [61]. SEPs can also be described as "short-latency" if the signal occurs within the first 40 ms from a stimulus in the upper limbs, and within 50 ms for the lower limbs. Peaks and troughs longer than 45 ms have a higher risk of variability as they are more susceptible to cognitive factors [63]. For this reason, the short-latency SEPs are more useful to study because they have less variability among normal patients with typically functional nervous systems [61].

Figure 2.7 depicts an example of SEP extracted from normal patients [44]. Figure 2.7a depicts the median nerve stimulation SEP test setup of two patients. The stimulus was introduced on the wrist and the SEPs were recorded along the median nerve en route to the somatosensory cortex. The bottom waveform shows the bipolar response of the stimulus between two of the depicted chest electrodes and the top waveform depicts the N20 and P23 peaks in their expected locations.

Figure 2.7b the SEPs recorded from an impulse introduced to the tibial nerve, en route to the brain. On the left, a normal tibial stimulated SEP is depicted, and an abnormal SEP on the right. The normal patient's SEP shows normal P37 and N45 peaks, while the abnormal SEP responses show attenuated responses and delayed latencies even before the onset of the stimulation.

SEPs are commonly used to investigate patients who could have multiple sclerosis and myoclonus. They are also used as a guide to decision making in post-traumatic and anoxic ischaemic coma in the ICU, as well as intraoperatively monitoring the efficiency of the sensory pathways during spinal curvature corrections [44].

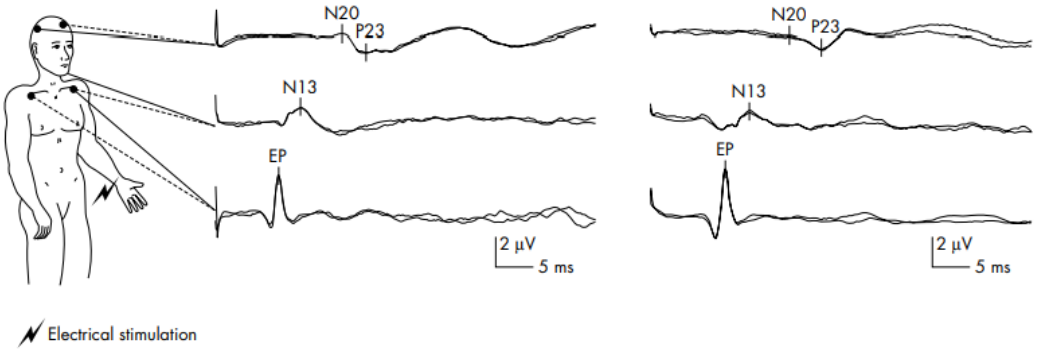


(a) Depiction of short-latency somatosensory evoked potentials (SEPs) occurring normally after stimulation of the median nerve (left) and normal median nerve short-latency SEPs relative to signals on the right of Fig 2.7b (right)

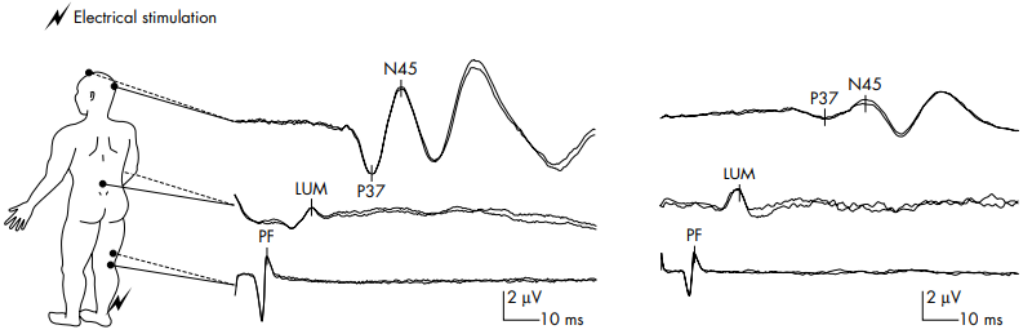


(b) Posterior tibial nerve SEP measured en route to the brain (left) and a dispersed P37 trough with lingering latency relative signals on the right of Fig 2.7a (right)

Figure 2.7: Examples of measured SEP signals [44]

### 2.5.3 Auditory Evoked Potentials

Auditory evoked potentials (AEPs) are the evoked potentials generated in the brain when an auditory stimulus is introduced. They are generated by fluctuations in the electrical potential across neuronal membranes in the auditory system [64].

Similar to the SEPs, AEPs can only be detected and recorded relative to a stimulus, and in this case an auditory stimulus. AEP signals are much smaller than the EEG signals in which they are found, therefore the only way to extract them from the EEG signal is by introducing multiple occurrences of identical stimuli and averaging the response monitored in the EEG signal. The EEG signals will vary widely in a certain time-frame and the AEP will be detected as the constant signal in the same time-frame [64].

To generate usable AEPs, the stimuli introduced is the sound of consistent clicks or tonebursts. The auditory stimulus needs to be delivered at a comfortable, audible level for the patient, and not too loud for patient when awake. To monitor the AEPs on the scalp, the electrodes are placed according to the

International 10-20 system, as depicted in Figure 2.2, and should be placed by $Cz$, or on other points on the same midline as $C_z$ (e.g. $F_z$ or $P_z$), with the same earlobe electrode reference [64].

There are two classifications used in AEPs. The first is the transient AEPs which are generated by the auditory stimulus and wear off before the next stimulus is introduced. The second classification is the steady-state AEPs, which are generated when successive stimuli are delivered before the AEP decays. They then depict sinusoidals with the same frequency as the stimulus introduced. The transient responses can be further classified into the:

- Fast response which occurs around 6 - 10 ms;
- Middle response which occurs around 10 - 50 ms;
- Slow response which occurs around 50 - 250 ms;
- Late response which occurs at times after 250 ms.

A normal AEP signal is depicted in Figure 2.8. The brainstem auditory evoked potential (BAEP) is the fast response. It is commonly resistant to the effects of anesthetics, and is often used to test the reliability of the auditory pathways during neurosurgical procedures. The middle-latency auditory evoked potential (MLAEP) is the middle response commonly used to measure the effects of an anesthetic on a patient. It has been shown that the shape of the MLAEP in normal awake awake patients differs from that of patients in anesthesia [65], [66]. The slow and late evoked potentials are considered to be too sensitive to the effects of anesthesia, and therefore cannot be used [64].

Mantzaridis and Kenny [65] developed a new AEP index, AEPidx, used to evaluate a patient's depth of anesthesia. This AEPidx is a mathematical derivative of the absolute difference between every two successive segments of the AEP waveform. Unfortunately, the details for this index are proprietary knowledge. Fortunately, it has also been found that the latencies of the MLAEP signals can be used to monitor the depth of anesthesia a patient experiences because the latencies of the different peaks and troughs of the signal are delayed the deeper a patient drifts into anesthesia [65], [66]. The $N_b$ trough's latency has been shown to have the strongest correlation to the AEPidx to monitor the depth of anesthesia [65].

## 2.6 Pharmacokinetics and Pharmacodynamics

The patient needs to be closely and carefully monitored during the procedure to prevent any adverse effects that the anesthetics could have on the patient. To

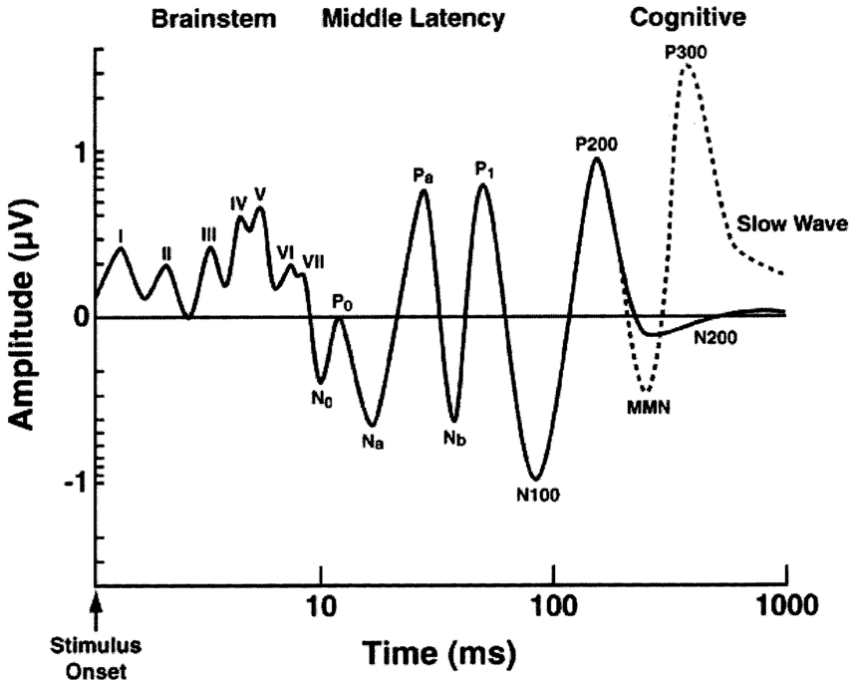


Figure 2.8: An example of a healthy, awake patient's AEP [67]

administer appropriate amount of anesthetic to the patient, we need a thorough understanding of pharmacokinetcs (PK) and pharmacodynamics (PD).

Pharmacokinetics describe the movement of administered drugs within the patient's body. This includes absorption, distribution, metabolism and elimination of the drug. The movement of a drug is highly dependent on patient-specific parameters, which include age, sex, weight, and height, as well as the chemical properties of each drug. Pharmacodynamics describe what the drug does to the body once it has entered the body. This involves receptor binding, post-receptor effects and chemical interactions [68].

### 2.6.1 PK-PD models

There is different pharmacokinetic and pharmacodynamic (PK-PD) theory related to the type of anesthetic drug being administered, and therefore, different PK-PD models are needed for different types of anesthesia.

#### 2.6.1.1 PK model for volatile anesthetics

For inhalation anesthesia, where a gas such as isoflurane is used to induce and maintain anesthesia, the PK model consists of a five-component compartmental model depicted in Figure 2.9 [21]. In this model, the anesthetic is first delivered to the lungs. The anesthetic is then distributed to the various compartments and back via the rate constants $k_{ij}$, where $i$ is the origin

compartment and $j$ is the destination. The rate constants with destination 0 represents the elimination rate constants. The compartments include the vessel rich group (VRG), which includes the brain, heart, liver, kidneys and spinal cord; the muscle group; the fourth compartment, which is the fat around the vessel-rich organs; and the fat group.

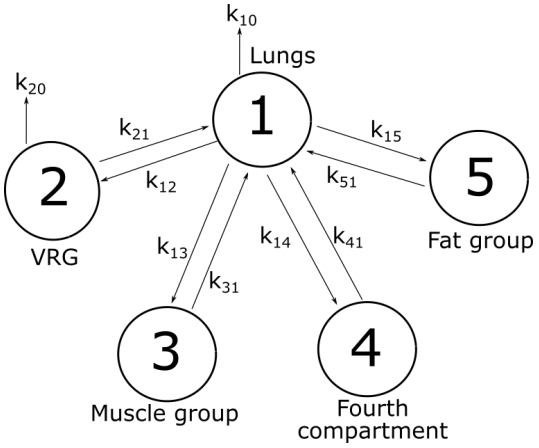


Figure 2.9: 5-compartmental model of the PK of the patient for inhalation anesthesia [21]

#### 2.6.1.2 PK model for intravenous anesthetics

For intravenous anesthesia, where the drug is directly infused into the patient's bloodstream, the three-compartmental mamillary model is commonly considered. Although one- and two- compartmental PK models do exist, their functionality is restricted to a very small number of anesthetic agents [20]. In the three-compartmental PK model, the amount of drug leaving one compartment is the input of the adjacent compartment [20], depicted in Figure 2.10.

The compartment $V_1$ is the primary compartment, which represents the first point of entry of the anesthetic, being the blood; compartment $V_2$ is the fast compartment which represents muscle; and $V_3$ is the slow compartment, which represents fat. The parameters $q_1, q_2$ and $q_3$ represent the drug quantities in each compartment over time and the $k_{ij}$ parameters are rate constants representing the mass flow from the $i$ to the $j$ compartment [68].

Various PK-PD models have been developed and are available for use. These different models have been developed from testing the interaction of the anesthetics to different patients with similar characteristics. From there, different assumptions were made per model and parameters were determined to fit these models. Many of the models were designed based on young, healthy

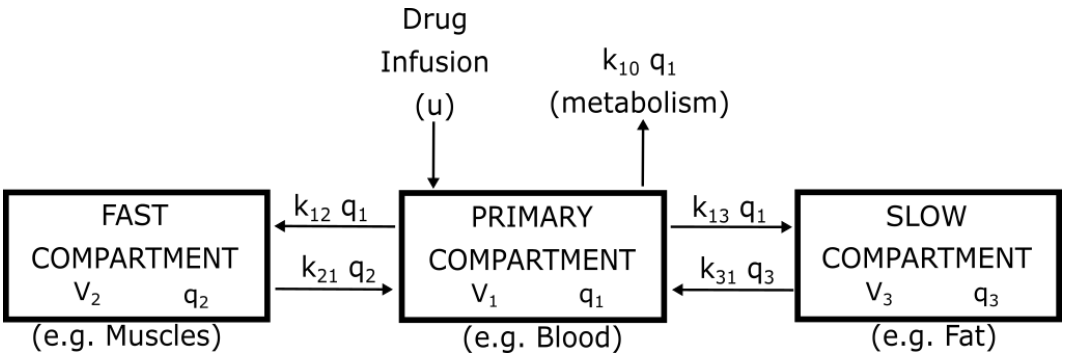


Figure 2.10: 3-compartmental mamillary model of the PK of the patient for intravenous anesthesia

adults and a smaller percentage of models is based on the obese and on paediatrics.

The models used for healthy, young adults undergoing general anesthesia with the drug propofol include the Marsh [22], [69] and Schnider [22], [68] models; and for children, the Paedfusor [23] and Kataria [24] models are used. There is also an overarching Eleveld model [70] which is compatible with a wide variety of patients, but it has not been included in the target-controlled infusion anesthetic pumps because it is relatively new [37].

## 2.7 Conclusion of the anesthesiology literature review

Using the in-depth research conducted regarding anesthesiology and the types and methods available to sedate a patient, the methodology of administering general anesthesia using the intra-ear monitor designed in [10] can be drawn up in subsequent Chapter 4.

# Chapter 3

# Literature Review: Control systems

A control system is a system that governs the behaviour of a defined variable. It controls the variable by either keeping it constant in the face of external disturbances, or it changes the parameter according to a given trajectory [5].

Control systems are commonly used to control complex systems that would be harder to control manually. As functional as control systems are, they need to be meticulously designed and rigorously tested before implementing. In the face of external disturbances, these systems could yield disastrous results. If they encounter unforeseen disturbances, they run the risk of failing and the failure of the controller alone could jeopardize the functionality of the whole system [71].

Examples of control systems in everyday life would include the cruise control of a car and the automated flight control sequences of an aeroplane. The human body can also be seen in terms of a number of control systems that keep the body functioning normally. One of these physiological control systems is heart rate control, controlling how much blood, nutrients and oxygen is supplied to the body and its various organs under various circumstances [71].

There are a number of types of control systems available. They all have unique approaches to the control problem and have varied levels of complexities, but the end goal of each type of control system is to drive the behaviour of the system under control.

## 3.1 Proportional-Integral-Derivative (PID) Control

Proportional-Integral-Derivative (PID) controllers are one of the most used controllers in industry. They have gained popularity because of the simplicity

of their structure, ease of design and relatively low implementation costs [72].

PID controllers are made of three separate controllers that work together to provide control of a system. The three controllers are used to adjust the controller output to be: proportional to that of the error signal, which is the difference between the reference signal and the signal measured from the system; to remove the residual error aggregated from the previous values of the error signal; and to reduce the effect that sharp, sudden signal disturbances will have on the system [73].

PID is widely used in industry because of low implementation cost, but it could be risky to implement for a highly complex system such as the human body. In a medical setting, there is the risk of stability issues if there are disturbances during the procedure as the controller could potentially administer a correcting amount of drug regardless of the effect that this unprecedented infusion would have on the drug concentration in the patient, which could, potentially, be fatal [74].

### 3.1.1 Classic PID control structure

The classic PID control structure is depicted in Figure 3.1. The signal $y$ and $y_{SP}$ are the output and the set-point of the output, respectively. The signal $e$ is the error signal, which is the difference between the output and the set-point and $u_{PID}$ is the control input to the plant from the PID controller.

The three controllers, the P-, I- and D-controllers, each contribute to the performance of the PID controller. The proportional (P) feedback control of the controller is linearly proportional to the error of the controller and the control signal is instantaneously related to the system error [73]. Therefore, the proportional control signal is:

$$u_P(t) = k_P\, e(t) \tag{3.1}$$

The parameter $k_P$ is the proportional gain that amplifies the error signal.

The integral (I) feedback control signal is linearly proportional to the integral of the system error. This is used to decrease the steady-state error of the error signal from the set-point [73]. Its control signal is in the form:

$$u_I(t) = k_I \int_{t_0}^{t} e(\tau) d\tau \tag{3.2}$$

The parameter $k_I$ is the integral gain. The integral translates to a summation of all the previous values of the error signal.

The derivative (D) feedback control signal is used to decrease the overshoot of the signal and improve the closed-loop stability of the system. This is

achieved by having the derivative gain term $k_D$ proportional to the rate of change of the system error [73]. The control signal is thus:

$$u_D(t) = k_D\,\dot{e}(t) \tag{3.3}$$

Therefore, the plant input $u_{PID}$ in Figure 3.1 is:

$$u_{PID} = k_P\,e(t) + k_I \int_{t_0}^{t} e(\tau)d\tau + k_D\,\dot{e}(t) \tag{3.4}$$

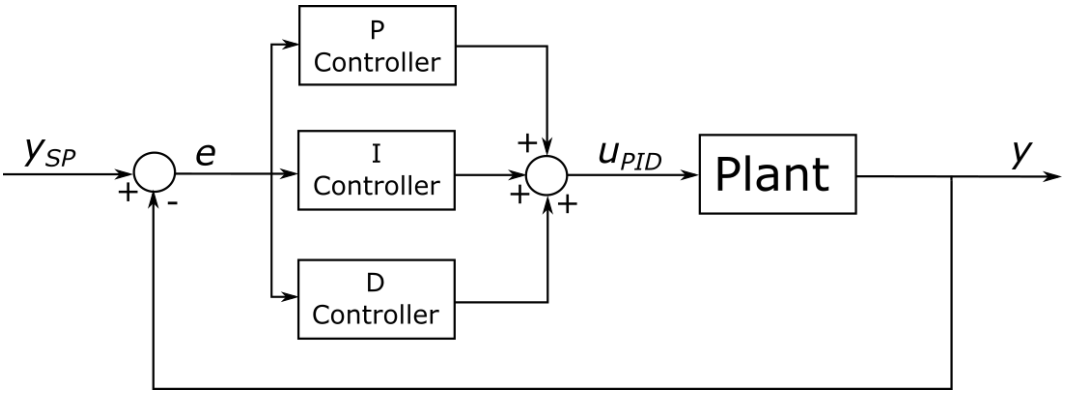


Figure 3.1: The basic PID control structure

Selecting PID parameters appropriately for the system has been researched widely. There are a couple of tuning methods that stand out.

#### 3.1.1.1 "Ziegler-Nichols" tuning method

Ziegler and Nichols developed their popular "Ziegler-Nichols" tuning method and published their work in two papers [75], [76]. Basically, their tuning method involves calculating controller parameters based on testing the plant in an open-loop and then testing the plant in a closed-loop [73], [77].

#### 3.1.1.2 Predictive PID

Predictive PID is another tuning method available for the PID controller. The control structure includes the prediction of the output of the plant and the controller then recalculates the control action to be undertaken by using the data of the future set-point [78].

The algorithm for predictive PID involves reformulating the generalized predictive controller with steady-state weighting into a model-based PID control structure [79].

#### 3.1.1.3 Integral Performance Criteria

Integral performance criteria are also used when designing PID controllers, for selecting parameters that give the desired response [80], [81]. All performance criteria are dependent on the error signal and in a general sense, the lower the value of the performance criteria, the more stable the system is.

The Integral Squared Time Error (ISTE), in (3.5), highlights the larger errors and emphasizes consistent errors [82]. Lastly, there is also the IST$^2$E, which is the Integral of the Squared Time-squared weighted Error and the IST$^3$E which is the Integral of the Squared Time-cubed weighted Error [80].

$$ISTE = \int_0^t t(e(t)^2)\,dt \tag{3.5}$$

$$IST^2E = \int_0^t t^2(e(t)^2)\,dt \tag{3.6}$$

$$IST^3E = \int_0^t t^3(e(t)^2)\,dt \tag{3.7}$$

The paper [80] gives the tuning rules which highlight the integral performance criteria values required for tuning the PID controller.

### 3.1.2 Fuzzy PID

The classic PID structure does have the drawback of being insufficient to control more complex systems, such as those containing time delays, significant oscillations, as well as systems containing non-linearities or multi-input multi-output systems (MIMO) plants [83], [84]. To make provision for these problems, investigations have been undertaken to combine fuzzy logic control technology with the classic PID controller for better performance.

Fuzzy logic is closely linked to human thinking and natural language processing of information. In control terms, fuzzy logic control is a control algorithm that can set linguistic control strategies, like *if-then* rules, into an automatic control strategy [85].

The fuzzy logic controller is essentially made of three components as depicted in Figure 3.2 [72]. The *Fuzzification* interface involves measuring the input and converting the data into fuzzy set activation levels to provide input to the Fuzzy Inference Mechanism. The *Fuzzy Inference Mechanism* is made of the "data base" and "linguistic control rule base" which classify the incoming data values according to the defined rule base. From here, the system's "decision making" logic decides on the fuzzy control action that will take place. Lastly, the *Defuzzification* interface takes the fuzzy control action and transcribes it into non-fuzzy control action [85].

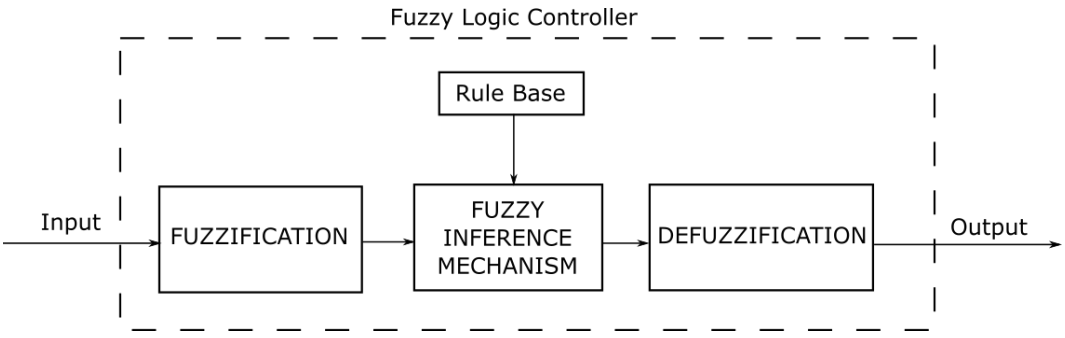


Figure 3.2: Components of a fuzzy logic controller [85]

## 3.2 Model Predictive Control (MPC)

Model predictive controllers are advanced control systems which solve on-line optimization problems to minimize output error and control effort, subject to the constraints and dynamics of system states and controls. A unique feature is that they make use of a model of the system within the controller to optimize the control actions taken.

The changes in the manipulated variable are carefully selected based on the prediction of system outputs. The system predicts several future actions to be taken on the manipulated variable over the "prediction horizon", but only the first computed change is implemented. After the implementation, the model output is computed and the model parameters are updated. Then, the possible future actions are predicted again over the same length of the prediction horizon.

### 3.2.1 Principles of Model Predictive Control

The operation principle of an MPC controller is depicted in Figure 3.3. The MPC controller predicts the future behaviour and dynamics of the system over a defined prediction horizon and, over the period which the MPC computes control actions, called the control horizon, it determines the inputs to be delivered to the system to optimize the open-loop performance objective function [86].

The first computed control action is executed during an interval of $\delta$ from time $t$, and the controller has to recalculate the control actions, prediction and optimization, from $t+\delta$. This process is repeated for every $\delta$ sample time-units [86].

Another advantage of using the MPC controller is the simplicity of including constraints in the controller. Most systems handle constraints by implementing overrides, logic-based saturation or through split range controllers. Such constraint implementations are difficult to design, modify and maintain.

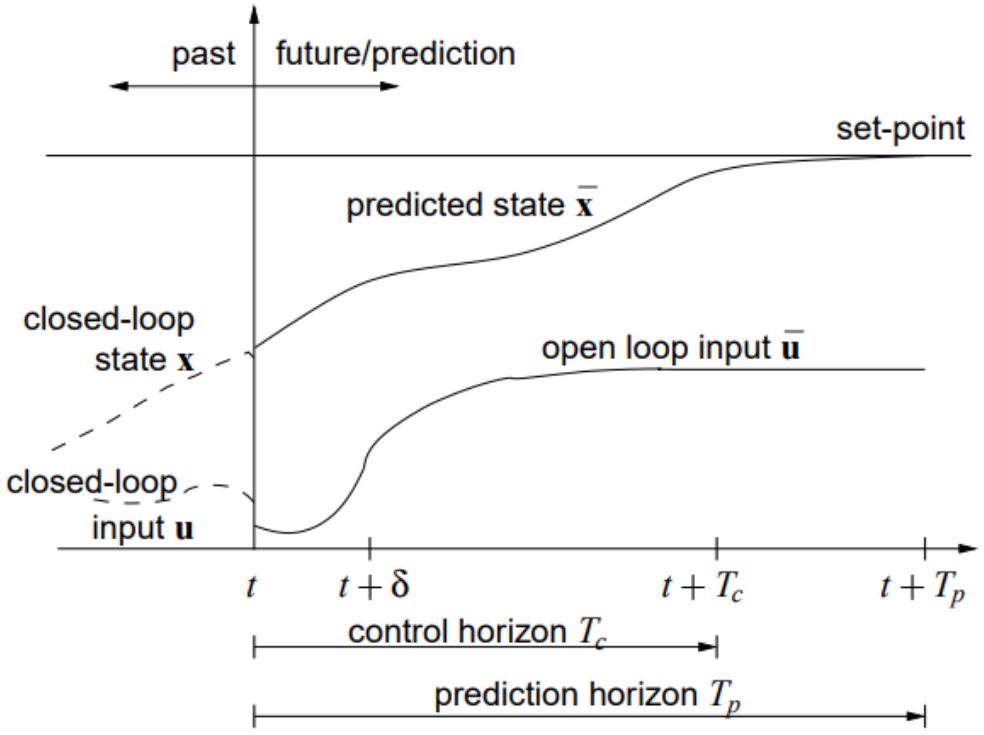


Figure 3.3: The basic operating principle of the MPC

In an MPC controller, the system constraints can be included directly into the controller and the controlling algorithm is able to find optimal solutions that operate within those working constraints [87].

### 3.2.2 MPC model structure

The model structure of an MPC controller is depicted in Figure 3.4. The plant model is a state-space or a transfer function description of the system. The plant model has its manipulated variables, $u(k)$, and the optional inclusion of measured disturbances $v(k)$, as inputs. The outputs include the measured outputs $y(k)$ and the optionally included unmeasured outputs $y_u(k)$. The disturbance models, $d(k)$ for the input disturbance model and $y_{od}(k)$ for the output disturbance model, can be included optionally [88].

The measurement noise differs from the unmeasured input and output disturbances, as measurement noise specifies the expected noise model for the measured data, and can be implemented without the unmeasured output disturbance or the unmeasured input disturbance.

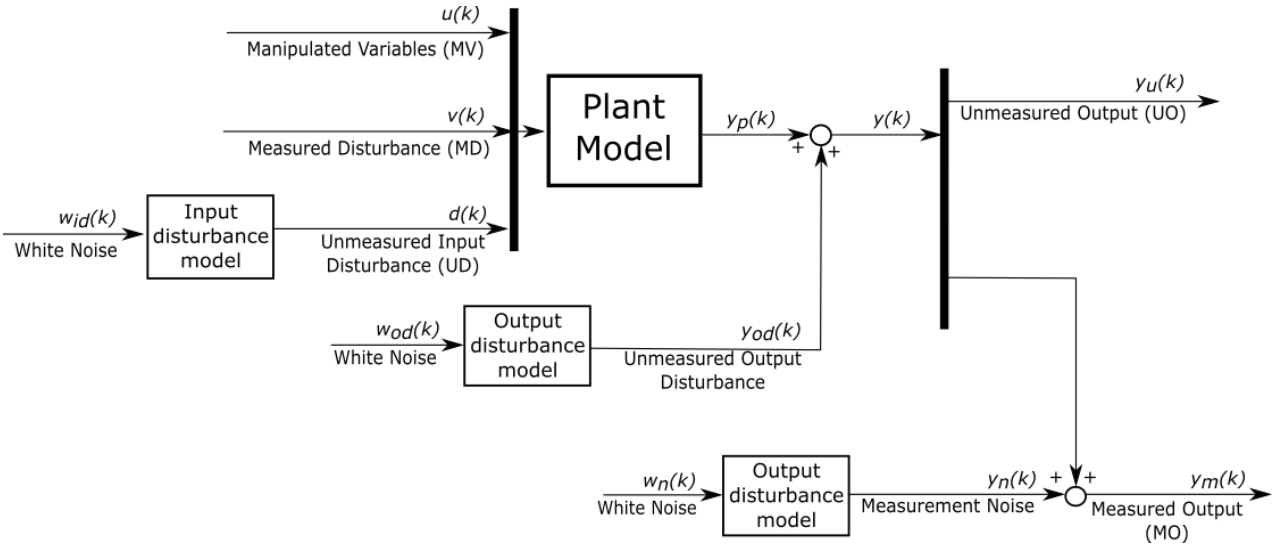


Figure 3.4: The model structure of MPC [88]

### 3.2.3 Linear MPC

Linear MPC is defined as an MPC controller incorporating a linear model of the system under control. These linear models are commonly described as state-space models, but they could also be represented as transfer functions, also known as input-output models. Models in state-space form are represented in the form:

$$x(k) = A\,x(k-1) + B\,u(k-1) \qquad y(k) = C\,x(k)$$

where $x$ is the vector of states, $u$ is the vector of inputs, and $y$ is the vector of outputs. The parameter $k$ is the discrete-time sample number. The matrices $A, B$ and $C$ are the system matrices for the state-space model [87].

State-space descriptions are favourable because of the simple depiction of multi-variable systems, easy analysis of closed-loop properties and simple implementation of on-line computation [89] Additionally, the use of the state-space representation of models has opened the door for linear systems theory, which includes linear quadratic regulator theory [90], Kalman filtering theory [91] and internal model principles [87].

Linear models are the favoured models to use for MPC controllers as they can be solved quickly and the optimization problem can be represented as a linear or quadratic problem.

### 3.2.4 Non-linear MPC

In many systems, non-linearities are introduced because of the desire to have models that closely resemble the dynamics of the system in the real world.

These non-linearities are commonly introduced by incorporating the fundamentals of a system, like the conservation of mass, momentum and energy in physical systems, or the relationships of chemical kinetics in chemical processes [89].

MPC controllers that use non-linear models are well suited for systems which have process conditions that vary significantly over the course of operation. Despite the complexities of such systems, the use of non-linear MPC has actually been promoted by the availability of increasing computing power [89]. For systems with highly non-linear models, some of the following techniques are used to achieve sufficient control.

#### 3.2.4.1 Adaptive MPC

The first method available is the use of adaptive MPC. As a non-linear system controlled by an MPC runs, the prediction accuracy can degrade over time and the MPC's performance can quickly become obsolete. Adaptive MPC can adapt the prediction model for various operating conditions. The adaptive MPC controller does this by dividing the model into various linear models at different operating points. These linear models then have linear constraints and solve a linear cost function. Therefore, at the beginning of each control interval, the adaptive MPC controller calculates the prediction using model parameters appropriate for the current running conditions [92].

#### 3.2.4.2 Gain-scheduled MPC

This method differs from the adaptive MPC because instead of having different model parameters for various operating conditions, the gain-scheduled MPC switches between various MPC controllers which operate in different operating conditions of the non-linear model. The various MPC controllers will then have linear constraints and solve a linear cost function. This method could be more memory intensive as multiple MPC controllers need to be saved in the system's memory for switching, but the computational power of using this method can be reduced by preventing the inactive controllers from computing predictions during operation [93].

#### 3.2.4.3 Non-linear MPC

If the non-linear plant model cannot be simplified by various operating points with linear constraints and cost functions, then non-linear MPC would need to be used. Computationally, this is the most demanding method as the optimization function becomes non-convex and finding the global optimum becomes complex. This method uses the most accurate representation of the plant and the predictions made by the controller more accurate than the those determined by the other methods [94].

## 3.3 Control system performance evaluation

An important aspect of control system design also lies in the evaluation of the performance of the control system during and after the design. This can help the control engineer determine that the design meets the design specifications set and that the designed system is ready to be implemented.

In the context of automated control of anesthesia, the control objectives are described as: controlling the average value of the manipulated variable to remain within a given limit, minimizing controller oscillation within the given limits, and guaranteeing stability in the controller performance by either reducing the oscillations a controller experiences or keeping the oscillations within the defined performance limits [95], [96].

A suitable set of performance evaluation criteria is given below.

### 3.3.1 Time-domain specifications

An important part of control system design involves considering the time response of the system. The performance specifications of a control system involve certain requirements that the system needs to adhere to when a step input is introduced to the system.

A typical step response of a control system is depicted in Figure 3.5. The parameter $t_r$ is the rise time, which specifies the time between 10% and 90% of the final value. The settling time $t_s$ defines the time taken for the system's step response oscillations to decay. It is often defined as the time taken for the system's oscillations to reach the range of 5%, 2% or 1% of the final value. [73].

The parameters $t_p$ and $M_p$ are the peak time and overshoot, respectively. The peak time defines the time taken for a step response to reach its maximum value, and the overshoot defines the maximum amount that a system response overshoots its final value, and this is often stated as a percentage [73]. Depending on the application of the controller, the a certain amount of overshoot could be allowed, which then defines the system as an underdamped system. Otherwise, if no overshoot is allowed for the application, the system is then defined as an overdamped system and the system's step response will rise smoothly to the final value with no oscillations.

### 3.3.2 Integral Performance Criteria

Integral performance criteria [98], [99] can also be used to evaluate the performance of a control system. All performance criteria are dependent on the error signal, which is the difference between the reference signal and the system output.

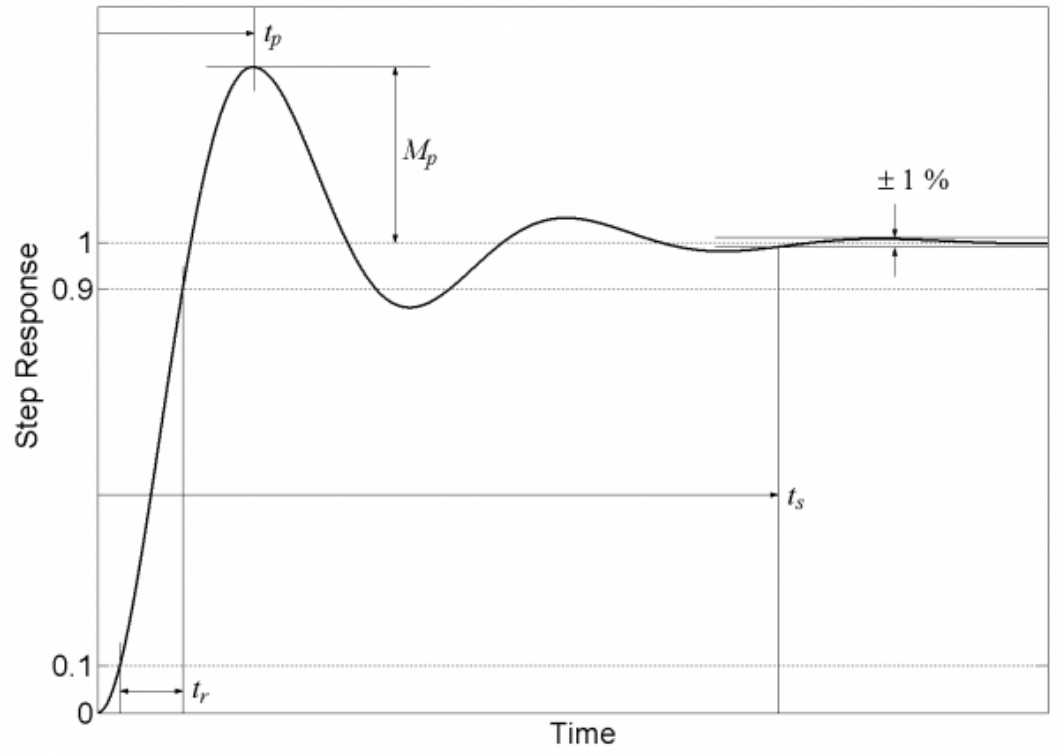


Figure 3.5: A typical step response of a control system [97]

The integral performance criteria used include the Integral Absolute Error (IAE), with its equation in (3.8). It determines the integral of the error signal over the entire simulation and all errors hold the same weight. There are other performance criteria. These include the Integral Squared Error (ISE), in (3.9), squares the error signal and then determines the integral. This highlights larger errors more than the rest of the errors in the system. The Integral Time-weighted Absolute Error (ITAE), in (3.10), highlights recurring errors in the error signal.

$$IAE = \int_0^t |e(t)|\, dt \tag{3.8}$$

$$ISE = \int_0^t e(t)^2\, dt \tag{3.9}$$

$$ITAE = \int_0^t t|e(t)|\, dt \tag{3.10}$$

### 3.3.3 Performance error-based evaluation parameters

According to [96], [100], [101], the performance of a closed-loop control system used for muscle relaxants can be evaluated using performance error(PE)-based evaluation parameters. These include the median performance error (MDPE), median absolute performance error (MDAPE), and wobble.

The performance error (PE) of a given period is calculated as:

$$PE = \frac{\text{Measured value} - \text{Reference value}}{\text{Reference value}} \cdot 100 \tag{3.11}$$

The MDPE is a measure of the bias of the controller performance. It describes if the measured values are symmetrically above or below the reference value, with a positive MDPE or a negative MDPE, respectively. It is determined as:

$$MDPE_i = Median\{PE_{ij}, j = 1, ..., N_i\} \tag{3.12}$$

where $N_i$ is the number of PE values obtained for the subject $i$.

The MDAPE is a measure of the amplitude of possible bias and errors from the reference value the controller experiences. It is determined as:

$$MDAPE_i = Median\{|PE_{ij}|, j = 1, ..., N_i\} \tag{3.13}$$

with $N_i$ as the number of PE values obtained for the subject $i$.

Wobble represents the oscillations of the controller and it measures the intrasubject variability in the measured values. It is determined as:

$$Wobble_i = Median\{|PE_{ij} - MDPE_i|, j = 1, ..., N_i\} \tag{3.14}$$

## 3.4 Conclusion of the control systems literature review

Using the research conducted regarding control system and various types available, the design of a closed-loop control system administering general anesthesia can be undertaken in Chapter 4. The MPC controller will be used as it provides the benefit of incorporating the patient model into the controller for optimized control actions.

# Chapter 4

# Methodology

## 4.1 Introduction

This study will focus on designing a closed-loop controller interfacing intra-ear monitoring with general anesthesia.

In order to achieve this aim as well as to answer the research questions, the design and implementation of such a system needs to be thought through and analysed. Considering the information listed in the literature review and applying the relevant information, a practical design of a closed-loop control system can be achieved.

## 4.2 System design

The system will be designed is to read the current depth of anesthesia experienced by the patient, then deliver the desired amount of propofol intravenously to a patient during general anesthesia. It is recommended that such a system should be designed for application during the maintenance phase of anesthesia [3]. Automating the induction phase could be feasible, but it is more intricate and involved because the anesthesiologist is required to sedate the patient and monitor that the patient does not show any signs of awareness through movement, increased breathing rate or increased heart rate.

The signals monitoring the patient's depth of anesthesia will be read into a control system that will compare the current depth to the desired set-point. If the depth of anesthesia experienced is lower than the specified set-point, the system will administer anesthetic to deepen the anesthesia. If the depth of anesthesia experienced is greater than the set-point, the system will pause the infusion so the patient can metabolize some of the anesthetic that is already in his/her system, lightening the depth of anesthesia experienced and this will slowly return the patient back to the desired level of anesthesia.

As this process will be continuous throughout the maintenance phase, it will be implemented as a closed-loop control system. The system architecture is depicted in Figure 4.1.

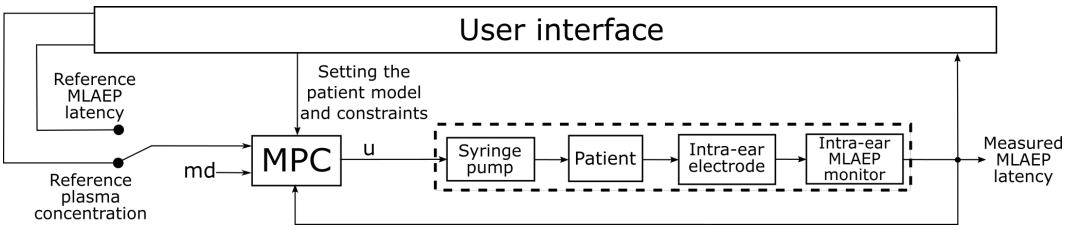


Figure 4.1: Block diagram of the system architecture

### 4.2.1 Reference

The reference signal is the set-point governing the desired depth of anesthesia the system will be targeting. For the system, the reference can be selected as either the desired latency of the $N_b$ trough in the MLAEP, which will be read from the intra-ear monitor [10], or the anesthetic plasma concentration, required to keep the patient sedated.

### 4.2.2 MPC Controller

It will be advantageous to incorporate some information about the patient into the system so the infusion algorithm of the controller is able to base its calculations on the patient's parameters. Therefore, a Model Predictive Controller (MPC) is used with a model of the patient incorporated into the controller.

Linear MPC will be used for the closed-loop control of anesthesia because of the linearized patient model described by the PK-PD model. The controller will determine how much anesthetic needs to be infused into the patient during the maintenance phase based on measurements of the patient's current depth of anesthesia and the reference signal.

The output of the MPC is $u$ and this will be the signal to drive the anesthetic infusion pump administering anesthetic to the patient. The measured disturbance, $md$, is the amount of disturbance that the system would need to account for.

### 4.2.3 Plant

The plant is depicted by the dashed lines in Figure 4.1. The plant includes the anesthetic infusion pump, the patient, the intra-ear electrode reading the EEG

signals from the patient and the intra-ear monitor extracting the MLAEP from the EEG signals to determine the $N_b$ latency.

### 4.2.4 $N_b$ latency output

The intra-ear monitoring system will be monitoring the latency of the $N_b$ trough throughout the procedure, and that will be the measured output fed back into the system to close the loop.

### 4.2.5 User interface

For a practical system implementation, a user interface will be necessary to allow an anesthesiologist to control the operation of the closed-loop control system. It will be used to input patient data for the PK-PD model used in the MPC controller as well as to set the reference plasma concentration or latency. It will also be used to monitor the measured latency and plasma concentration from the patient to alert the anesthesiologist of the level of anesthesia currently experienced by the patient.

## 4.3 Simulation

The system will be simulated using a Simulink model which is available in MATLAB. MATLAB is a programming language predominantly used for numeric and other algebraic computations. It comes with its own Integrated Development Environment (IDE) and a vast number of libraries, apps and built-in functions [102], [103]. One of these includes the simulation software Simulink.

Simulink is a MATLAB add-on that allows for graphical simulation, modeling and analysis of dynamic systems. It allows for the graphical user interface (GUI)-based construction of block diagrams to design and model various systems using a wide variety of pre-defined and custom block libraries. Simulink also aids in a system-level approach to design, automatic code generation, testing and verification of designed systems [104].

In Figure 4.2, the Simulink model used to simulate the closed-loop control system is depicted. The elements within the model are described below.

### 4.3.1 Reference

The Simulink model allows for two types of reference signals to be used: a reference latency or a reference plasma concentration. Either of these two references can be selected by connecting the switch to the desired reference.

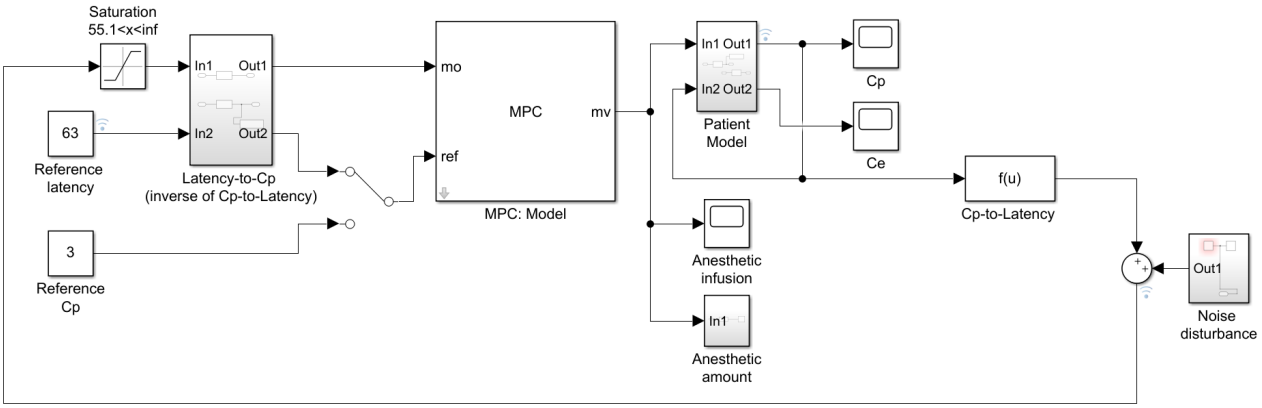


Figure 4.2: Block diagram of the system structure in Simulink

The reference plasma concentration, in $\mu g.ml^{-1}$, drives the system to infuse propofol to reach the specified plasma concentration in the patient.

The reference latency is derived from the desired plasma concentration, $C_p$, required during the maintenance phase. According to [37], the recommended $C_p$ concentration for the maintenance phase is 3 $\mu$g.ml$^{-1}$. From the dose-response model (4.3), the corresponding latency is 63.0267 ms.

### 4.3.2 Patient model

The patient model consists of the blocks depicted in Figure 4.3. The model consists of the state-space model of the Paedfusor PK model and the transfer function of the patient's PD model. The PK model is used to determine the plasma concentration which is then used to determine the latency of the patient's $N_b$ trough at that specific time. The PD model is used to determine the concentration of the anesthetic in the patient's brain, called the effect-site, at a specific time.

The patient's PK model is a state-space representation the patient. The state-space model has infusion rate as the input $u$, the plasma concentration as the output $C_p$ and three states $q_1, q_2$, and $q_3$, which represent the drug mass in each compartment of the 3-compartmental model, as mentioned in Section 2.6. The full state-space representation of the PK model is:

$$\begin{bmatrix} \dot{q}_1(t) \\ \dot{q}_2(t) \\ \dot{q}_3(t) \end{bmatrix} = \begin{bmatrix} -(k_{10} + k_{12} + k_{13}) & k_{21} & k_{31} \\ k_{12} & -k_{21} & 0 \\ k_{13} & 0 & -k_{31} \end{bmatrix} \begin{bmatrix} q_1(t) \\ q_2(t) \\ q_3(t) \end{bmatrix} + \begin{bmatrix} 1 \\ 0 \\ 0 \end{bmatrix} u \tag{4.1}$$

$$C_p = \begin{bmatrix} 1 & 0 & 0 \end{bmatrix} \begin{bmatrix} q_1(t) \\ q_2(t) \\ q_3(t) \end{bmatrix} + 0 \cdot u \tag{4.2}$$

The output of the PK is the input of the PD model. Both their outputs are similar, however they have a time delay difference. The effect of the effect-site concentration, $C_e$ on the 3-compartmental PK model is small and insignificant, thus it can be assumed that the effect-site will have a similar end concentration as $C_p$, but the concentration will only be reached later than that of $C_p$, at the rate $k_{e0}$ [22]. The equation for the PD model is:

$$C_e = \frac{k_{e0}}{s + k_{e0}} C_p$$

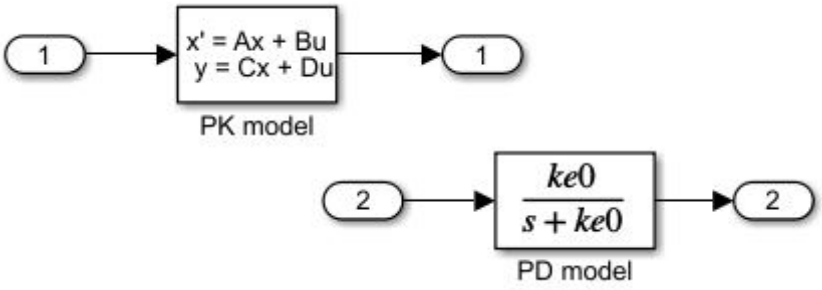


Figure 4.3: Diagram of the PK-PD in the *Patient Model* block

### 4.3.3 MPC

Simulink provides the MPC Designer software, to assist in the development of MPC controllers, and to allow a number of controller parameters to be defined.

The internal model used in the MPC design is the state-space Paedfusor PK model of the average patient in [66]: an 8.6 year old patient who weighs 29.2 kg. The patient's state-space model used is similar to that shown in (4.3.2) and (4.2).

The parameters of the MPC are listed in Table 4.1. The sample time ($T_s$) selected for the MPC block was determined from [37], where the intravenous propofol maintenance infusion is administered every 10 seconds. As recommended by [105], the prediction horizon is chosen as a value computing an adequate amount of future predictions, saving computing resources. The control horizon is chosen as 10% of the prediction horizon. The manipulated variable upper and lower limit were set based on the guidelines in [106], where the lowest infusion rate possible is 0 $mg.min^{-1}$ and the highest is 250 $mg.kg^{-1}.min^{-1}$.

Adjusting the robustness of the controller block can be achieved by using the Control-Loop Performance slider in the MPC Designer, shown in Appendix C. The robustness of the system is adjusted to reduce the step response's overshoot and to shorten the settling time. By adjusting the slider, the manipulated variable rate weight and the output variable weight are adjusted.

Table 4.1: MPC parameters

| Parameter | Value |
|---|---|
| Sample time ($T_s$) | 10 s |
| Prediction horizon | 20 |
| Control horizon | 2 |
| **Constraints** | |
| MV minimum constraint | 0 mg.min$^{-1}$ |
| MV maximum constraint | 7.3 mg.min$^{-1}$ |
| **Weights** | |
| MV | 0 |
| MV Rate | 0.1457 |
| OV | 0.4116 |

MV: Manipulated Variable
OV: Output Variable

In the practical system, the output of the MPC is the signal which drives the infusion pump administering anesthetic to the patient. For the simulated system, the infusion pump is considered as a simple pass-through block between the MPC and the patient model.

### 4.3.4 MLAEP latency and plasma concentration correlations

To date, there has been limited research conducted toward the use of the MLAEP latency to control closed-loop anesthesia. Many studies that do have MLAEP in anesthesia only study the influence that anesthesia has on MLAEP and not necessarily the correlation of the amount of anesthetic administered to the patient and the change in MLAEP and their latencies [65], [66], [107]–[109]. Additionally, there is little to no literature that uses the MLAEP latency as a control variable in a closed-loop control system.

With the $N_b$ trough latency as the measurement signal from the patient, the trough can be correlated to the plasma concentration in the patient with help from the results in [66]. This paper uses the MLAEP measured from paediatric anesthesia to draw up correlations between the various MLAEP peaks and troughs, and the propofol plasma concentration $C_p$. These latencies measured include the $P_a$, $N_a$, $N_b$ and $P_1$ peaks and troughs, as mentioned in Section 2.5.3.

It is important to note that the study in reference [66] was conducted on children. Children and healthy adults have different PK models and character-

istics and this could pose a problem when attempting to use the same data to relate $C_p$ to MLAEP latencies in healthy adults. Kuhnle [66] does cite similar studies conducted on adults, but unfortunately the results from those papers [110], [111] do not correlate the $C_p$ to MLAEP latencies, as needed here.

The issue with reference [110] is that the measurements are taken at various stages in the induction and maintenance of anesthesia, and there is inter-patient variability when it comes to the time at which these various stages of anesthesia are reached. In reference [111], propofol is not used and different anesthetic drugs will have different PK characteristics. Therefore, there is no proper data available to generate the relation between $C_p$ and MLAEP latency for healthy adults. For these reasons, the system was designed using paediatric patients.

#### 4.3.4.1 $C_p$-to-latency

Data from Kuhnle [66] are used to define logistic functions, to establish a relation between $C_p$ and MLAEP latency

Unfortunately, the details of the lines of best fit from Kuhnle [66] have not been disclosed, therefore the logistic functions needed to be estimated. From the line of best fit from the $C_{plasma}$ vs Peak $N_b$ graph in Kuhnle [66], a couple of assumptions needed to be made. The value of the latency at 0 $\mu g.ml^{-1}$ is assumed to be 55 ms and the upper limit of the logistic equation is assumed to be 99 ms. One more assumption made is that the plasma concentration at 63 ms is 3 $\mu g.ml^{-1}$.

Using these assumptions, the logistic function can be estimated by using a basic sigmoid function with two parameters commonly used for subitizing calculations [112]. The function is estimated using the form:

$$f(x) = \frac{L}{1 + e^{-k(x-x_0)}} + c$$

with $L$ as the height of the sigmoid function, $k$ as the slope of the sigmoid function, $x_0$ as the $x-$value of the mid-point and $c$ as the $f(x)$-intercept, or the latency when the plasma concentration is 0. The sigmoid function used in the $C_p$-to-latency of Figure 4.2 is therefore:

$$f(x) = \frac{44}{1 + e^{-1.5(x-4)}} + 55 \tag{4.3}$$

Lastly, the simulated system considers the intra-ear electrode and monitor as a simple pass-through block between the the patient model and the *$C_p$-to-latency* block.

#### 4.3.4.2 Latency-to-$C_p$

The logistic function (4.3) is used to convert the plasma concentration to latency. For the reference, the inverse of the function is used, to convert the reference latency to the reference plasma concentration needed by the MPC. This inverse function, computed from (4.3), is therefore:

$$\begin{aligned} x(f) &= \frac{-log(\frac{L}{f-c} - 1) + k\,x_0}{k} \\ &= \frac{-log(\frac{44}{f-55} - 1) + 6}{1.5} \end{aligned} \tag{4.4}$$

With these correlations of the MLAEP latencies and $C_p$, we can convert the latencies acquired during anesthesia, to the corresponding $C_p$.

The contents of the *Latency-to-Cp* block are depicted in Figure 4.4. Both $f(u)$ blocks contain the equation (4.4). The top block converts the measurement latency to a measurement $C_p$ and the bottom block converts the reference latency to the reference $C_p$.

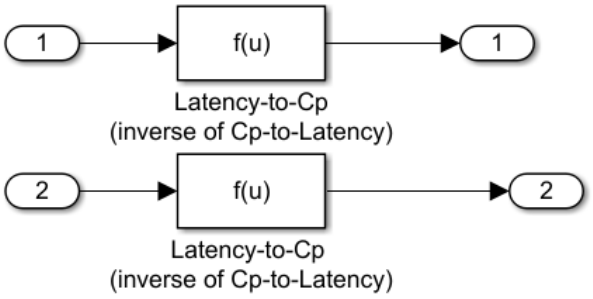


Figure 4.4: The contents of the block *Latency-to-Cp (Inverse of Cp-to-Latency)* in Figure 4.2

### 4.3.5 Anesthetic amount

The block *Anesthetic amount* is used to calculate the amount of simulated anesthetic administered to the patient during the simulation. The contents of the block is depicted in Figure 4.5.

The manipulated variable, which is the output of the MPC, is the anesthetic infusion rate in $mg.min^{-1}$. The block *Anesthetic amount* takes this output and firstly, divides the infusion rate by 60 to determine the infusion rate in $mg.sec^{-1}$. The block then integrates that value to get the quantity of anesthetic administered to the patient.


Figure 4.5: The contents of the block *Anesthetic amount*

In a practical system, this block could be used to interface the MPC output and the infusion pump and it would drive the infusion of the anesthetic pump.

### 4.3.6 Noise disturbance

It is likely that such a system would encounter some measurement noise. To account for it, a noise disturbance block was added to the main Simulink model. The noise disturbance block contains a band-limited white noise generator.

Adding the noise disturbance directly to the measured latency of the Simulink model causes a major problem for the control loop. The latency in (4.4), $f$ in this case, cannot be 55 ms or smaller for two reasons: a latency of 55 ms would cause the fraction to become undefined because $c$, being the $f(x)$-intercept of (4.3), is 55 and any value smaller than 55 ms would cause force the equation to take the logarithm of a negative number, which would also be undefined. To account for this, a saturation block has been added to the input of the *Cp-to-Latency* block. To prevent (4.4) from becoming undefined, the block's lower limit has been set as 55.1 ms, which represents a plasma concentration of 0 $\mu g.ml^{-1}$.

For the design of the system, the band-limited white noise generator will remain inactive.

### 4.3.7 System step response

The aim of the design is to control the delivery of an anesthetic to a patient for the maintenance phase of anesthesia. The system would need to keep the patient's plasma concentration at a desired level and that level must be reached as fast as possible without any overshoot in the step response.

Using the information stated above, the step-response of the average patient can be generated. Figure 4.6a depicts the latency step-response of the patient and Figure 4.6b shows the corresponding plasma concentration step-response. As depicted, the system's step response satisfies the requirements stated above.

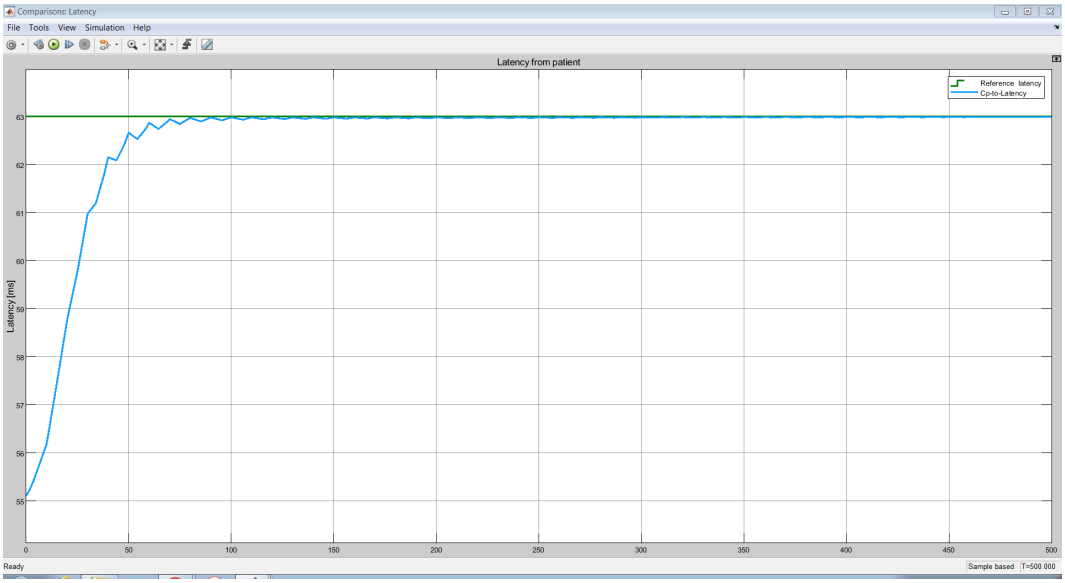


(a) Step response of the $N_b$ trough latency

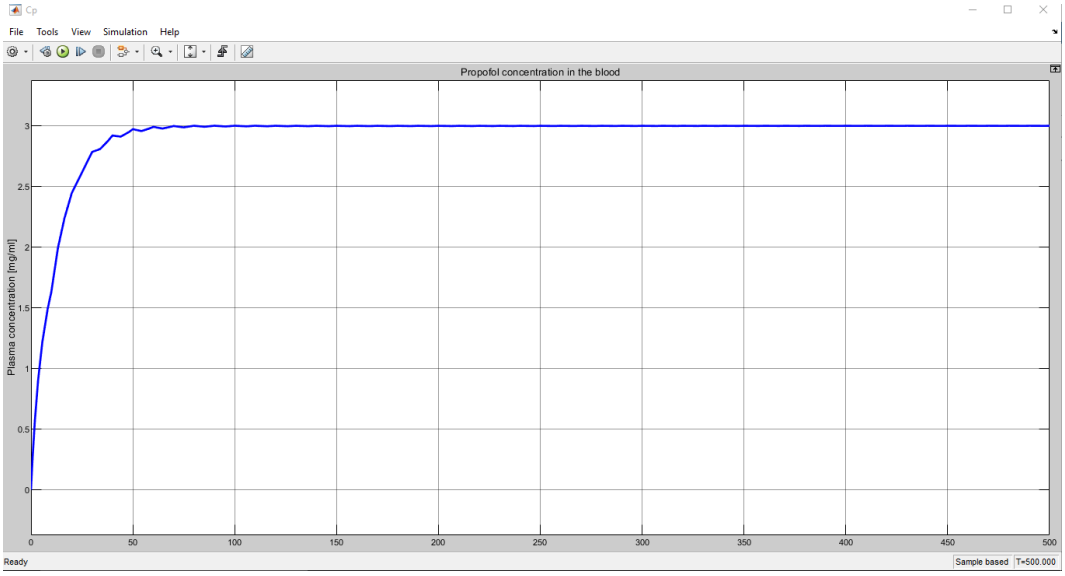


(b) Step response of the plasma concentration

Figure 4.6: Step response of the system on the average patient

# Chapter 5

# Comparing the MPC and PID controller

In this section, the MPC closed-loop controller, described in Section 4.3, is compared to a closed-loop controller using a PID control block. The practicality of using either control block is analysed in this section. The patient population that was used in the simulations was based on the patient population from [66] and the table of the patient population with all the corresponding Paedfusor PK-model parameters is listed in Table 5.1. The control loops were designed to reach the reference value as quickly as possible while not overshooting the reference value.

## 5.1 MPC

Figure 5.1 shows the performance of the MPC block over the patient population. The MPC controller design is based on the average patient in the patient population and the results of the design are depicted in Figure 5.1 and Figure 5.2 labelled as "Latency: Design standard" and "Cp: Design standard", respectively.

As seen from Figure 5.1, the step responses of the patients vary according to the patient's age. Patients that are younger than the average patient of 8.6 years overshoot the reference latency of 63 ms, and as expected, they overshoot the reference plasma concentration of 3 $\mu g.ml^{-1}$. This shows that the design criteria needs to be adjusted to accommodate inter-patient variability.

Patients that are younger than the average patient tend to overshoot the reference value because younger patients' pharmacokinetics are more aggressive than those of older patients. This is because of the smaller volumes used in younger patients' compartmental models in conjunction with the same rate transfer constants used for all the patients in the Paedfusor PK model. The system can be adjusted to accommodate the younger patients by setting the controller to be more robust. This would increase the settling time of the

Table 5.1: Patient population from [66]

| | Age | Height | Weight | V1 | V2 | V3 | k10 | k12 | k21 | k13 | k31 | ke0 |
|---|---|---|---|---|---|---|---|---|---|---|---|---|
| Average patient | 8.6 | | 29.2 | 13.385 | 27.744 | 169.953 | 0.0555 | 0.1140 | 0.04190 | 0.0550 | 0.00330 | 0.26 |
| Patient 1 | 2 | 95.494 | 12.322 | 5.649 | 11.708 | 71.720 | 0.072 | 0.11400 | 0.05500 | 0.04190 | 0.00330 | 0.26 |
| Patient 2 | 3 | 107.595 | 14.120 | 6.472 | 13.415 | 82.180 | 0.069 | 0.11400 | 0.05500 | 0.04190 | 0.00330 | 0.26 |
| Patient 3 | 5 | 107.701 | 15.300 | 7.013 | 14.537 | 89.049 | 0.067 | 0.11400 | 0.05500 | 0.04190 | 0.00330 | 0.26 |
| Patient 4 | 6 | 113.799 | 22.621 | 10.370 | 21.493 | 131.663 | 0.060 | 0.11400 | 0.05500 | 0.04190 | 0.00330 | 0.26 |
| Patient 5 | 8 | 115.397 | 24.480 | 11.222 | 23.259 | 142.480 | 0.059 | 0.11400 | 0.05500 | 0.04190 | 0.00330 | 0.26 |
| Patient 6 | 8 | 118.008 | 25.542 | 11.708 | 24.268 | 148.661 | 0.058 | 0.11400 | 0.05500 | 0.04190 | 0.00330 | 0.26 |
| Patient 7 | 8 | 130.315 | 26.427 | 12.114 | 25.110 | 153.815 | 0.057 | 0.11400 | 0.05500 | 0.04190 | 0.00330 | 0.26 |
| Patient 8 | 9 | 137.322 | 29.780 | 13.651 | 28.295 | 173.329 | 0.055 | 0.11400 | 0.05500 | 0.04190 | 0.00330 | 0.26 |
| Patient 9 | 10 | 139.124 | 30.795 | 14.116 | 29.260 | 179.236 | 0.055 | 0.11400 | 0.05500 | 0.04190 | 0.00330 | 0.26 |
| Patient 10 | 11 | 147.719 | 34.882 | 15.990 | 33.142 | 203.020 | 0.053 | 0.11400 | 0.05500 | 0.04190 | 0.00330 | 0.26 |
| Patient 11 | 12 | 149.051 | 36.940 | 16.933 | 35.098 | 214.999 | 0.052 | 0.11400 | 0.05500 | 0.04190 | 0.00330 | 0.26 |
| Patient 12 | 12 | 149.395 | 40.391 | 18.515 | 38.377 | 235.089 | 0.050 | 0.11400 | 0.05500 | 0.04190 | 0.00330 | 0.26 |
| Patient 13 | 15 | 165.883 | 41.669 | 11.834 | 24.529 | 150.256 | 0.095 | 0.11400 | 0.05500 | 0.04190 | 0.00330 | 0.26 |
| Patient 14 | 19 | 188.188 | 54.672 | 12.496 | 25.902 | 158.667 | 0.119 | 0.11400 | 0.05500 | 0.04190 | 0.00330 | 0.26 |

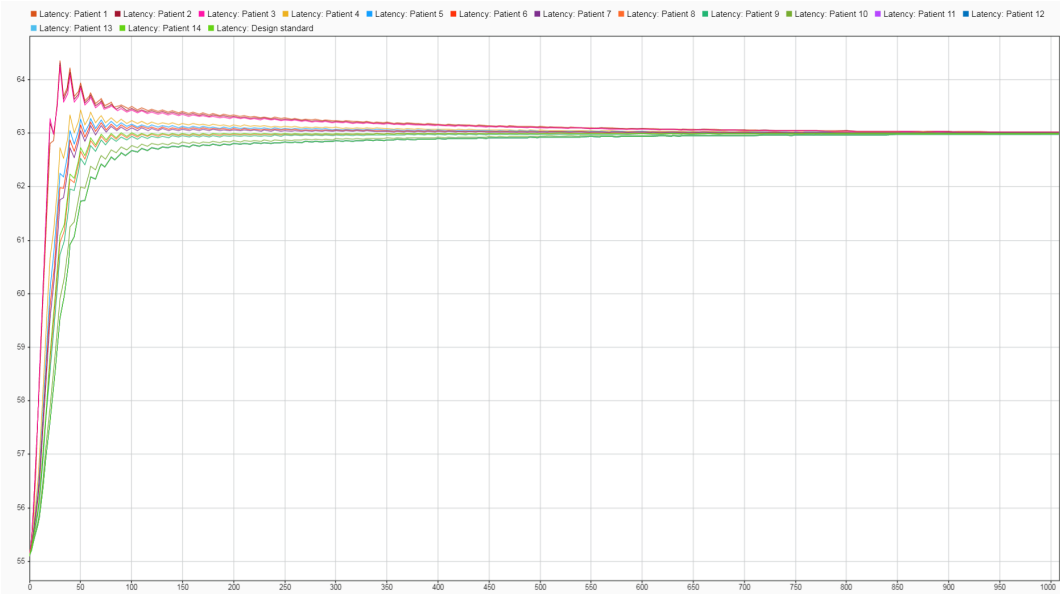


Figure 5.1: Patient latencies from the MPC control loop (in $ms$)


Figure 5.2: Patient plasma concentrations from the MPC control loop (in $\mu g.ml^{-1}$)

system's step response, but it would accommodate a wider variety of patient variability to keep from overshooting the set-point.

## 5.2 PID

To design the PID controller, a discrete-time two-degree-of-freedom PID controller was chosen. The controller parameters were designed using MATLAB's PID Tuner, as shown in Appendix D, which automatically calculates the appropriate proportional, integral and derivative terms based on a model of the plant specified, as well as the required step response which the user designs based on the user's desired response time and transient behaviour [113].

The tuner determines the controller output by applying the P, I, and D parameters independently, and the controller output, $u$, is implemented as:

$$u = P(b\,r - y) + I \cdot T_s \frac{1}{z-1}(r - y) + D\frac{N}{1 + N \cdot T_s \frac{1}{z-1}(c\,r - y)} \tag{5.1}$$

with $P$, $I$ and $D$ as the proportional, integral and derivative gains, $z$ as the discrete-time time step, $r$ as the reference signal, $y$ as the measured output, $N$ as the derivative filter coefficient, $b$ as the proportional setpoint weight, and $c$ as the derivative setpoint weight [114].

The control loop used for the PID controller simulation is depicted in Figure 5.3 and was designed based on the patient population's average patient and the results of the design are depicted in Figure 5.4 and Figure 5.5 labelled as "Latency: Design standard" and "Cp: Design standard", respectively. The same control criteria were used to design the PID controller: to reach the reference value as quickly as possible while not overshooting the reference value.

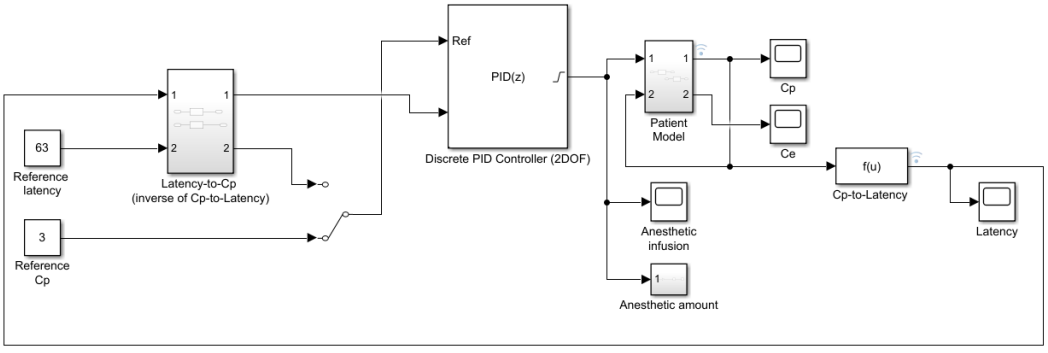


Figure 5.3: Simulink model for the PID controller

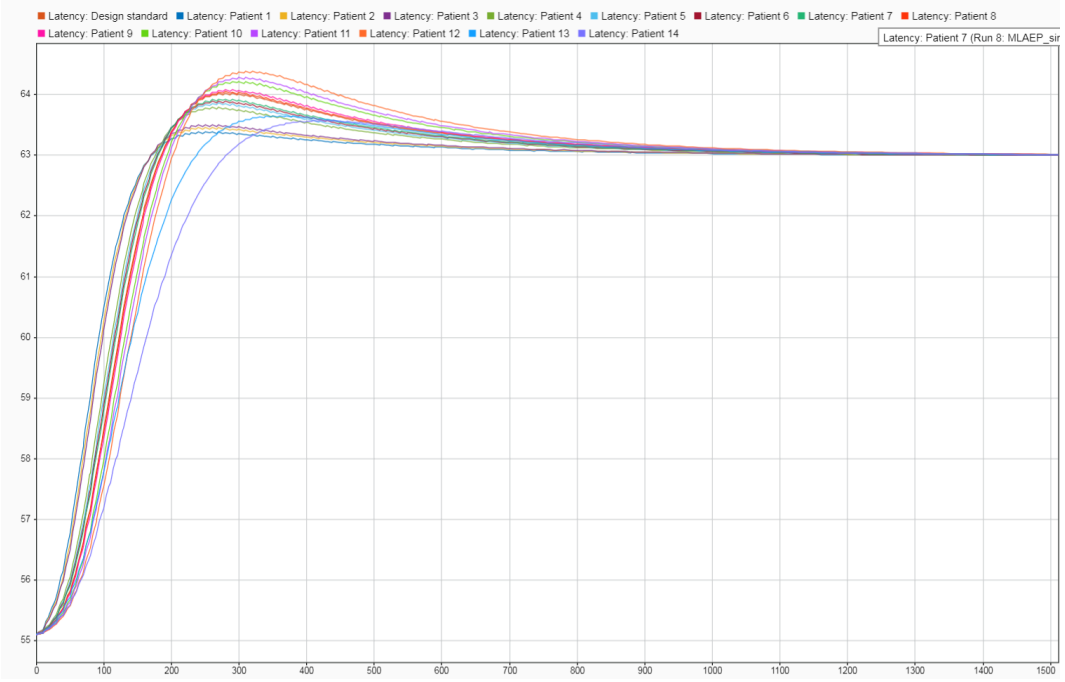


Figure 5.4: Patient latencies from the PID control loop (in $ms$)

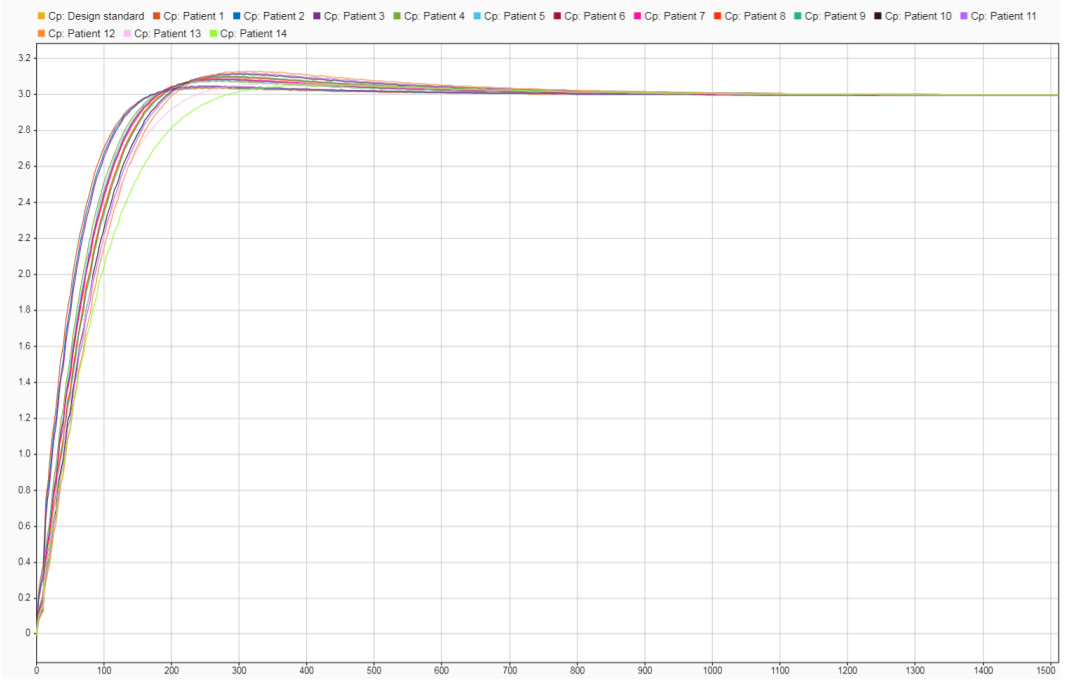


Figure 5.5: Patient plasma concentrations from the PID control loop (in $\mu g.ml^{-1}$)

Using the automatic tuner in the MATLAB PID Tuner, a system response with no overshoot was unattainable. The system was therefore designed with the least amount of overshoot attainable and the shortest possible settling time. This was achieved by designing the PID controller block with the following parameters:

Table 5.2: PID controller parameters

| PID parameter | Value |
|---|---|
| P | 2.7224 |
| I | 0.06354 |
| D | -6.0718 |
| N | 0.094885 |
| b | 0.11962 |
| c | 0.0072553 |

From Figure 5.4, the inter-patient variability also depends on the age of the patient relative to the average patient. Patients younger than the average patient have lower overshoots and quicker settling times when compared to the average patient. This is also because of the smaller compartment volumes used for the younger patients' models, so their pharmacokinetics reach steady state quicker. Patients that are older than the average patient have greater overshoots and longer settling times. This is true except for the last two patients, whose settling time is longer, but the overshoot is lower than that of the average patient.

## 5.3 MPC compared to PID

To get a better understanding of the differences in the PID and MPC controllers on the system, both system's step responses and execution times are compared to determine which controller is more fitting to implement.

### 5.3.1 Step response comparison

To compare the performance of the MPC and the PID, the latency and Cp design standards were plotted together to compare their step responses. The comparison of "Latency: Design standard" are plotted in Figure 5.6 and the "Cp: Design standard" comparisons plotted in Figure 5.7.

From the plasma concentration comparison in Figure 5.7, it can be identified that the MPC has a faster step response and no overshoot. The PID step response has a slower settling time and overshoots the reference 3 $\mu g.ml^{-1}$ to a maximum of 3.04 $\mu g.ml^{-1}$. This would make the MPC controller a better fit for the system because it reaches steady state faster and more safely because of no overshoot.

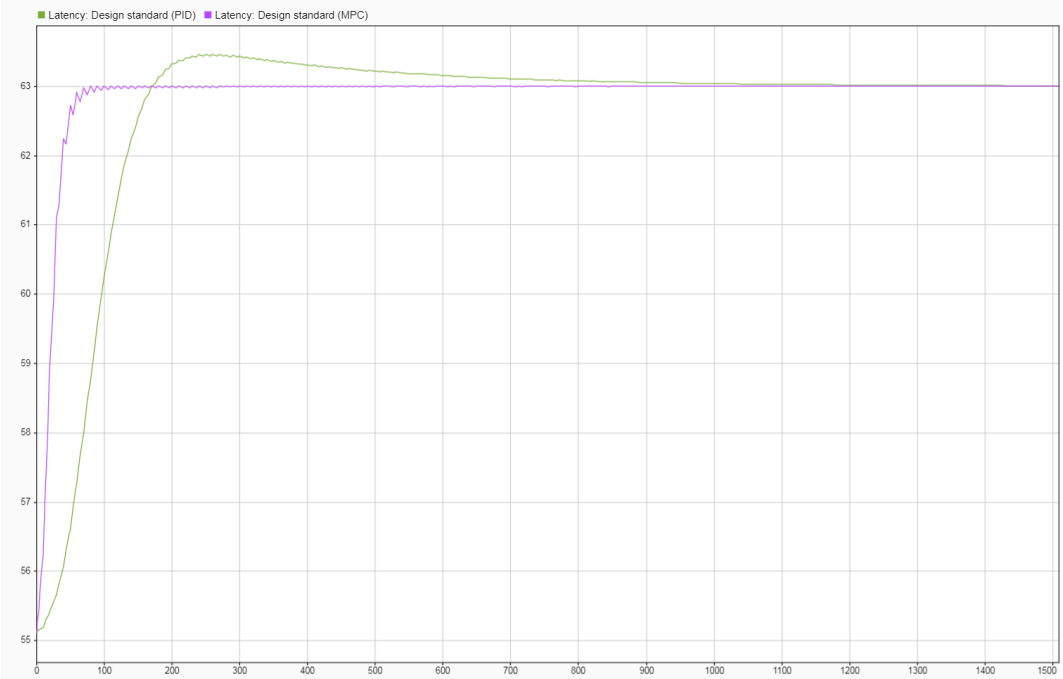


Figure 5.6: Comparison of the simulated latencies of the MPC and PID controller (in $ms$)

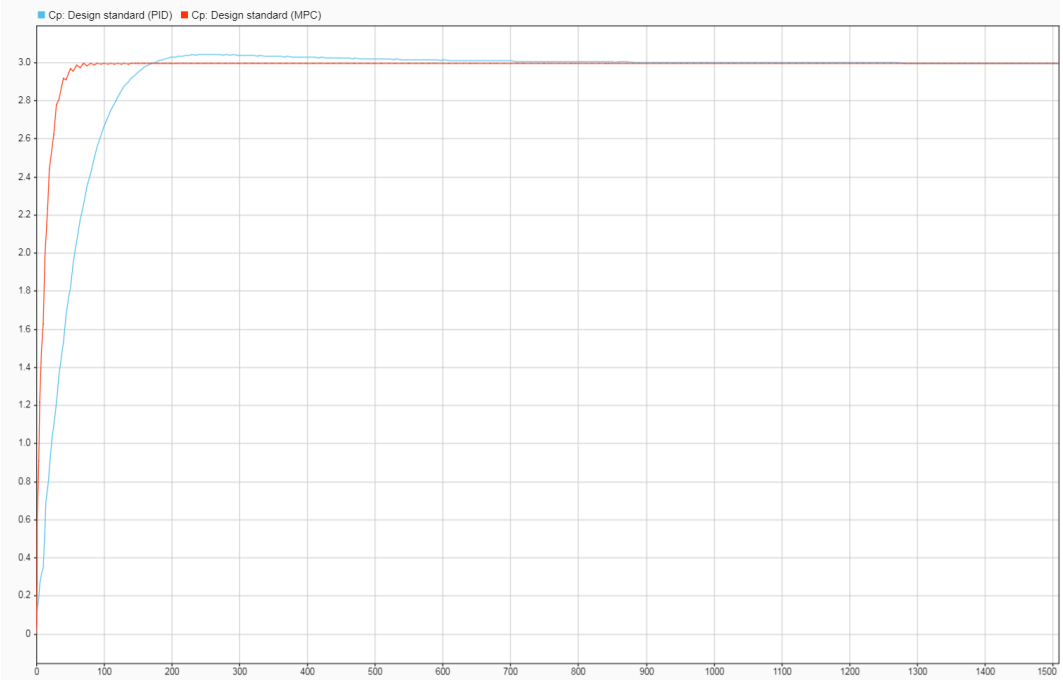


Figure 5.7: Comparison of the simulated plasma concentrations of the MPC and PID controller (in $\mu g.ml^{-1}$)

### 5.3.2 Execution time comparison

To determine which system would be more resource intensive, the two control systems' execution times were also recorded for the simulated patients over a 2000 second window. Simulink, as a model-based design and simulation software package, is not optimized for real-time simulations, so it does not run the simulation for the duration specified in the design. Rather, Simulink uses interpreted code and simulates the specified simulation duration [115]. The execution times of each patient's simulation based on how long it took to simulate 2000 seconds of processing is tabulated in Table 5.3.

Table 5.3: Execution times for all 14 patients according to the MPC or PID controller used

| | MPC [s] | PID [s] |
|---|---|---|
| Patient 1 | 8.926 | 5.497 |
| Patient 2 | 5.436 | 6.906 |
| Patient 3 | 5.641 | 6.026 |
| Patient 4 | 6.473 | 5.110 |
| Patient 5 | 8.534 | 5.238 |
| Patient 6 | 4.853 | 5.221 |
| Patient 7 | 4.195 | 7.299 |
| Patient 8 | 3.880 | 5.833 |
| Patient 9 | 8.281 | 5.040 |
| Patient 10 | 10.259 | 5.038 |
| Patient 11 | 10.433 | 5.685 |
| Patient 12 | 4.921 | 5.222 |
| Patient 13 | 8.106 | 5.107 |
| Patient 14 | 4.941 | 6.452 |
| Average | 6.777 | 5.691 |

For the MPC control loop, the average execution time was 6.777 s and the PID controller control system executed for an average time of 5.691 s. The data also indicates that the PID controller remains more consistent in controlling infusion of the different patients with varying PK models. This indicates that the PID system would be less resource intensive in a practical setting as it does not need as much processing power to execute the control loop as the MPC controller would need.

From the data gathered from both the MPC and PID controllers, it would be fair to conclude that the MPC controller is the more suited controller to use in this setting. Despite the fact that the MPC requires more processing power to operate than the PID, it is more appropriate for this setting because of its faster settling time and no overshoot. This would help for a more seamless transition from the induction to the maintenance phase of anesthesia.

## 5.4 Changing the reference

Changing the reference of the closed-loop control system would change the plasma concentration which the system would aim to achieve in a patient. This in turn would change the plasma concentration experienced by the patient.

### 5.4.1 Background

In anesthesia, it is not uncommon for the anesthesiologist to alter the depth of anesthesia experienced by the patient. One of the main reasons for altering the amount of anesthetic delivered to a patient, and subsequently deepening the level of anesthesia experienced by the patient, is to avoid awareness during anesthesia. Awareness occurs when too little anesthetic is delivered to the patient's brain and the patient remains conscious. Total intravenous anesthesia (TIVA) systems are designed using the pharmacokinetics of the average of a certain patient population [37]. It will, therefore, be incorrect to assume that the system's internal PK model can cater adequately for a larger patient population.

For example, the anesthesiologist can administer the mandatory amount of anesthetic and notice that the patient exhibits signs of consciousness because of signs like movement or hyperactive haemodynamics, or the patient shows signs of drug resistance because of prior experience of awareness, excessive alcohol use or the use of amphetamines, cocaine or opiates [116], which would lead the anesthesiologist to increase the level of anesthetic delivered, to ensure an adequate depth of anesthesia. Providing "light anesthesia" to a patient can be intentional. Surgeries like cardiac, obstetric or paediatric surgery require the anesthesiologist to intentionally administer light anesthesia because of the adverse effects that anesthetics can have when coupled with severe bleeding, septic shock and possible cardiac arrest [116].

### 5.4.2 System design

For these reasons, the system should be able to alter the level of anesthesia when the anesthesiologist deems it necessary. The Simulink model has been modified by adding a block that introduces the ability to modify the reference plasma concentration and is depicted in Figure 5.8. The system has an added summation block and the block "Changes to the Reference Cp" which includes a signal builder, depicted in Figure 5.9. The signal builder is the block that will be used to generate the various alterations to the reference plasma concentration.

To simulate changes in the level of anesthesia experienced by a patient, the reference plasma concentration was altered according to the regime set by

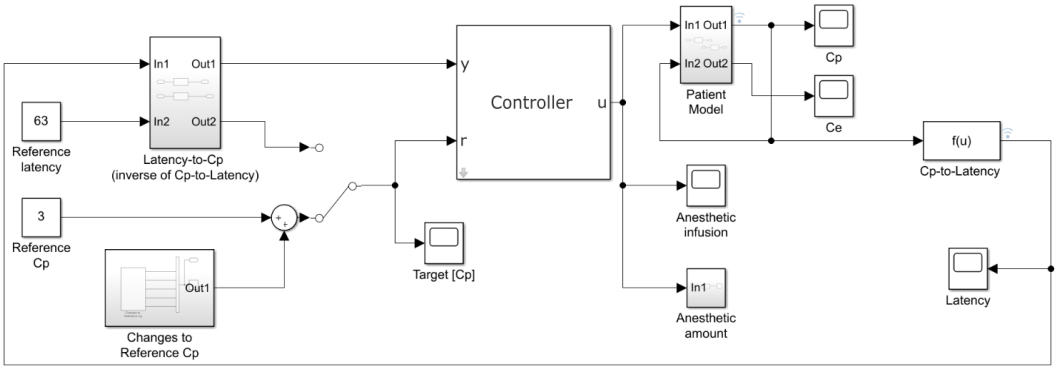


Figure 5.8: Simulink model of the changing reference simulation

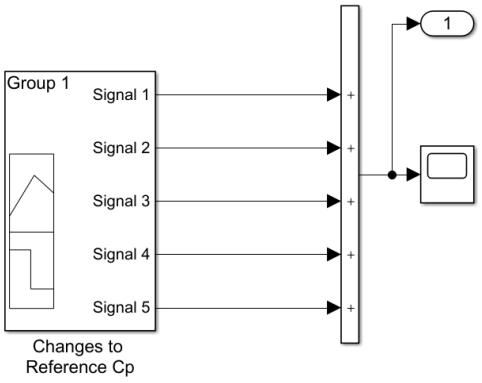


Figure 5.9: Signal builder block in the changing reference simulation

the signal builder. The alterations are depicted in Figure 5.10. The regime is listed below:

Table 5.4: Changing the plasma concentration as depicted in Figure 5.10

| Time Period | Alteration [$\mu$g.ml$^{-1}$] | New C$_p$ [$\mu$g.ml$^{-1}$] |
|---|---|---|
| 0 s - 500 s | - | 3 |
| 500 s - 1000 s | + 0.2 | 3.2 |
| 1000 s - 1500 s | + 0.4 | 3.6 |
| 1500 s - 2000 s | - 0.6 | 3 |
| 2000 s - 2500 s | - 1 | 2 |
| 2500 s - 3000 s | - 0.5 | 1.5 |

### 5.4.3 Results

To draw comparisons between the controller performances, MPC and PID controllers were simulated with changes to the reference plasma concentration for the simulated patient population. The plasma concentration results from

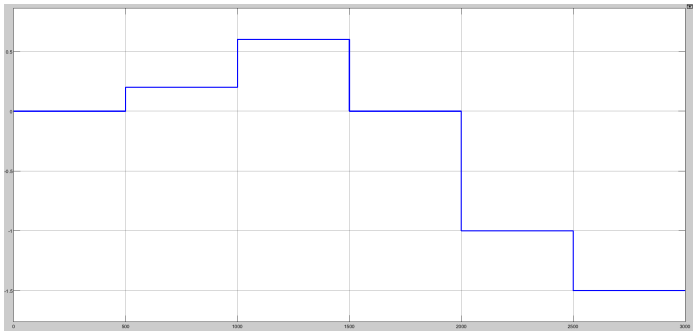

Figure 5.10: The reference signal generator for the "Changes to Reference Cp" block in the Simulink model

the MPC controller simulations are depicted in Figure 5.11, and the results from the PID controller simulations are depicted in Figure 5.11.

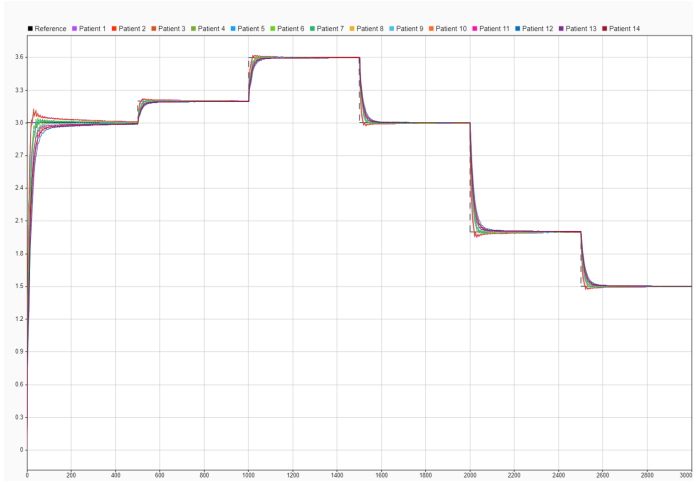


Figure 5.11: Plasma concentrations of the patient population with the MPC controller with changes to the reference plasma concentration

To compare the performances of both controllers, the MDPE, MDAPE and wobble of the simulations were calculated. The simulated patient populations' MDPE, MDAEP and wobble are compared in Figures 5.13a, 5.13b and 5.13c, respectively.

As mentioned in , MDPE represents the bias of a controller's performance, with a positive MDPE representing the controller's performance being above the reference value and a negative MDPE representing a controller's performance being below the reference value. The MDAPE represents the magnitude of the error between the reference value and the measured value. Lastly, the wobble represents the oscillations of the controller and it measures the intra-subject variability in the measurements.

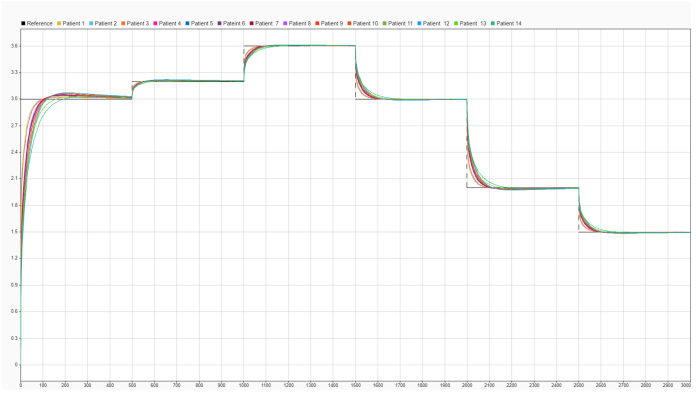

Figure 5.12: Plasma concentrations of the patient population with the PID controller with changes to the reference plasma concentration

Figure 5.13a depicts that the PID controller has a tendency to overshoot the reference value than the MPC controller. This depicts that the PID controller is more likely to overdose the anesthetic administered than the MPC controller. The MDPE of the MPC controller shows that it would underdose the anesthetic for some younger patients, and overdose the anesthetic for some of the older patients.

The MDAPE in Figure 5.13b depicts that the PID controller has greater errors in the control performance than the PID. This shows that in more control operations, the PID controller does not follow the reference value as closely as the MPC controller does.

Lastly, the wobble of the PID controller is generally greater than that of the MPC controller. This depicts that the PID controller has greater oscillations in its control of the simulated patients' plasma concentration. This, combined with the greater MDAPE of the PID controller, shows that the PID controller could be less stable than the MPC controller in administering anesthetic, which could be potentially dangerous to the patient.

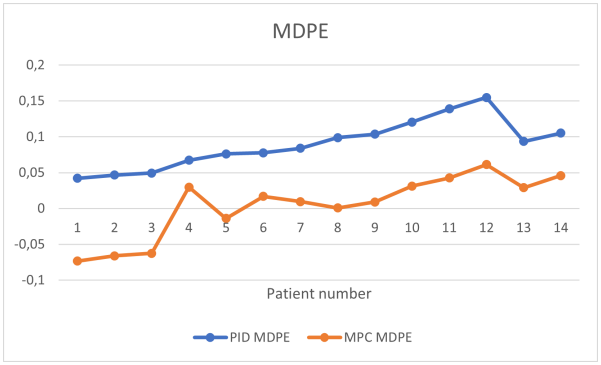


(a) MDPE of the simulated patient population for the MPC and PID controller

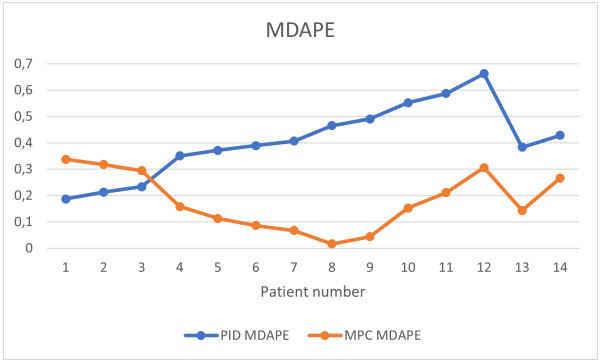


(b) MDAPE of the simulated patient population for the MPC and PID controller

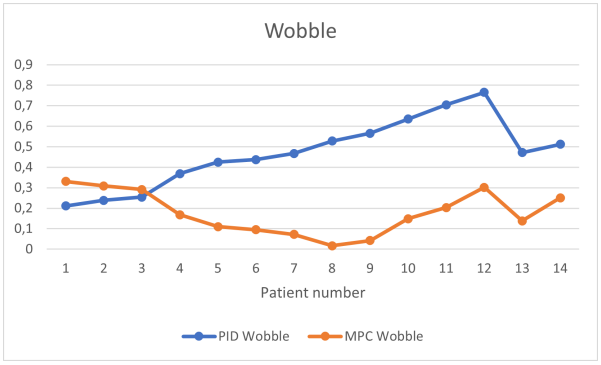


(c) Wobble of the simulated patient population for the MPC and PID controller

Figure 5.13: Performance error comparisons of the MPC and PID controllers

# Chapter 6

# Simulations based on possible application scenarios

This chapter expands on the design of the MPC control loop and analyses the effect of measurement noise that could be encountered during the maintenance phase of anesthesia that the system would need to make provision for.

## 6.1 Measurement noise

To simulate the influence of measurement noise on the system, the band-limited white noise block in the *Noise disturbance* block, depicted in Figure 4.2, is activated to add noise to the measured latency.

### 6.1.1 Background

To determine the magnitude of the noise levels to be added to the system, signal-to-noise ratios (SNR) were used. SNR is defined as the ratio of the power of a desired signal relative to the power of the noise within the signal [117]. It can be described as a unit-less ratio, or more commonly, it can be described in decibels (dB). SNR is calculated as either

$$SNR = \frac{P_{Signal}}{P_{Noise}} \tag{6.1}$$

or

$$SNR_{dB} = 10\,log_{10}\,\frac{P_{Signal}}{P_{Noise}}\ dB \tag{6.2}$$

or

$$SNR_{dB} = 20\,log_{10}\,\frac{V_{Signal}}{V_{Noise}}\ dB \tag{6.3}$$

### 6.1.2 Simulation design

To simulate the measurement noise scenarios, the band-limited white noise generator within the *Noise disturbance* block in Figure 4.2 was activated and used.

The power of the reference latency signal from the simulation over 500 seconds was calculated using

$$P_{\substack{Reference\\latency}} = \lim_{N\to+\infty}\left(\frac{1}{2N+1}\sum_{n=\infty}^{\infty}|x(n)|^2\right)$$

with $N$ as the total number of samples in a 500 second window, $n$ as the sample number and $x(n)$ as the step function that is the reference latency. The power of the reference latency was calculated as 15 dB. The SNR values used to simulate the added noise were 40 dB, 30 dB, 20 dB, 15 dB, 10 dB, 5 dB, 0 dB and -3 dB.

### 6.1.3 Results

The latency results with added measurement noise are depicted in Figure 6.1, and the corresponding plasma concentration results are depicted in Figure 6.2.

The MDPE, MDAPE and wobble of the measurement noise simulations are depicted in Figures 6.3a and 6.3b. These performance characteristics depict that as the measurement noise increases, the bias and the magnitude of the error of the controller performance increases.

From the performance error characteristics in Figure 6.3b, it is clear that the influence of measurement noise experienced by the system remains relatively consistent below 10 dB and it starts increasing relatively linearly from 5 dB, therefore the system would be more stable if the noise input to the system was limited to about 15 dB.

From reference [37], the maintenance plasma concentration of propofol in children should range between 2 $\mu g.ml^{-1}$ and 4 $\mu g.ml^{-1}$ for cases lasting longer than 30 minutes and when an opioid is given alongside. From the results, all the noise ranges remain within those thresholds, except the plasma concentration of the -3 dB case. From analysing the noise simulation results as well as Figure 6.3b, the maximum acceptable signal to noise ratio is chosen as 15 dB. The plasma concentration in that scenario ranges from 3.1 $\mu g.ml^{-1}$ to 2.9 $\mu g.ml^{-1}$, and the corresponding latency is within the threshold of 66 and 60 ms from the 63 ms reference.

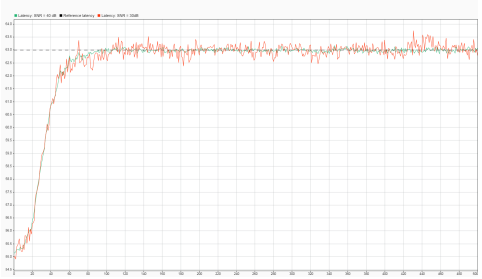

(a) Measured latencies with 40 dB and 30 dB SNR (in $ms$)

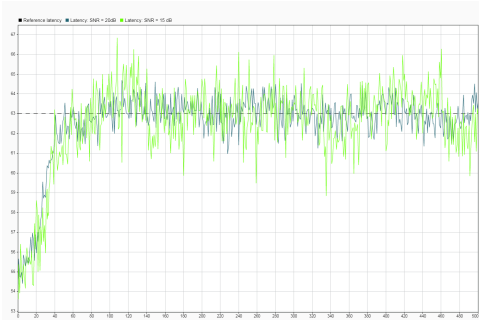

(b) Measured latencies with 20 dB and 15 dB SNR (in $ms$)

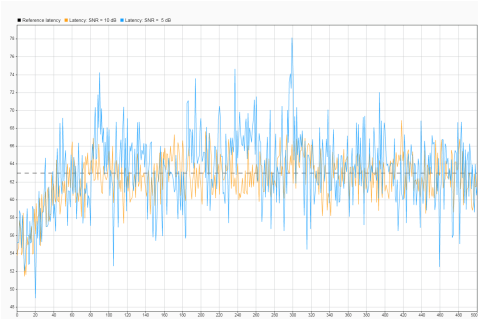

(c) Measured latencies with 10 dB and 5 dB SNR (in $ms$)

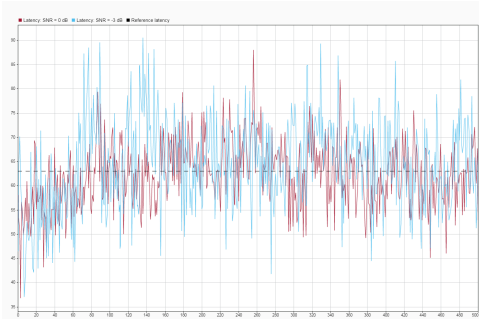

(d) Measured latencies with 0 dB and -3 dB SNR (in $ms$)

Figure 6.1: Measured latencies with added noise

## 6.2 Final system

This chapter has has elaborated on the various adjustments to the depth of anesthesia experienced by a patient and the anesthesiologist has the responsibility of making sure that the patient stays comfortable while undertaking these adjustments. The final system will therefore need to include the various modifications made to the main system. The final system with all the modifications is depicted in Figure 6.4.

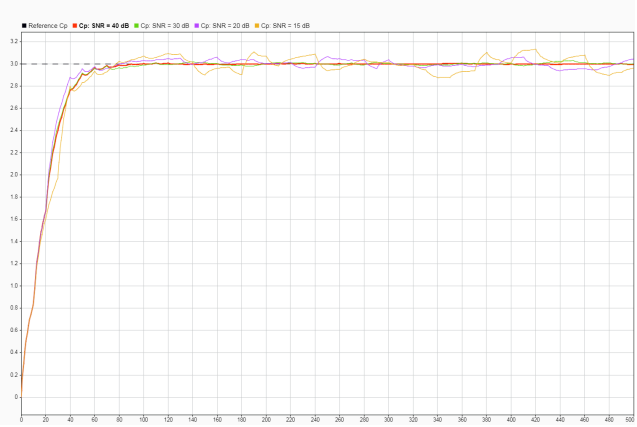

(a) $Cp$ with 40 dB, 30 dB, 20 and 15 dB SNR (in $\mu g.ml^{-1}$)

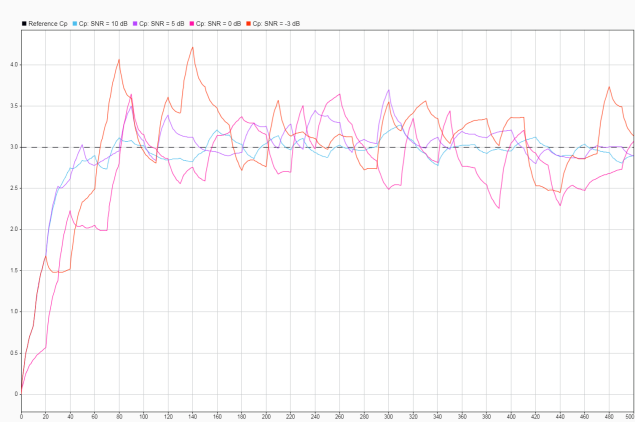

(b) $Cp$ with 10 dB, 5 dB, 0 dB and -3 dB SNR (in $\mu g.ml^{-1}$)

Figure 6.2: $Cp$ with noise added to the measured latency

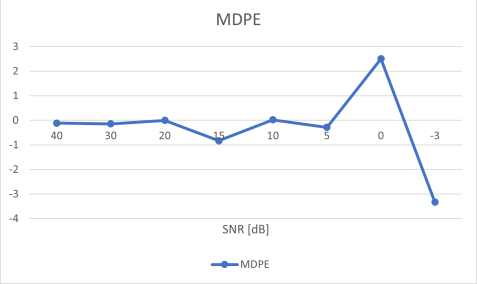


(a) MDPE values of the noise simulations over the noise range

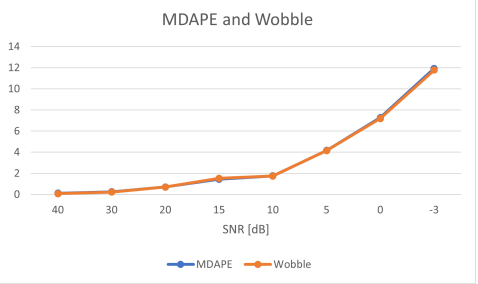


(b) MDAPE and wobble values of the noise simulations over the noise range

Figure 6.3: Performance error characteristics for the measurement noise simulations

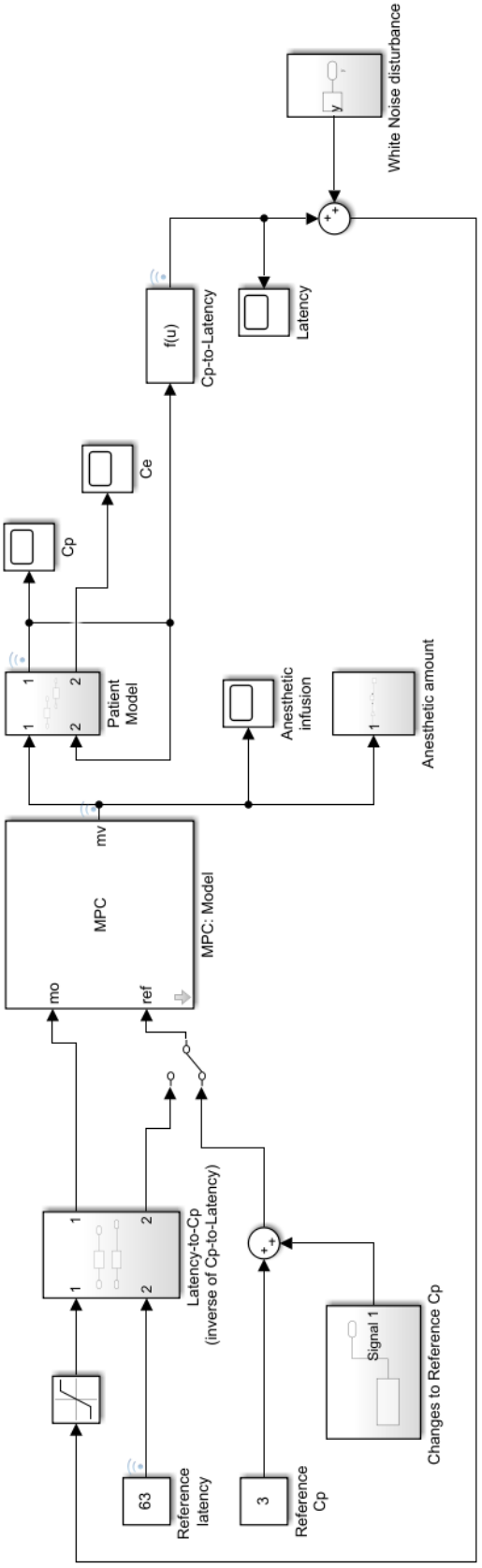


Figure 6.4: The final closed-loop control system with all the modifications included

# Chapter 7

# Discussion

This chapter expands on the results obtained in the preceding chapters. The focus of this chapter is to place the results, and the entirety of the research project, into perspective and it expands on how the system could be incorporated in a surgical setting.

## 7.1 The system in practice

For the whole system to operate efficiently, a number of components need to be put together and their compatibility with each other must be tested for correct operation.

The intra-ear electrodes from the novel intra-ear monitor [10] need to be fitted into the patient's ear and then connected to the monitor to read the signals. The monitor is then connected to the controlling computer through a wired connection or through the OpenBCI Cyton wireless Bluetooth USB module [10], [118]. The computer will run the algorithms that extract the MLAEP from the EEG data as well as send the MLAEP information to the closed-loop controller.

When the closed-loop controller has calculated the amount of anesthetic to be infused, it will transmit infusion instructions to the infusion pump. A digitally-controlled infusion pump will receive the infusion instructions and control the syringe containing the anesthetic. The anesthetic is then pumped into the patient and the loop is complete and it can recycle. The control loop is depicted in Figure 7.1.

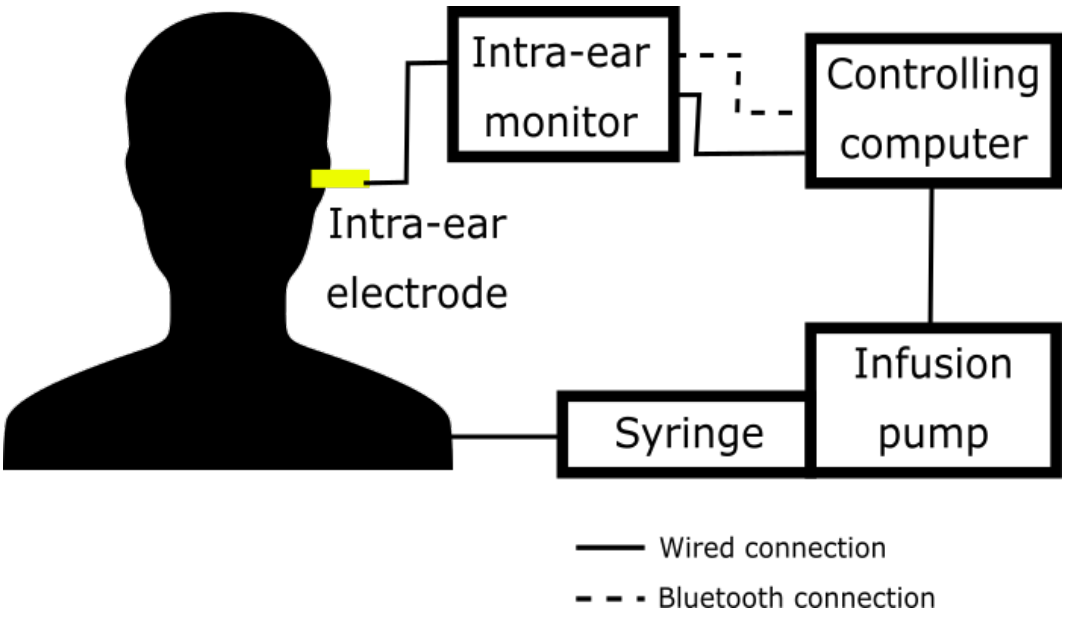


Figure 7.1: The implementation of the system in practice

## 7.2 Overview of general anesthesia with the closed-loop control system included

General anesthesia consists of 3 phases: induction, maintenance and emergence [3]. To incorporate the closed-loop control system into the practice of anesthesiology, the routines used to prepare the systems needed to sedate a patient, as well as routines for the preparation of the patient, will need to be adjusted. Preparation procedures need to be done separately and thoroughly to ensure that both the closed-loop control system and normal processes of anesthesia happen effectively without hindering each other's performance in any way.

### 7.2.1 Preparation

The anesthesiologist will prepare for the procedure as well as prepare the patient according to the normal pre-anesthesia care and checks used in practice, similar those mentioned in [37], [119].

During the preparations conducted by the anesthesiologist, the closed-loop control system would need to be prepared. The anesthesiologist would need to allow for multiple channels of intravenous infusion to accommodate the infusion of the anesthetic, opioid and analgesic during the induction phase [32], and a separate channel would be needed to connect the syringe of the closed-loop control system's infusion pump to the patient for the maintenance phase. This can be achieved by using a multi-lumen connector to accommodate the numerous lines of infusion, depicted in Figure 7.2 [37]. Each line should

have anti-reflux and anti-siphon valves to prevent the anesthetic or other drugs from flowing back into the syringes.

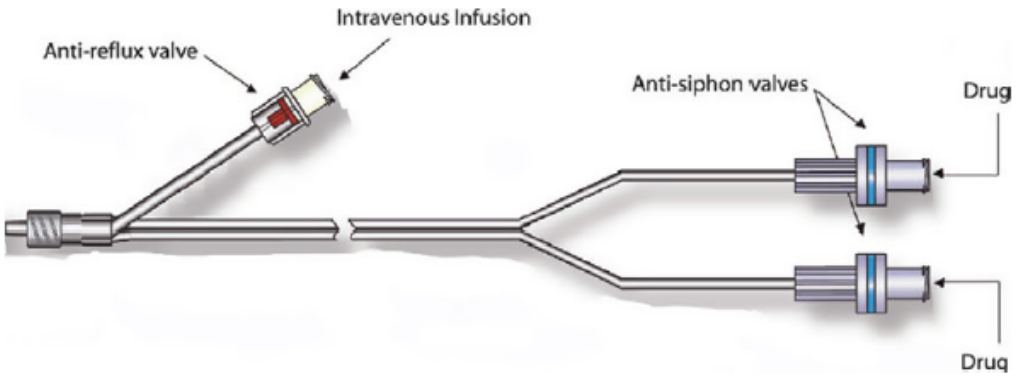


Figure 7.2: An example of a multi-lumen connector with anti-reflux and anti-siphon valves [37]

### 7.2.2 Induction

In the induction phase, the anesthesiologist prepares the patient for the anesthesia and the surgery by pre-medicating the patient with the desired anesthetic. From there, the patient is monitored closely by the anesthesiologist to determine the depth of anesthesia experienced by the patient.

Once the anesthesiologist deems the patient to be at an appropriate level of anesthesia, the anesthesiologist will then enter the desired plasma concentration for the maintenance phase into the closed-loop control system. This level could vary slightly for different patients because of inter-patient variability. Then maintenance phase can begin.

### 7.2.3 Maintenance

The patient will be kept at the desired depth of anesthesia by the system. The anesthesiologist will not be required to dedicate his/her full attention to the patient, as the system will be controlling the delivery of anesthetic to the patient to keep the patient at the specified depth of anesthesia based in the propofol plasma concentration.

During the maintenance phase, the surgery could require a number of situations that the system would need to accommodate. The anesthesiologist could be required to alter the level of anesthesia the patient experiences if the patient exhibits signs of awareness, like movement or an increasing heart rate, or the patient could be experiencing a drop in blood pressure [116]. This will

be done by entering an new reference plasma concentration into the system, either higher or lower than the previous value, and the system will adjust accordingly, as described in Section 5.4.

### 7.2.4 Emergence

Once the surgery is complete, the emergence phase will begin to return the patient back to consciousness. Anesthesiologists are less likely to switch off an infusion system at the end of a procedure because the surgeon could still need to do some work on the patient [120]. Therefore, the anesthesiologist will be required to decrease the reference plasma concentration to allow the patient to return to consciousness. This can be done by just setting the controller to achieve a plasma concentration of about 1.5 $\mu g.ml^{-1}$ [37], allowing the patient to slowly gain consciousness.

## 7.3 Motion artefacts

Another factor that would be interesting to investigate is the influence of motion artefacts on the system.

### 7.3.1 Introduction

Motion artefacts are undesired signals generated in biological systems, which stem from the movement of one component of the system relative to another [121]. For this system, the motion artefact to be considered would be caused by motion between metal, the intra-ear electrode, and the electrolyte, being the electrode gel on the surface of the external auditory canal, depicted in Figure 2.3.

### 7.3.2 Background

The most likely sources of artefacts that could influence the intra-ear system would be eye movements or muscle activity, such as the movements of the jaw. Jaw movements are of greater concern with regards to motion artefacts within the inner ear [122]. Jaw motion can cause changes in the shape of the ear canal, which would adjust the positioning of the intra-ear electrode. The motion between the electrode and the electrode gel during that adjustment would then generate an artefact voltage.

According to [10], the intra-ear monitor will be playing an audio stimulus in the patient's ear and from that ear, the AEP will be recorded. The patient should only register the single stream of audio stimulus to the one ear for accurate MLAEP information to be recorded from the ear of interest.

One factor that was considered in the design is mitigating the influence that bone conduction in the opposite ear would have on the system. Bone conduction is when vibrations are transmitted through the skull and then received by the inner ear. These vibrations will then be registered by the brain as sound [123]. In this case, the audio stimulus in the ear of interest would be transmitted into the desired ear, as well as through the skull into the opposite inner ear. There would then be two audio stimuli perceived by the brain and the brain would respond to both stimuli. To mitigate this, the system generates white noise into the opposite ear to mask the bone conduction [10].

### 7.3.3 Motion artefact simulation

According to [121], artefact voltages ($V_a$) generated between a metal and an electrolyte can be calculated as:

$$\begin{aligned} V_a &= \Delta Q / C \\ &= \Delta Q \ \phi / (\sigma \, S_0) \\ &= [K \, \tau \, \phi / S_0] \, [1 - exp(-t/\tau)] \end{aligned} \tag{7.1}$$

with $\phi$, the electrochemical potential $[mV]$, $S_0$, the total surface area of the electrode $[mm^2]$, and $K$ is the exposed area per unit time $[mm^2.s^{-1}]$. The parameter $\tau$ is the dielectric relaxation time constant $[ms]$, and $t$ is the contact time of $K$ over a certain area $S_0$ $[ms]$.

To determine the artefact voltages that could potentially plague this system, it would be beneficial to simulate the possible voltages that could be generated. With knowledge of the types of electrodes used in the system, the parameters $S_0$ and $K$ can be determined. Unfortunately, a couple of the parameters used to calculate $V_a$ can only be determined experimentally [121]. Furthermore, there have been no experiments recorded where the electrochemical potential or the dielectric relaxation time constant of gold and the specific concentration of sodium chloride (NaCl) in the Ten20 electrode gel, used in [10], have been recorded. Therefore, it would be hard to simulate the exact amount of artefact voltage that moving the intra-ear electrode would generate.

However, with these two unknowns, it is possible to plot a 3-dimensional mesh of the possible artefact voltages that can be determined. The x- and y-axes can be the two variables, the electrochemical potential and the dielectric relaxation time constant, and the z-axis will be the artefact voltages possible from the combination of the x- and y-axes calculated using (7.1).

Some assumptions need to be made because of the number of unknown variables available. Firstly, the intra-ear electrode is assumed to have the

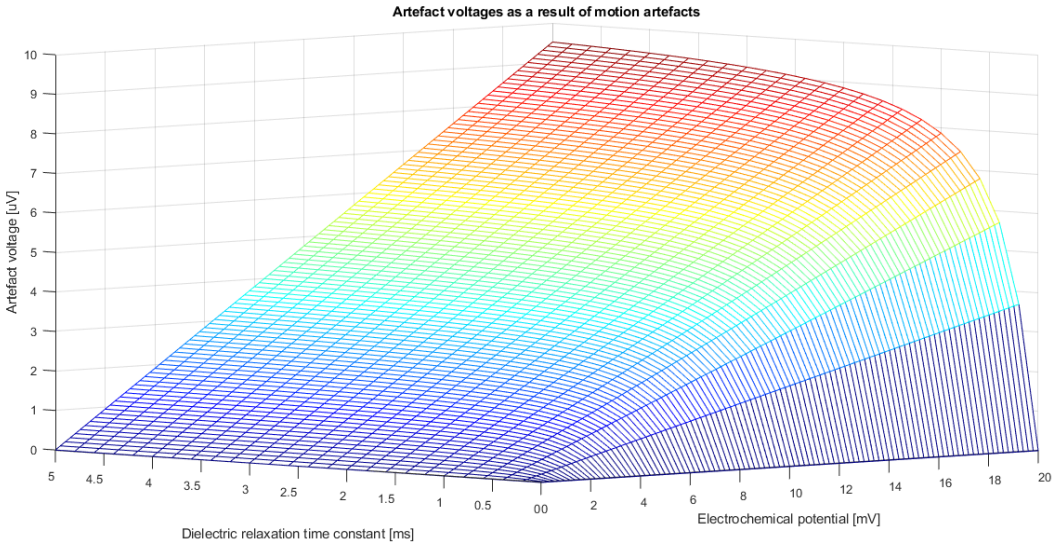


Figure 7.3: Simulated range of artefact voltages

same surface area as the gold-cup electrodes used for the earlobe plugs [10]. Secondly, the EEG recording of the intra-ear monitor only records the EEG signals once the audio stimulus is generated. Any signals that linger for longer than this sample time would be filtered out as a DC offset [10], or they could corrupt the EEG signal measured for the duration of the movement. To calculate a possible minimum $V_a$ that could be generated, the motion time of the electrode is assumed to lie within this sample time of 125 ms [10] and it is thus simulated at 500 $\mu$s.

### 7.3.4 Results

From Figure 7.3, it is clear to see that under these conditions, artefact voltages generated will lie between 0 and 10 $\mu$V. The MLAEP voltage levels recorded by the intra-ear monitor lie within the same range after the filtering and averaging algorithms are applied to the raw EEG signals recorded [10], so motion artefacts will influence the readings of the MLAEP signals for the closed-loop system. It is likely that unintended jaw movements could occur for a couple of seconds. So using the 500 $\mu$s simulation as a baseline, motion lasting longer than 500 $\mu$s could corrupt a fair amount of $V_a$ measurement samples until the motion stops.

According to [9], anesthesia only shows a clear influence on the delay of the MLAEP peaks and troughs. The deeper the patient drifts into anesthesia, the greater the delay. The amplitude of the peaks and troughs do not show any notable change as the patient drifts deeper into anesthesia.

An example of the MLAEP plot read from the intra-ear system is depicted in Figure 7.4. In this case, the additional artefact voltage generated would

slightly increase the amplitude of MLAEP readings at certain points in the signal. If the artefact were to fall on a trough, the voltage would be increased slightly, but the system would still be able to identify it as a trough with respect to the surrounding Pa- and P1-peaks. However, if the artefact were to fall on any other point, it could make the system miscalculate the latency.

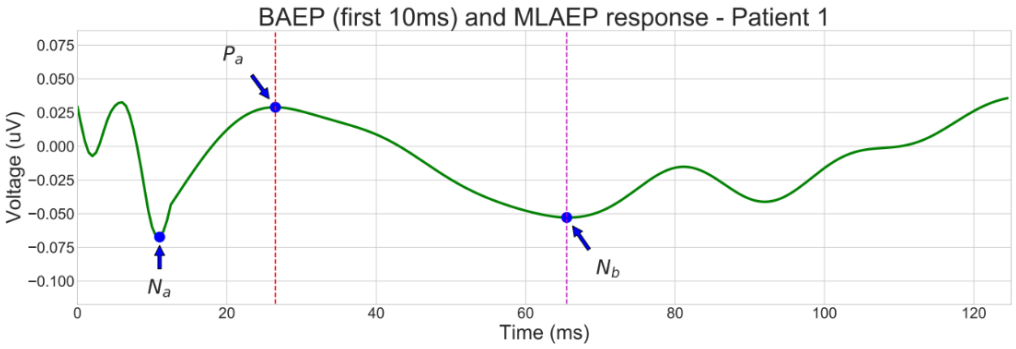


Figure 7.4: An example of the MLAEP signal acquired from the intra-ear system [10]

Therefore, it would be a good idea to design an algorithm that could detect and filter out any artefact voltages generated during the reading of MLAEP signals during anesthesia.

## 7.4 Advantages of incorporating the system in practice

There are a number of advantages associated with using such a system in practice.

### 7.4.1 Benefits to anesthesiology

As mentioned in [1], there is a great shortage of workers in South Africa's healthcare sector and this includes a shortage in anesthesiology. This system could provide the necessary support needed in hospitals and bridge the gap in the shortage of anesthesiologists.

Unlike an anesthesiologist, the system is not susceptible to fatigue caused by the irregularity of an anesthesiologist's daily schedule and the constant focus needed from the anesthesiologist during lengthy surgeries [1]. It is able to provide consistent, accurate doses of anesthetic regardless of the number of hours it has to maintain a patient in anesthesia. Once the anesthesiologist has administered the required induction procedure, the system can then take over the maintenance phase and the anesthesiologist is only needed to oversee the

administration of anesthetic from the system and intervene when necessary. This does not demand as much focus from the anesthesiologist and can possibly be done from a separate control centre or from a smart device.

With this newly found freedom, the anesthesiologist could administer the induction phase to another patient and set up the closed-loop control system to control the delivery of anesthetic during the maintenance phase to each patient. Once the maintenance phases begin, the anesthesiologist could oversee this number of patients from a control room that gives information on each procedure, and the MLAEP latency measured from the patient through each system could alert the anesthesiologist if there is a need for an intervention in any of the procedures. This allows for fewer anesthesiologists to be needed in a single hospital and the anesthesiologists available could be distributed more evenly across the South African population.

### 7.4.2 Wider usability

Additionally, the system can be operated by an individual with lower qualification than an anesthesiologist. Since the setup of the system and the sedation of the patient will primarily be handled by the anaesthesiologist, the individual with the lower qualification can take over when the patient enters the maintenance phase. What is important is that the anesthesiologist should still have higher-level oversight over the system in the control room. This would allow for quick, on-site recognition and resolution of issues that the user might encounter with the system or the patient.

## 7.5 Concerns of using the system in practice

Before the system is tested and implemented in practice, a couple of concerns need to be addressed.

### 7.5.1 Thorough testing is needed

The system would need to be tested rigorously through animal tests as well as to be tested on live patients to make sure that the system works adequately. The system was designed using the Paedfusor PK model, so the system can initially only be used in paediatric anesthesia.

The system would also need to be reviewed by various anesthesiologists to determine if it works to the satisfaction of the various anesthesiologists and boards of approval. With their support, the system could be be rolled out and used in numerous hospitals with confidence based on the accreditation from the various anesthesiologists and the necessary boards required to implement such a system, like the South African Society of Anesthesiologists.

As mentioned in [120], anesthesiologists are not very familiar with the use of plasma concentration in monitoring depth of anesthesia. This could be because there are no measures of anesthetic plasma concentration available to be used in medical settings. Anesthesiologists have a better knowledge of the effect that a certain amount of infused anesthetic will have on a patient, rather than the influence on the plasma concentration that the infused anesthetic will have. Therefore, anesthesiologists will have to be familiarized with the influence of plasma concentration on the depth of anesthesia a patient experiences, or the system will need to be used with a general guide describing the influence that various plasma concentrations have on a patient.

### 7.5.2 Processing power

For the whole system to operate efficiently, the processing power of the various components needs to be sufficient. The concatenation of the intra-ear monitor, controller PC and the digitally-controlled infusion pump, which would need to be built specifically to work with this system, would need to be compatible with each other to deliver the necessary dose of anesthetic to the patient timeously.

The processing power of the controlling PC is of greatest concern in this case because it will be running software filtering the MLAEP data from the raw EEG streamed from the intra-ear monitor [10] and the whole control system and if it does not process the information it transmits and receives timeously, it can delay the whole loop and the patient will not receive the correct dose of anesthetic. The average dosing sampling time of 10 seconds [37] should be sufficient for the the whole process to run its cycle before the next dosage required, but it would need to be thoroughly tested to ensure that the whole process can be completed within the sampling interval of 10 seconds.

If it is found in a particular setting that the implementation cost of the MPC closed-loop control system is too high because of the increased processing power required, the PID closed-loop control system can be considered as a more affordable alternative. As shown in Section 5.3, although the PID controller has a slower settling time and a larger overshoot, the infusion algorithm runs faster. The overshoot of the system's step response does also fall within a usable range according to [37] as it states that the plasma concentration needed during the maintenance phase of anesthesia ranges between 2.5 and 4 $\mu g.ml^{-1}$.

### 7.5.3 Measurement noise

If the closed-loop control system were to be operated in an environment susceptible to noise, it would be beneficial if the noise were capped at SNR of 15 dB as mentioned in Section 6.1. However, if the SNR was to drop below

15 dB, a noise filter may need to be incorporated into the system. The filter would need to raise the SNR to 15 dB or higher, as described in Section 6.1. The filter would need to be added to the feedback path, after the latency measurement is recorded and before by the "Latency-to-Cp" block in Figure 6.4.

## 7.6 Limitations

A major limitation in the implementation of the system is related the patient population that would benefit from this system. The reason the Paedfusor model was used in the design is that the look-up tables relating the MLAEP latencies to the propofol plasma concentrations, depicted in [66], are not available for the other PK models used in practice, like the Schnider and Marsh models.

To incorporate other PK models, further research and tests need to be conducted into finding the correlation between the plasma concentration and MLAEP latencies for the patient populations that make up the other PK models. With this information, correlations similar to those in [66], and the corresponding functions, like that in Equation (4.3), can be determined. These correlations could then be used in conjunction with the corresponding PK models used for adults, like the Schnider, Marsh and Eleveld PK models, within the MPC controller. From there, the system could be further developed for use with adults.

Additionally, without definite information about the data points in [66], the estimated sigmoid function in (4.3) and its inverse in (4.4) will vary according to the estimations made by the users of the information. Further tests would need to be conducted to acquire more data so establish industry-standard correlations of the plasma concentration and latencies.

## 7.7 Possible additions to improve the system

Using these findings and this design of this system as a springboard, there are a number of additions that can be investigated to improve the system.

### 7.7.1 Prototyping

Prototyping is the natural next step for the system. Before tests are conducted using the system, a digitally-controlled anesthetic infusion pump needs to be built for the control system. The advantage of building an infusion pump is that the infusion pump will be driven through instructions given from the

closed-loop control system, directly. The infusion pump can also be built according to specifications which satisfy the needs of the anesthesiologist and the specific test case used for testing the system. It can also be a more affordable alternative to the infusion pumps that are on the market [124].

The block *Anesthetic amount*, mentioned in Section 4.3.5 can be adapted to drive the infusion pump. This would be done by translating the amount of anesthetic infused to the the distance the syringe's plunger needs, depicted in Figure 7.5, to move to administer the specified amount of anesthetic required.

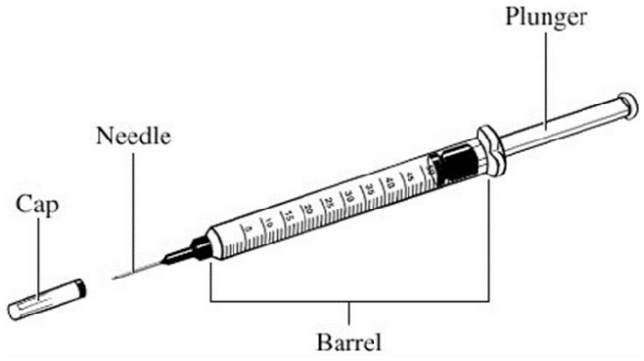


Figure 7.5: Diagram of a syringe [125]

To account for the transition speeds that the anesthetic infusion pump would capable of for situations such as those in Section 5.4, the MPC block would need to be adjusted. The MPC includes constraints that specify the maximum and minimum rate of change of the manipulated variable. This would be beneficial to include in the MPC for the system to account for the capabilities of the anesthetic infusion pump as it will have maximum speed specifications.

There should also be a user interface developed for easy control of the whole system. This user interface would be responsible for the input of the plasma concentration required for the maintenance phase and the adjustment of the selected plasma concentration. It would also be used to indicate that the infusion is in progress and used to monitor the current MLAEP latency and plasma concentrations read from the patient. Additionally, the user interface could also display other information like the patient's heart rate and breathing rate to get a holistic view of the patient during anesthesia on one display.

The system will then need further additions to alert the anesthesiologist about the state of the infusion pump. These additions will could include adding default alarms for situations in which the infusion has stopped because: the end of the procedure has been reached or the syringe has been disconnected from the multi-lumen connector; the syringe is running out of anesthetic or is

empty; the main power supply has been disconnected or the stand-by battery is running low [37].

### 7.7.2 Using other vital signs available in the inner ear

It has been found that from the inner ear, other vital signs can be acquired alongside MLAEP. These include heart rate, heart rate variability, blood oxygenation levels, body temperature and respiratory rate [126]. The availability of these other vital signs pave the way for the closed-loop control system to be adapted to administer other drugs. Provided that the PK model of the drugs to be infused is available, the system can be adapted to infuse a variety of drugs other than propofol.

General anesthesia involves the administration of drugs for hypnosis, to provide: unconsciousness; analgesia, for pain suppression; and neuromuscular blocking drugs, to prevent movement during surgery [34]. By using the relationship between heart rate variability and the sensation of pain a patient experiences [127], a separate closed-loop control system can be developed to administer an analgesic during general anesthesia.

Depending on the processing power of the available controller, these various closed-loop control systems could be incorporated into one machine and the system could operate as a multi-input multi-output (MIMO) system. This means that the various measurements read from a single patient could be read into the one machine. The machine would then collect the measurements and assigns them to their appropriate controllers and each controller sends output signals to the appropriate infusion pump to administer the correct amount of drug to the patient.

### 7.7.3 Further developments to accommodate the induction phase

The system could also be improved by designing it to also administer drugs for the induction phase. This is a more involved stage in anesthesia because the anesthesiologist administers the drugs at specific quantities and monitors the patient's response to those doses until the patient is deemed fully anesthetized and ready to begin the maintenance phase of anesthesia.

As mentioned in [10], the intra-ear monitor has a built-in accelerometer and it measures accelerometer data in three axes. These measurements could be used to monitor the movements of the patient while the system administers the appropriate doses of anesthetic for the induction phase. Alongside the movement of a patient, the system could also incorporate other vital sign information, like heart rate and breathing rate [116]. If the anesthesiologist

deems the measurements taken adequate for a fully anesthetized patient, the system could then switch into "maintenance phase mode".

The infusion regime conducted for the induction phase differs from that of the maintenance phase, therefore multiple MPC controllers could be applied to allow for the different control sequences of the two phases.

### 7.7.4 Machine learning implementation

Furthermore, there may be potential for a machine learning implementation of the system. Machine learning is the automatic detection of patterns in large amounts of data and from the patterns that have been determined, future predictions can be made on new data introduced or other decision making processes can be executed [128].

Since the induction phase is more involved because of the inter-patient variability involved in sedating the patients adequately and the anesthesiologist needs to keep a close eye on how the patient responds to the drugs being administered, it would be interesting to investigate the patterns that a number of patients exhibit when undergoing the induction phase so that the machine learning algorithm could implement the anesthetic infusion regime required to sedate a patient during the induction phase.

To train the machine learning algorithm, it would need to collect plenty of training data consisting of a number signals from many patients as they undergo the induction phase. The algorithm would need to be trained on the data from patients' vital signs and, potentially, anesthetic plasma concentrations as patients are sedated. Once thoroughly trained, the algorithm would then administer anesthetic to a patient during the induction phase to adequately sedate a patient from the induction phase and once acceptable sedation is achieved, the system could switch to the maintenance phase of anesthesia.

# Chapter 8

# Conclusion

From previous work, it has been shown that it is possible to determine the depth of anesthesia a patient experiences by monitoring the patient's EEG signals [38]. From the EEG signals, the auditory evoked potentials can be derived and they correlate well with the depth of anesthesia experienced [7]. The latency of the MLAEP signals tends to increase as the patient experiences deeper levels of anesthesia. It has also been discovered that these signals can be acquired inside the patient's ear as a non-invasive form of signal acquisition [10], [45].

Using this information, a closed-loop control system has been designed that is able to keep a simulated patient adequately sedated. The closed-loop control system uses the latency of the of the MLAEP's $N_b$-trough to determine the plasma concentration of propofol within the patient. If this plasma concentration falls below that specified by the anesthesiologist, the system will increase the infusion of propofol to the patient. When the desired latency or plasma concentration is reached, the system is designed to monitor and maintain the plasma concentration at that specified level.

From the simulations, it has been shown that the MPC controller is a better controller to use for the closed-loop control of anesthetic delivery compared to the PID controller because of its faster settling time and its ability to suppress the step response's overshoot better than the PID.

Additionally, the MPC control system has shown that it is capable of adequately manipulating the plasma concentration within a simulated patient to alter the depth of anesthesia experienced by managing reference value changes. This is done without overshooting the new plasma concentration set during the process.

The simulations conducted have shown that the SNR experienced can be quite low, yet the system is robust enough to maintain a plasma concentration between the desired values of 2-4 $ug.ml^{-1}$ [37]. To keep the deviation of the plasma concentration as low as possible, it would be best to keep the SNR to a minimum of 15 dB.

Motion artefacts have been shown to have a potential influence on the system and could cause problems in the operation of the system. If the electrodes were to move during operation, they would introduce artefact voltages to the system that could corrupt sections of the MLAEP measured. Measures would need to be investigated to mitigate the influence of motion artefacts if they are shown to have an influence on the MLAEP readings of the system in practice.

## 8.1 Review of research questions

The tests and simulations in this thesis were conducted in an attempt to answer the research questions stated in Section 1.5. The research questions will then be individually addressed below.

### 8.1.1 Closed-loop control interfacing intra-ear monitoring and general anesthesia

Based on the simulations performed, closed-loop control can be used to interface intra-ear monitoring and general anesthesia. A model predictive controller (MPC) has shown to perform adequately for this application because it allows for the incorporation of a patient model within its control algorithm. With the patient model incorporated and the the performance criteria specified, the controller's step response is able to achieve a short settling time with no overshoot.

### 8.1.2 MLAEP latencies used as a control signal

There is currently no ubiquitous method to measure the anesthetic plasma concentration. It has, however, been found that MLAEP signal latencies correlate well with the concentration of anesthetic within a patient [66]. Therefore, MLAEP latencies have shown to be appropriate control signals.

### 8.1.3 System usability with a wide range of patients

The usability of the closed-loop control system is currently limited to paediatric patients in general anesthesia because of the limited research in the correlations of the MLAEP latencies and the anesthetic plasma concentration in other patient populations.

Based on the simulations conducted, the system is able to keep a wide range of simulated paediatric patients adequately sedated despite the wide range of inter-patient variability in anesthesia. The MPC controller would need to be made more robust to account for the rigorous pharmacokinetics of younger patients.

### 8.1.4 The anesthesiologist's user requirements

The system has been designed with an idea of the actions that the anesthesiologist might want to undertake during the maintenance phase of anesthesia. The system has shown that it is able to steadily change the simulated patient's plasma concentration to that set as the system's reference during the simulated maintenance phase. This can be used to increase the plasma concentration, deepening the anesthesia experienced, or lightening the anesthesia by decreasing the reference plasma concentration.

## 8.2 Future work

Using this work as a springboard, there is research to be conducted that could advance this system. The system could enter a prototyping phase to test the system's usability in animal tests first, and then in paediatric anesthesia. Further research could be conducted to acquire the necessary MLAEP latency and plasma concentration correlation to make the system available to wider range of patients. The system could also be adapted to a administer other drugs used in surgery. Lastly, further research could be conducted to improve the system's capability to administer the induction phase of anesthesia. Provided that sufficient data could be collected, a machine learning-based implementation could be undertaken. A machine learning-based implementation would be beneficial as it may allow for the automation of the induction phase of anesthesia, which is a more meticulous process to automate.

# Appendices

# Appendix A

# Notes from the private conversation with Dr Theodi Lombard, MBChB, DA(SA)

# Meeting with Anesthesiologist: Dr Theodi Lombard

Circumstances to change depth of anesthesia:

- Awareness
  - if their hemodynamics show (hypertensive) or move: ↑ infusion
- if blood pressure ↓ or patient is bleeding: ↓ infusion

- better to risk awareness than very low BP
  → awareness is not life-threatening, but it is traumatic

- Anesthesia is: causing sleep
  : muscle relaxing
  : keeping patient pain-free
  } Separate drugs do these

The LORD is my light and my salvation – whom shall I fear?
The LORD is the stronghold of my life – of whom shall I be afraid?
Psalm 27:1

W.r.t changing depth of anesthesia

a) Targeting Cp (Reference Cp)
- they don't necessarily know what Cp they are after
  → they would need to read it from a chart to know what Cp does what to the patient

- mainly use volatile anesthetics
- MAC value 1 is their target

- TIVA isn't as familiar to them

b) Having second patient model that translates [mg] of propofol to Cp
- better because they know what 10mg propofol does to a patient

The LORD Himself goes before you and will be with you;
He will never leave you nor forsake you.
Deuteronomy 31:8

• Reliability is the biggest concern

TCI systems : input age
weight
height

and the systems can infuse the necessary reliable effect

BUT don't forget that patients will react differently
- old people have slower arm-brain circulation

∴ a) Needs chart

Waking patient:
- rather dial the patient down than put off
- if they put things off, it takes long to switch off and surgeon could still want to do a few things
∴ rather dial it down to waking concentrations

God is working in you, giving you the desire
to obey Him and the power to do what pleases Him.
Philippians 2:13

I can do everything through Him who gives me strength.
Philippians 4:13

# Appendix B

# MATLAB code

## B.1 Average patient PK model initialization

```
% PK SIMULATION

age = 8.6;
weight = 29.2;


if age >= 0 && age <= 12
    V1= 0.4584 * weight;
    k10 = 0.1527 * weight.^(-0.3);

elseif age == 13
    V1 = 0.400 * weight;
    k10 = 0.0678;

elseif age == 14
    V1 = 0.342 * weight;
    k10 = 0.0792;

elseif age == 15
    V1 = 0.284 * weight;
    k10 = 0.0954;

elseif age == 16
    V1 = 0.22857 * weight;
    k10 = 0.119;
end

k12 = 0.114;
k13 = 0.0419;
k21 = 0.055;
k31 = 0.0033;
ke0 = 0.26;

V2 = V1 * k12/k21;
V3 = V1 * k13/k31;

```

## B.2 Paediatric patient population PK model initialization

```
% RANDOMIZED PAEDIATRIC PATIENT POPULATION

paed = struct('age', age, 'weight', weight, 'height', 125.9);

% Random patient generator
% x = sd*randn(range, 1) + mean

% ages = 4.3*randn(14, 1)+8.6
ages = [18.7070, 5.9529,11.8167,7.7726,12.4210,5.3111,
        2.5702,2.4838,10.6992,7.8373,7.7570,14.7030,
        9.8538,9.4506];
% weights = 14.6*randn(14, 1)+29.2
weights = [36.9395,15.2998,41.6690,34.8815,12.3224,
           29.7802,22.6213,30.7950,25.5419,26.4274,
           14.1195,24.4799,40.3913,54.6722];
% heights = 26.2*randn(14, 1)+125.9;
heights = [95.4944,188.1882,165.8832,130.3149,
           118.0084,107.5953,147.7186,107.7013,
           113.7987,149.0508,137.3217,149.3948,
           139.1240,115.3965];


ages = sort(round(ages));
weights = sort(weights);
heights = sort(heights);

paed.age = ages;
paed.weight = weights;
paed.height = heights;

age_data = zeros(1, 14);
height_data = zeros(1, 14);
weight_data = zeros(1, 14);
V1_data = zeros(1, 14);
V2_data = zeros(1, 14);
V3_data = zeros(1, 14);
k10_data = zeros(1, 14);
k12_data = zeros(1, 14);
k21_data = zeros(1, 14);
k13_data = zeros(1, 14);
k31_data = zeros(1, 14);
ke0_data = zeros(1, 14);
```

## B.3 Paediatric patient population PK model initialization

```
% PK SIMULATION
% n = 1; % Patient number in sturct

age = paed.age(n);
weight = paed.weight(n);
height = paed.height(n);


if age <= 12
    V1= 0.4584 * weight;
    global k10
    k10 = 0.1527 * weight.^(-0.3);

elseif age == 13
    V1 = 0.400 * weight;
    global k10
    k10 = 0.0678;

elseif age == 14
    V1 = 0.342 * weight;
    global k10
    k10 = 0.0792;

elseif age == 15
    V1 = 0.284 * weight;
    global k10
    k10 = 0.0954;

elseif age >= 16
    V1 = 0.22857 * weight;
    global k10
    k10 = 0.119;
end

global k12
k12 = 0.114;
global k13
k13 = 0.0419;
global k21
k21 = 0.055;
global k31
k31 = 0.0033;
global ke0
ke0 = 0.26;

V2 = V1 * k12/k21;
V3 = V1 * k13/k31;

age_data(n) = age;
height_data(n) = height;
weight_data(n) = weight;
V1_data(n) = V1;
V2_data(n) = V2;
V3_data(n) = V3;
k10_data(n) = k10;
k12_data(n) = k12;
k21_data(n) = k21;
k13_data(n) = k13;
k31_data(n) = k31;
ke0_data(n) = ke0;

```

## B.4 MPC initialization

```
% MPC ccontroller block initialization

% PK Model
%  Cp = Cp_Schnider(age, wight, height, gender);

% PD Model
%  Ce = Ce_Schnider(Cp);

% PK model (from "Optimized PID control of depth
%                 of hypnosis in anesthesia")

A = [-(k10+k12+k13)     k21     k31;
                k12     -k21      0;
                k13        0   -k31];

B = [1 1 ; 0 0 ; 0 0 ];

C = [1/V1 0 0];

D = 0;

Cp = ss(A, B, C, D);
Cp = setmpcsignals(Cp, 'MV', 1, 'UD', [2])

%[b, a] = ss2tf(A, B, C, D);

%Cp = tf(b, a);


% PD model (from "Optimized PID control of depth
%                 of hypnosis in anesthesia")
%Ce = tf(ke0, [1, ke0]) * Cp;


% Nb-to-Cp correlation(from "Impact of propofol on MLAEP in children")
%{According to Fig 8 in "Pharmacokinetic models for propofol—defining and
illuminating the devil in the detail", the output of PK, Cp, is in [ug/ml],
so we don't need to convert the logistic function's units
%}
% f(x) = L/(1+m*e^(-k*t)) + c

L = 44;
k = 0.8853
x0 = 0;
c = 55;
m = 440;

% Nb latency-to-Cp
%f(x) = (-log(L./(x-c)-1)+k*x0)./k; % beware: exclude all elements x<55

tfCe = tf(ke0, [1, ke0]);


% according to "Guidelines for Intravenous Dosing"
    % Lower constraint MV = 0 mg/kg/min
    % Upper constraint MV = 250 ug/kg/min


init_Cp = 4;    % Initial plasma concentration of propofol in patient
global ref_Cp
ref_Cp = 3;     % Reference plasma concentration

%% create MPC controller object with sample time
mpcCp = mpc(Cp, 10);
%% specify prediction horizon
mpcCp.PredictionHorizon = 20;
%% specify control horizon
mpcCp.ControlHorizon = 2;
%% specify nominal values for inputs and outputs
mpcCp.Model.Nominal.U = 0;
mpcCp.Model.Nominal.Y = 0;
%% specify constraints for MV and MV Rate
mpcCp.MV(1).Min = 0;
```

```
mpcCp.MV(1).Max = 0.250.*weight; %
%% specify overall adjustment factor applied to weights
beta = 0.54881;
%% specify weights
mpcCp.Weights.MV = 0*beta;
mpcCp.Weights.MVRate = 0.08/beta;
mpcCp.Weights.OV = 0.75*beta;
mpcCp.Weights.ECR = 100000;
%% specify simulation options
options = mpcsimopt();
options.RefLookAhead = 'off';
options.MDLookAhead = 'off';
options.Constraints = 'on';
options.OpenLoop = 'off';
%% run simulation
%sim(mpcCp, 21, mpcCp_RefSignal, mpcCp_MDSignal, options);


```

## B.5 MPC controller simulation for all 14 patients

```
% The MPC Automated Simulation

% ***DO YOU WANT TO CLEAR THE LOG?**
Simulink.sdi.clear

% Initialize the MPC using the average patient from the population in
% Khunle
pkpd_model = 'D:\Desktop\Masters from Laptop\MATLAB\Masters\PKPD
models\PKPD_Paedfusor.m';
run(pkpd_model);

mpc_model = 'D:\Desktop\Masters from Laptop\MATLAB\Masters\MPC\MPC.m';
run(mpc_model);

simulink_model = 'D:\Desktop\Masters from
Laptop\MATLAB\Masters\Simulink\Main\MLAEP_simulink_model.slx';
tic
sim(simulink_model);
toc

% Initialize the patient population
patient_pop = 'D:\Desktop\Masters from Laptop\MATLAB\Masters\PKPD
models\paediatric_patients2.m';
run(patient_pop);

% Run the 14 patients through the system
n=1;
while n <= 14
    pkpd_model = 'D:\Desktop\Masters from Laptop\MATLAB\Masters\PKPD
    models\PKPD_Paedfusor_edits.m';
    run(pkpd_model);

    mpc_model = 'D:\Desktop\Masters from Laptop\MATLAB\Masters\MPC\MPC.m';
    run(mpc_model);

    simulink_model = 'D:\Desktop\Masters from
    Laptop\MATLAB\Masters\Simulink\Main\MLAEP_simulink_model.slx';
    tic
    sim(simulink_model);
    toc

    n=n+1
end

```

## B.6 PID initialization

```
% PK-PD-latency

% In the loop:
% 1: Infusion into patient to get the Cp
% Optional: Cp-to-Ce
% 2: Cp to latency conversion

% In the MPC
% 1: Convert the latency to Cp
% 2: Convert the Cp to the necessary infusion rate


% In the loop:

% PK Model
%  Cp = Cp_Schnider(age, wight, height, gender);

% PD Model
%  Ce = Ce_Schnider(Cp);

% PK model (from "Optimized PID control of depth
%                  of hypnosis in anesthesia")

A = [-(k10+k12+k13)      k21      k31;
    k12      -k21     0;
    k13      0    -k31];

B = [1; 0; 0];

C = [1/V1 0 0];

D = 0;

[b, a] = ss2tf(A, B, C, D);

Cp = tf(b, a);


% PD model (from "Optimized PID control of depth
%                  of hypnosis in anesthesia")
Ce = tf(ke0, [1, ke0]) * Cp;


% Nb to Cp conversion (from "Impact of propofol
%                            on MLAEP in children")
%{
According to Fig 8 in "Pharmacokinetic models for propofol—defining and
illuminating the devil in the detail", the output of PK, Cp, is in [ug/ml],
so we don't need to convert the logistic function's units
%}
L = 44;
k = 1.5;
x0 = 4;
c = 55;


syms f(x)
% Cp-to-Nb latency
%f(x) = L/(1+exp(-k*(x-x0)))+c;


% Nb latency-to-Cp
%f(x) = (-log(L./(x-c)-1)+k*x0)./k; % beware: exclude all elements x<55

tfCe = tf(ke0, [1, ke0]);

opt = pidtuneOptions('DesignFocus','reference-tracking')
PID_C = pidtune(Cp, 'pid2')
```

## B.7 PID controller simulation for all 14 patients

```
% The PID Automated Simulation

% ***DO YOU WANT TO CLEAR THE LOG?**
 Simulink.sdi.clear

% ////////////////////////// FOR USE ON PERSONAL LAPTOP \\\\\\\\\\\\\\\\\\\\\\

% Initialize the MPC using the average patient from the population in
% Khunle
pkpd_model = 'C:\Users\TPSetati\Google Drive\Masters from Laptop\MATLAB\Masters\PKPD models\PKPD_Paedfusor.m';
run(pkpd_model);

controller_parameters = 'C:\Users\TPSetati\Google Drive\Masters from Laptop\MATLAB\Masters\PID\PID.m';
run(controller_parameters);

simulink_model = 'C:\Users\TPSetati\Google Drive\Masters from Laptop\MATLAB\Masters\Simulink\Main PID\2019\MLAEP_simulink_model_PID.slx';
tic
sim(simulink_model);
toc

% Initialize the patient population
patient_pop = 'C:\Users\TPSetati\Google Drive\Masters from Laptop\MATLAB\Masters\PKPD models\paediatric_patients.m';
run(patient_pop);

% Run the 14 patients through the system
n=1;
pkpd_model = 'C:\Users\TPSetati\Google Drive\Masters from Laptop\MATLAB\Masters\PKPD models\PKPD_Paedfusor_edits.m';

while n <= 14

    run(pkpd_model);

    simulink_model = 'C:\Users\TPSetati\Google Drive\Masters from Laptop\MATLAB\Masters\Simulink\Main PID\MLAEP_simulink_model_PID.slx';
    tic
    sim(simulink_model);
    toc

    n=n+1
end
```

## B.8 Measurement noise simulation

```
% The Measurement Noise Automated Simulation

% ***DO YOU WANT TO CLEAR THE LOG?**
Simulink.sdi.clear

signal_power = 31.6832  % Calculated from the latency. The amplitude as the difference between fully anesthetized (63 ms) and fully awake (55 ms)
SNR_dB = [40, 30, 20, 15, 10, 5, 0, -3]
SNR = 10.^((SNR_dB)/10)
noise_power = signal_power ./ SNR
s = numel(noise_power)

% http://facstaff.cbu.edu/rprice/lectures/tuning.html
IAE = zeros(s, 1); % Integral absolute error: penalizes all errors equally
ISE = zeros(s, 1); % Integral Squared Error. Penalizes large errors more than small
ITAE = zeros(s, 1); % Integral Time Weighted Absolute Error. Penalizes persistant errors
ITSE = zeros(s, 1); % Integral Time Squared Error.


% Initialize the MPC using the average patient from the population in
% Khunle
% pkpd_model = 'D:\Desktop\Masters from Laptop\MATLAB\Masters\PKPD models\PKPD_Paedfusor.m';
pkpd_model = 'C:\Users\TPSetati\Google Drive\Masters from Laptop\MATLAB\Masters\PKPD models\PKPD_Paedfusor.m';
run(pkpd_model);

i = 1;
for r = 1:s
    noise_power_used = noise_power(4)
    seed = round(50000*rand(1, 1))
    % mpc_model = 'D:\Desktop\Masters from Laptop\MATLAB\Masters\MPC\MPC.m';
    mpc_model = 'C:\Users\TPSetati\Google Drive\Masters from Laptop\MATLAB\Masters\MPC\MPC.m';
    run(mpc_model);

    A_noise = 8/sqrt(SNR(i));
    mod1 = tf(A_noise, 1);
    indist = [mod1];
    setindist(mpcCp,'model',indist);

    %simulink_model = 'D:\Desktop\Masters from Laptop\MATLAB\Masters\Simulink\Measurement noise\MLAEP_simulink_model_edits_with_measurement_noise.slx';
    simulink_model = 'C:\Users\TPSetati\Google Drive\Masters from Laptop\MATLAB\Masters\Simulink\Measurement noise\MLAEP_simulink_model_edits_with_measurement_noise.slx';
    sim(simulink_model);

    t = transpose(1:1:numel(cp_data));
    IAE(i) = trapz(abs(cp_data-ref));
    ISE(i) = trapz((cp_data-ref).^2);
    ITAE(i) = trapz(t.*(abs(cp_data-ref)));
    ITSE(i) = trapz(t.*((cp_data-ref).^2));

    i = i+2;



end

IAE


```

# Appendix C

# MATLAB/Simulink MPC Designer

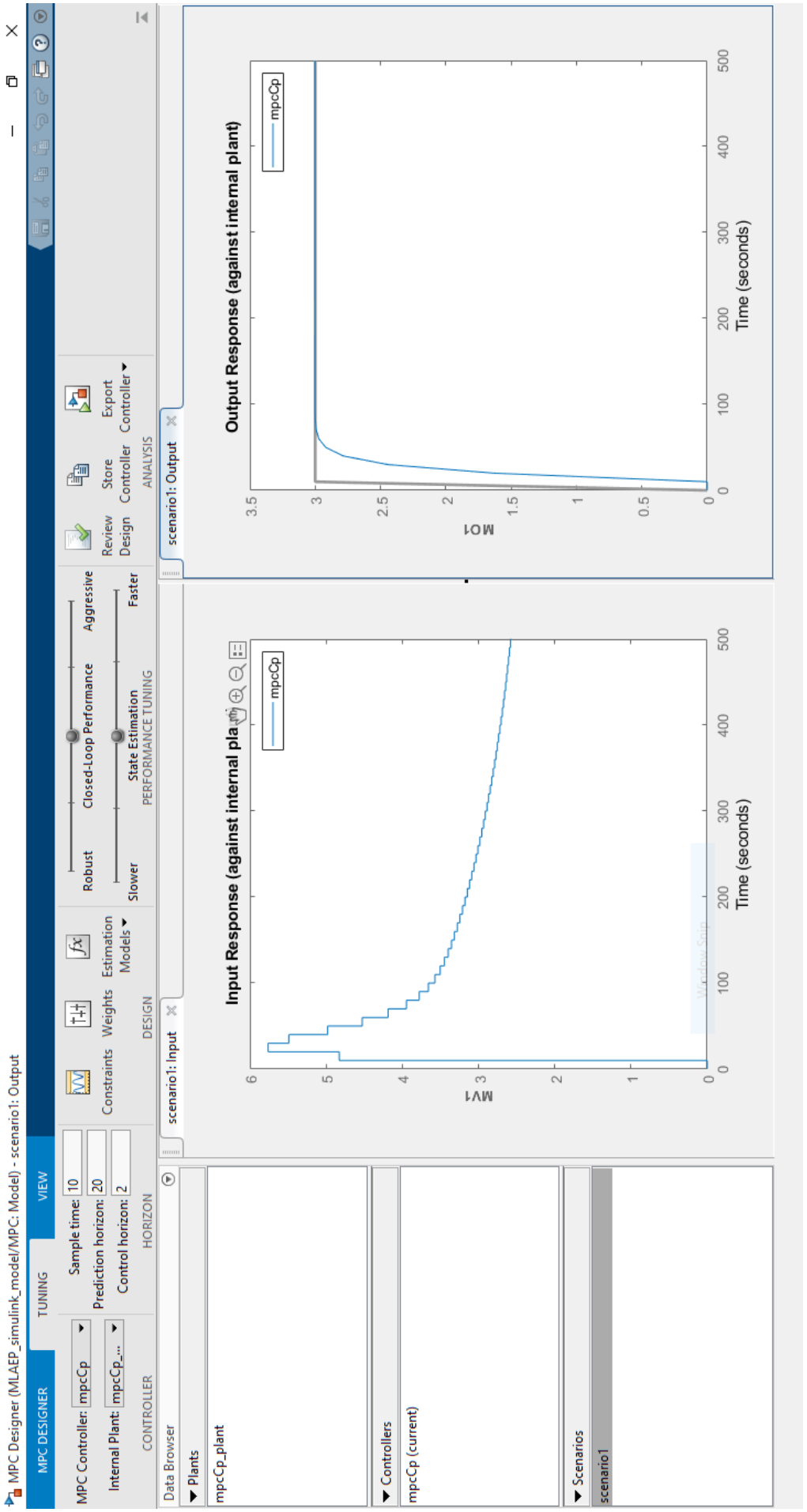

# Appendix D

# MATLAB/Simulink PID Tuner

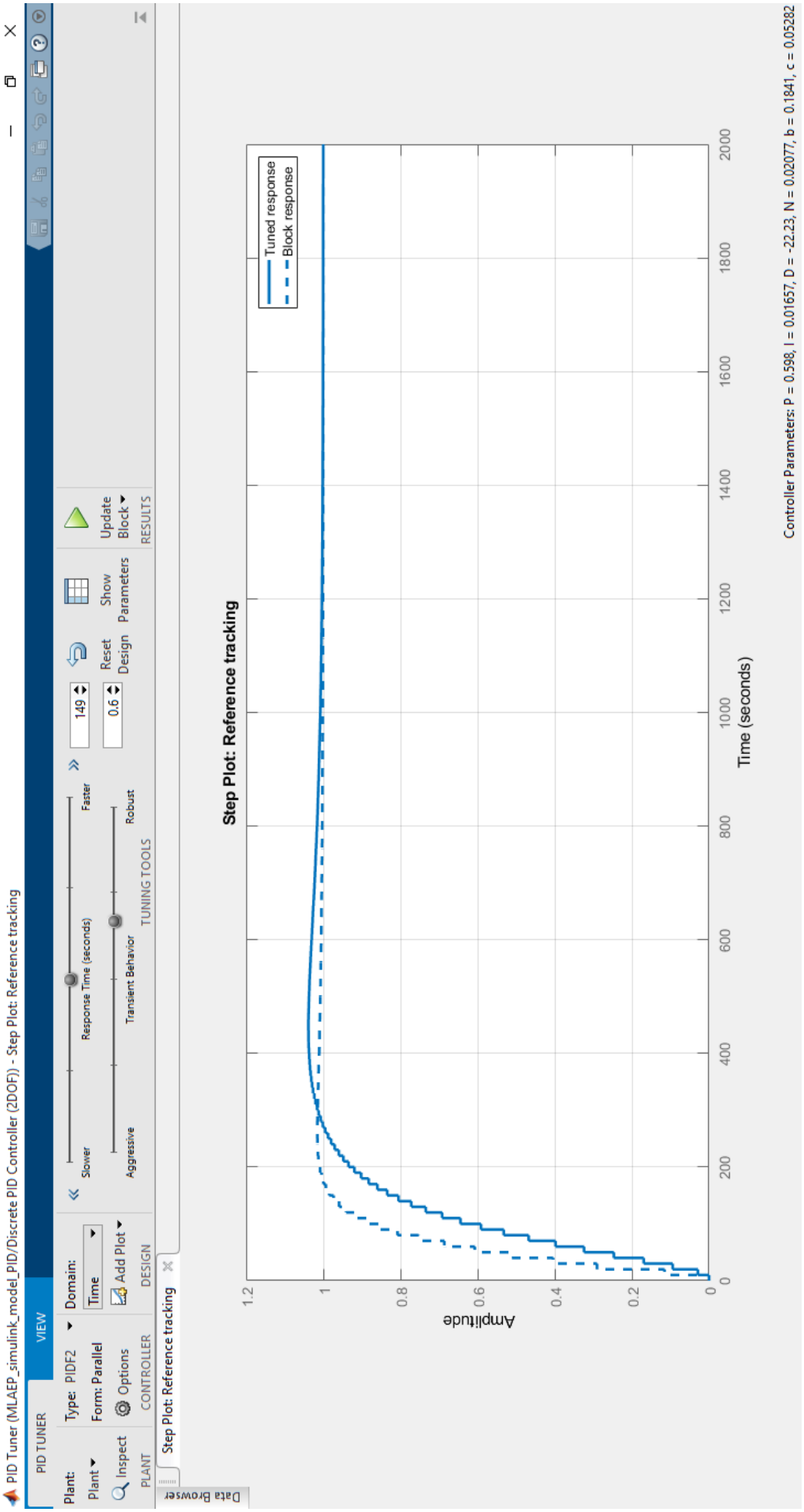

# Bibliography

[1] H. K. et al., "Sasa practice guidelines 2018 revision", *Southern African Journal of Anaesthesia and Analgesia 2018*, vol. 4, no. 6, pp. 1–119, 1993.

[2] S. J. Swierzewski. (Oct. 2001). "Anesthesia types of anesthesia", [Online]. Available: http://www.healthcommunities.com/before-after-surgery/overview-types-anesthesia.shtml (visited on 02/21/2020).

[3] C. W. Frei, "Fault tolerant control concepts applied to anesthesia", *Available at SSRN 1946892*, 2000.

[4] J. Diedericks, "Anesthetics", *Continuing Medical Education*, vol. 30, no. 6, p. 192, Jun. 2012.

[5] (Aug. 2013). "Control system", [Online]. Available: https://www.britannica.com/technology/control-system (visited on 04/25/2020).

[6] C. Rosow and P. J. Manberg, "Bispectral index monitoring", *Anesthesiology Clinics of North America*, vol. 19, no. 4, pp. 947–966, 2001.

[7] B. Oken and T. Phillips, "Evoked potentials: Clinical", in *Encyclopedia of neuroscience*, Elsevier Ltd, 2009, pp. 19–28.

[8] M. I. Al-Kadi *et al.*, "Evolution of electroencephalogram signal analysis techniques during anesthesia", *Sensors*, vol. 13, no. 5, pp. 6605–6635, 2013.

[9] D. Schwender *et al.*, "Midlatency auditory evoked potentials and motor signs of wakefulness during anaesthesia with midazolam.", *British journal of anaesthesia*, vol. 79, no. 1, pp. 53–58, 1997.

[10] C. Wessels, "Design of an in-ear eeg device to detect consciousness levels and be used in monitoring anesthesia levels of a patient in a medical setting.", M.S. thesis, Stellenbosch University, Mar. 2019.

[11] H. C. Hemmings and T. D. Egan, *Pharmacology and Physiology for Anesthesia E-Book: Foundations and Clinical Application*. Elsevier Health Sciences, 2012.

[12] S. Bibian, "Automation in clinical anesthesia", Ph.D. dissertation, University of British Columbia, 2006.

[13] J. A. Méndez *et al.*, "Adaptive computer control of anesthesia in humans", *Computer methods in biomechanics and biomedical engineering*, vol. 12, no. 6, pp. 727–734, 2009.

[14] I. Nacu *et al.*, "Advanced model-based control studies for the induction and maintenance of intravenous anaesthesia", *IEEE Transactions on biomedical engineering*, vol. 62, no. 3, pp. 832–841, 2014.

[15] J.-O. Hahn *et al.*, "Robust closed-loop control of hypnosis with propofol using wavcns index as the controlled variable", *Biomedical Signal Processing and Control*, vol. 7, no. 5, pp. 517–524, 2012.

[16] L. Oakden-Rayner. (Jun. 2018). "The end of human doctors - understanding automation", [Online]. Available: https://lukeoakdenrayner.wordpress.com/2017/05/03/the-end-of-human-doctors-understanding-automation/ (visited on 04/02/2020).

[17] Wood Library Museum. (2019). "History of Anesthesia", [Online]. Available: https://www.woodlibrarymuseum.org/history-of-anesthesia/ (visited on 11/13/2019).

[18] Michigan Medicine. (2019). "Monitoring during anesthesia", [Online]. Available: https://www.uofmhealth.org/health-library/rt1592 (visited on 04/13/2020).

[19] E. N. Brown *et al.* (Dec. 2010). "General anesthesia, sleep, and coma: Nejm", [Online]. Available: https://www.nejm.org/doi/pdf/10.1056/NEJMra0808281?articleTools=true (visited on 06/14/2019).

[20] C. Hull, "Pharmacokinetics and pharmacodynamics", *British Journal of Anaesthesia*, vol. 51, no. 7, pp. 579–594, 1979.

[21] M. Behne *et al.*, "Clinical pharmacokinetics of sevoflurane", *Clinical Pharmacokinetics*, vol. 36, no. 1, pp. 13–26, Jan. 1999, ISSN: 1179-1926. DOI: 10.2165/00003088-199936010-00002.

[22] A. Absalom *et al.*, "Pharmacokinetic models for propofol - defining and illuminating the devil in the detail", *British journal of anaesthesia*, vol. 103, no. 1, pp. 26–37, 2009.

[23] A. Absalom *et al.*, "Accuracy of the 'paedfusor'in children undergoing cardiac surgery or catheterization", *British Journal of Anaesthesia*, vol. 91, no. 4, pp. 507–513, 2003.

[24] A. Rigouzzo *et al.*, "Pharmacokinetic-pharmacodynamic modeling of propofol in children", *Anesthesiology: The Journal of the American Society of Anesthesiologists*, vol. 113, no. 2, pp. 343–352, 2010.

[25] T. E. Miller and T. J. Gan, *Closed-loop systems in anesthesia: Reality or fantasy?*, 2013.

[26] A. Husney *et al.* (Dec. 2018). "General, regional, and local anesthesia", [Online]. Available: https://myhealth.alberta.ca/Health/Pages/conditions.aspx?hwid=stg124289& (visited on 06/14/2019).

[27] S. F. Malamed, *Handbook of local anesthesia*. Elsevier Health Sciences, 2004.

[28] (Jul. 2018). "Local anaesthesia", [Online]. Available: https://www.nhs.uk/conditions/local-anaesthesia/ (visited on 06/14/2019).

[29] (). "Regional anesthesia", [Online]. Available: https://www.longdom.org/scholarly/regional-anesthesia-journals-articles-ppts-list-4074.html (visited on 06/14/2019).

[30] A. Husney and J. M. Freedman, *Regional anesthesia*, Aug. 2019.

[31] B. Dalens, "Regional anesthesia in children", *Anesthesia & Analgesia*, vol. 68, no. 5, pp. 654–672, 1989.

[32] B. Musizza and S. Ribaric. (Dec. 2010). "Monitoring the depth of anaesthesia", [Online]. Available: https://www.mdpi.com/1424-8220/10/12/10896 (visited on 06/14/2019).

[33] B. J. Anderson and O. Bagshaw, "Practicalities of total intravenous anesthesia and target-controlled infusion in children", *Anesthesiology: The Journal of the American Society of Anesthesiologists*, vol. 131, no. 1, pp. 164–185, 2019.

[34] S. Bibian *et al.*, "Clinical anesthesia and control engineering: Terminology, concepts and issues", in *2003 European Control Conference (ECC)*, IEEE, 2003, pp. 2430–2440.

[35] R. D. Miller *et al.*, "Miller's anesthesia", eng, in, Saint Louis: Elsevier, 2014, ch. 20, pp. 509–539, ISBN: 0702052833.

[36] P. F. White, "A history of intravenous anesthesia", in *The Wondrous Story of Anesthesia*, Springer, 2014, pp. 629–639.

[37] A. Nimmo *et al.*, "Guidelines for the safe practice of total intravenous anaesthesia (tiva): Joint guidelines from the association of anaesthetists and the society for intravenous anaesthesia", *Anaesthesia*, vol. 74, no. 2, pp. 211–224, 2019.

[38] I. J. Rampil, "A primer for eeg signal processing in anesthesia", *Anesthesiology: The Journal of the American Society of Anesthesiologists*, vol. 89, no. 4, pp. 980–1002, 1998.

[39] L. Voss and J. Sleigh, "Monitoring consciousness: The current status of eeg-based depth of anaesthesia monitors", *Best practice & research Clinical anaesthesiology*, vol. 21, no. 3, pp. 313–325, 2007.

[40] G. H. Klem, "The ten-twenty electrode system of the international federation. the internanional federation of clinical nenrophysiology", *Electroencephalogr. Clin. Neurophysiol. Suppl.*, vol. 52, pp. 3–6, 1999.

[41] M. Grigg-Damberger and N. R. Foldvary-Schaefer, *Sleep-related Epilepsy and Electroencephalography, An Issue of Sleep Medicine Clinics-E-Book*, 1. Elsevier Health Sciences, 2012, vol. 7.

[42] D. Looney *et al.*, "An in-the-ear platform for recording electroencephalogram", in *2011 Annual International Conference of the IEEE Engineering in Medicine and Biology Society*, IEEE, 2011, pp. 6882–6885.

[43] B. M. Gorman and D. R. Flatla, "A framework for speechreading acquisition tools", in *Proceedings of the 2017 CHI Conference on Human Factors in Computing Systems*, 2017, pp. 519–530.

[44] P. Walsh *et al.*, "The clinical role of evoked potentials", *Journal of neurology, neurosurgery & psychiatry*, vol. 76, no. suppl 2, pp. ii16–ii22, 2005.

[45] P. Kidmose *et al.*, "Auditory evoked responses from ear-eeg recordings", in *2012 Annual International Conference of the IEEE Engineering in Medicine and Biology Society*, IEEE, 2012, pp. 586–589.

[46] P. S. Myles, "Prevention of awareness during anaesthesia", *Best practice & research Clinical anaesthesiology*, vol. 21, no. 3, pp. 345–355, 2007.

[47] A. Sharma and R. J. Roy, "Design of a recognition system to predict movement during anesthesia", *IEEE Transactions on Biomedical engineering*, vol. 44, no. 6, pp. 505–511, 1997.

[48] I. Pichlmayr *et al.*, *The electroencephalogram in anesthesia: fundamentals, practical applications, examples*. Springer Science & Business Media, 2012.

[49] H. Schwilden *et al.*, "Closed-loop feedback control of propofol anaesthesia by quantitative eeg analysis in humans", *BJA: British Journal of Anaesthesia*, vol. 62, no. 3, pp. 290–296, 1989.

[50] J. Schüttler and H. Schwilden, "Feedback control of intravenous anesthetics by quantitative eeg", in *Control and Automation in Anaesthesia*, Springer, 1995, pp. 194–207.

[51] I. Rampil *et al.*, "Spectral edge frequency - a new correlate of anesthetic depth", *Anesthesiology: The Journal of the American Society of Anesthesiologists*, vol. 53, no. 3 Suppl, S12–S12, 1980.

[52] S. Bowles *et al.*, "Effects of anaesthesia on the eeg - bispectral analysis correlates with movement", in *Handbook of Spinal Cord Monitoring*, Springer, 1994, pp. 247–252.

[53] H. Q. Ontario *et al.*, "Bispectral index monitor: An evidence-based analysis", *Ont Health Technol Assess Ser*, vol. 4, no. 9, pp. 1–70, 2004.

[54] S. Bibian *et al.*, "Method and apparatus for the estimation of anesthetic depth using wavelet analysis of the electroencephalogram", US Patent 7,373,198, May 2008.

[55] T. Zikov, "Monitoring the anesthetic-induced unconsciousness (hypnosis) using wavelet analysis of the electroencephalogram", Ph.D. dissertation, University of British Columbia, 2002.

[56] A. B. Evans. (Apr. 2020). "Clinical utility of evoked potentials". S. R. Benbadis, Ed., [Online]. Available: https://emedicine.medscape.com/article/1137451-overview (visited on 02/22/2020).

[57] I. Singh. (). "The visual pathway of the brain", [Online]. Available: http://www.brainkart.com/article/The-Visual-Pathway-of-the-Brain_19029/ (visited on 09/14/2020).

[58] J. J. Stockard *et al.*, "Visually evoked potentials to electronic pattern reversal: Latency variations with gender, age, and technical factors", *American Journal of EEG Technology*, vol. 19, no. 4, pp. 171–204, 1979.

[59] G. Fein and F. F. Brown, "Gender differences in pattern reversal evoked potentials in normal elderly", *Psychophysiology*, vol. 24, no. 6, pp. 683–690, 1987.

[60] H. Hayashi and M. Kawaguchi, "Intraoperative monitoring of flash visual evoked potential under general anesthesia", *Korean journal of anesthesiology*, vol. 70, no. 2, p. 127, 2017.

[61] S. R. Passmore *et al.*, "The origin, and application of somatosensory evoked potentials as a neurophysiological technique to investigate neuroplasticity", *The Journal of the Canadian Chiropractic Association*, vol. 58, no. 2, p. 170, 2014.

[62] R. W. Homan *et al.*, "Cerebral location of international 10–20 system electrode placement", *Electroencephalography and clinical neurophysiology*, vol. 66, no. 4, pp. 376–382, 1987.

[63] G. Cruccu *et al.*, "Recommendations for the clinical use of somatosensory-evoked potentials", *Clinical neurophysiology*, vol. 119, no. 8, pp. 1705–1719, 2008.

[64] G. Plourde, "Auditory evoked potentials", *Best Practice & Research Clinical Anaesthesiology*, vol. 20, no. 1, pp. 129–139, 2006.

[65] H. Mantzaridis and G. Kenny, "Auditory evoked potential index: A quantitative measure of changes in auditory evoked potentials during general anaesthesia", *Anaesthesia*, vol. 52, no. 11, pp. 1030–1036, 1997.

[66] G. Kuhnle *et al.*, "Impact of propofol on mid-latency auditory-evoked potentials in children", *British journal of anaesthesia*, vol. 110, no. 6, pp. 1001–1009, 2013.

[67] T. McGee *et al.*, "Toward a strategy for analyzing the auditory middle-latency response waveform", *Audiology*, vol. 27, no. 2, pp. 119–130, 1988.

[68] F. Padula *et al.*, "Optimized pid control of depth of hypnosis in anesthesia", *Computer methods and programs in biomedicine*, vol. 144, pp. 21–35, 2017.

[69] N. J. Cowley *et al.*, "Assessment of the performance of the marsh model in effect site mode for target controlled infusion of propofol during the maintenance phase of general anaesthesia in an unselected population of neurosurgical patients", *European Journal of Anaesthesiology (EJA)*, vol. 30, no. 10, pp. 627–632, 2013.

[70] D. J. Eleveld *et al.*, "A general purpose pharmacokinetic model for propofol", *Anesthesia & Analgesia*, vol. 118, no. 6, pp. 1221–1237, 2014.

[71] D. J. Stone *et al.*, "Engineering control into medicine", *Journal of critical care*, vol. 30, no. 3, 652–e1, 2015.

[72] V. Kumar *et al.*, "A review on classical and fuzzy pid controllers", *International Journal of Intelligent Control and Systems*, vol. 16, no. 3, pp. 170–181, 2011.

[73] A. E.-N. Gene F. Franklin J. David Powell, "Feedback control of dynamic systems", in, 7th ed. Pearson Education Limited, 2015, ch. 4, pp. 216–237.

[74] M. M. Struys *et al.*, "Closed loops in anaesthesia", *Best Practice & Research Clinical Anaesthesiology*, vol. 20, no. 1, pp. 211–220, 2006.

[75] J. G. Ziegler, N. B. Nichols, *et al.*, "Optimum settings for automatic controllers", *trans. ASME*, vol. 64, no. 11, 1942.

[76] J. Ziegler and N. Nichols, "Process lags in automatic control circuits", *Trans. ASME*, vol. 65, no. 5, pp. 433–443, 1943.

[77] Y. Huang and S. Yasunobu, "A general practical design method for fuzzy pid control from conventional pid control", in *Ninth IEEE International Conference on Fuzzy Systems. FUZZ-IEEE 2000 (Cat. No. 00CH37063)*, IEEE, vol. 2, 2000, pp. 969–972.

[78] M. Moradi, "New techniques for pid controller design", in *Proceedings of 2003 IEEE Conference on Control Applications, 2003. CCA 2003.*, IEEE, vol. 2, 2003, pp. 903–908.

[79] R. Miller *et al.*, "Predictive pid", *ISA transactions*, vol. 38, no. 1, pp. 11–23, 1999.

[80] A. Ali and S. Majhi, "Integral criteria for optimal tuning of pi/pid controllers for integrating processes", *Asian Journal of Control*, vol. 13, no. 2, pp. 328–337, 2011.

[81] M. Zhuang and D. Atherton, "Tuning pid controllers with integral performance criteria", in *International Conference on Control 1991. Control'91*, IET, 1991, pp. 481–486.

[82] R. M. Price. (Jul. 2003). "Controller tuning", [Online]. Available: http://facstaff.cbu.edu/rprice/lectures/tuning.html (visited on 08/14/2019).

[83] J. Zumberge and K. M. Passino, "A case study in intelligent vs. conventional control for a process control experiment", *Control Engineering Practice*, vol. 6, no. 9, pp. 1055–1075, 1998.

[84] K. M. Passino, "Bridging the gap between conventional and intelligent control", *IEEE Control Systems Magazine*, vol. 13, no. 3, pp. 12–18, 1993.

[85] C.-C. Lee, "Fuzzy logic in control systems: Fuzzy logic controller. i", *IEEE Transactions on systems, man, and cybernetics*, vol. 20, no. 2, pp. 404–418, 1990.

[86] R. Findeisen and F. Allgöwer, "An introduction to nonlinear model predictive control", in *21st Benelux meeting on systems and control*, Technische Universiteit Eindhoven Veldhoven Eindhoven, The Netherlands, vol. 11, 2002, pp. 119–141.

[87] C. E. Garcia *et al.*, "Model predictive control: Theory and practice - a survey", *Automatica*, vol. 25, no. 3, pp. 335–348, 1989.

[88] (). "Mpc modeling", The MathWorks Inc., [Online]. Available: https://www.mathworks.com/help/mpc/gs/mpc-modeling.html (visited on 07/04/2020).

[89] J. B. Rawlings, "Tutorial overview of model predictive control", *IEEE control systems magazine*, vol. 20, no. 3, pp. 38–52, 2000.

[90] B. D. Anderson and J. B. Moore, *Optimal control: linear quadratic methods*. Courier Corporation, 2007.

[91] D. Simon, "Kalman filtering", *Embedded systems programming*, vol. 14, no. 6, pp. 72–79, 2001.

[92] (). "Adaptive mpc", The MathWorks Inc., [Online]. Available: https://www.mathworks.com/help/mpc/ug/adaptive-mpc.html (visited on 07/04/2020).

[93] (). "Gain-scheduled mpc", The MathWorks Inc., [Online]. Available: https://www.mathworks.com/help/mpc/ug/gain-scheduling-mpc.html (visited on 07/04/2020).

[94] M. Ulusoy. (). "Understanding model predictive control, part 4: Adaptive, gain-scheduled, and nonlinear mpc", [Online]. Available: https://www.mathworks.com/videos/understanding-model-predictive-control-part-4-adaptive-gain-scheduled-and-nonlinear-mpc-1530606851674.html (visited on 09/20/2020).

[95] J. F. Biebuyck *et al.*, "The use of computers for controlling the delivery of anesthesia", *The Journal of the American Society of Anesthesiologists*, vol. 77, no. 3, pp. 563–581, 1992.

[96] M. M. Struys *et al.*, "Performance evaluation of two published closed-loop control systems using bispectral index monitoring: A simulation study", *The Journal of the American Society of Anesthesiologists*, vol. 100, no. 3, pp. 640–647, 2004.

[97] (). "Control system basics", [Online]. Available: https://ledin.com/control-systems-basics/ (visited on 09/24/2020).

[98] J. Quevedo *et al.*, "A performance evaluation system of process control", *IFAC Proceedings Volumes*, vol. 25, no. 6, pp. 233–238, 1992.

[99] J. B. Riggs, *Chemical process control*. Ferret, 1999.

[100] J. R. Varvel *et al.*, "Measuring the predictive performance of computer-controlled infusion pumps", *Journal of pharmacokinetics and biopharmaceutics*, vol. 20, no. 1, pp. 63–94, 1992.

[101] M. Kansanaho *et al.*, "Model-driven closed-loop feedback infusion of atracurium and vecuronium during hypothermic cardiopulmonary bypass", *Journal of cardiothoracic and vascular anesthesia*, vol. 11, no. 1, pp. 58–61, 1997.

[102] (Apr. 2020). "What is matlab?: How it works: Skill career growth: Advantages", [Online]. Available: https://www.educba.com/what-is-matlab/ (visited on 08/05/2019).

[103] *What is matlab?*, The MathWorks, Inc.

[104] (). "Simulink", [Online]. Available: https://www.mathworks.com/help/simulink/ (visited on 08/05/2019).

[105] M. Melda Ulusoy, *Understanding model predictive control, part 3: Mpc design parameters*, Mar. 2020.

[106] J. Coetzee, *Guidelines for intravenous dosing*, Department of Anaesthesiology and Critical Care, Stellenbosch University, Stellenbosch, South Africa, 2018.

[107] M. Struys *et al.*, "Performance of the arx-derived auditory evoked potential index as an indicator of anesthetic depth", *Anesthesiology*, vol. 96, no. 4, pp. 803–816, 2002.

[108] E. W. Jensen *et al.*, "On-line analysis of middle latency auditory evoked potentials (mlaep) for monitoring depth of anaesthesia in laboratory rats", *Medical engineering & physics*, vol. 20, no. 10, pp. 722–728, 1999.

[109] C. Thornton *et al.*, "Effect of propofol on the auditory evoked response and oesophageal contractility", *British Journal of Anaesthesia*, vol. 63, no. 4, pp. 411–417, 1989.

[110] S. Palm *et al.*, "Dose–response relationship of propofol on mid-latency auditory evoked potentials (mlaep) in cardiac surgery", *Acta anaesthesiologica scandinavica*, vol. 45, no. 8, pp. 1006–1010, 2001.

[111] D. Schwender *et al.*, "The effects of anesthesia with increasing end-expiratory concentrations of sevoflurane on midlatency auditory evoked potentials", *Anesthesia & Analgesia*, vol. 81, no. 4, pp. 817–822, 1995.

[112] T. Leibovich-Raveh *et al.*, "A new method for calculating individual subitizing ranges", 2018.

[113] (). "Pid tuner", The MathWorks, Inc., [Online]. Available: https://www.mathworks.com/help/control/ref/pidtuner-app.html#:~:text=all%20in%20page-,Description,balance%20between%20performance%20and%20robustness.&text=You%20can%20interactively%20refine%20the,setpoint%20tracking%20or%20disturbance%20rejection. (visited on 07/04/2020).

[114] T. M. Inc. (2009). "Pid controller (2dof)", [Online]. Available: https://www.mathworks.com/help/simulink/slref/pidcontroller2dof.html (visited on 02/10/2020).

[115] (). "Optimize performance", The MathWorks, Inc., [Online]. Available: https://www.mathworks.com/help/simulink/performance%7B%5C_%7Dperformance.html (visited on 07/04/2020).

[116] N. Goddard and D. Smith, "Unintended awareness and monitoring of depth of anaesthesia", *Continuing Education in Anaesthesia, Critical Care & Pain*, vol. 13, no. 6, pp. 213–217, 2013.

[117] R. Kieser *et al.*, "Definition of signal-to-noise ratio and its critical role in split-beam measurements", *ICES Journal of Marine Science*, vol. 62, no. 1, pp. 123–130, 2005.

[118] (). "Cyton biosensing board (8-channels)", [Online]. Available: https://shop.openbci.com/products/cyton-biosensing-board-8-channel?variant=38958638542 (visited on 08/22/2020).

[119] H. Kluyts, *South african society of anaesthesiologists practice guidelines 2012 revision*, 2012 Revision, South African Society of Anaesthesiologists, 2012.

[120] D. Dr. Theodi Lombard MBChB, Private Communication, Pretoria, Gauteng, South Africa, 2020.

[121] A. Simakov and J. Webster, "Motion artifact from electrodes and cables", 2010.

[122] S. L. Kappel *et al.*, "Physiological artifacts in scalp eeg and ear-eeg", *Biomedical engineering online*, vol. 16, no. 1, p. 103, 2017.

[123] J. E. Hawkins. (Oct. 2018). "Transmission of sound by bone conduction", [Online]. Available: https://www.britannica.com/science/ear/Transmission-of-sound-by-bone-conduction (visited on 08/14/2020).

[124] (Nov. 2019). "Diy syringe pumps vs. commercial syringe pumps", [Online]. Available: https://www.chemyx.com/support/knowledge-base/applications/diy-syringe-pump-comparison/ (visited on 09/24/2020).

[125] M. Karpuz and A. Y. Özer, "Syringes as medical devices", *FABAD. J. Pharm. Sci*, vol. 41, pp. 27–37, 2016.

[126] innovation4life Intellectual Property (Pty) Ltd., *Vitaltrac - product profile*, Product profile for the VitalTrac from innovation4life, Stellenbosch, South Africa.

[127] J. Koenig *et al.*, "Heart rate variability and experimentally induced pain in healthy adults: A systematic review", *European Journal of Pain*, vol. 18, no. 3, pp. 301–314, 2014.

[128] K. P. Murphy, *Machine learning: a probabilistic perspective*. MIT press, 2012.